

การแสดงออกและการกลายพันธุ์เฉพาะตำแหน่งแอสพาราจีนไม่คงตัวของ  
ไซโคลเดกซ์ทรินไกลโคซิลแทรนส์เฟอเรสจาก *Paenibacillus* sp. RB01

นายวันชัย เย็นเพชร

วิทยานิพนธ์นี้เป็นส่วนหนึ่งของการศึกษาตามหลักสูตรปริญญาวิทยาศาสตรดุษฎีบัณฑิต

สาขาวิชาชีวเคมี ภาควิชาชีวเคมี

คณะวิทยาศาสตร์ จุฬาลงกรณ์มหาวิทยาลัย

ปีการศึกษา 2551

ลิขสิทธิ์ของจุฬาลงกรณ์มหาวิทยาลัย

EXPRESSION AND SITE-DIRECTED MUTAGENESIS AT LABILE ASPARAGINE RESIDUES OF  
CYCLODEXTRIN GLYCOSYLTRANSFERASE  
FROM *Paenibacillus* sp. RB01

Mr. Wanchai Yenpetch

A Dissertation Submitted in Partial Fulfillment of the Requirements  
for the Degree of Doctor of Philosophy Program in Biochemistry

Department of Biochemistry

Faculty of Science

Chulalongkorn University

Academic year 2008

Copyright of Chulalongkorn University

Thesis title                    EXPRESSION AND SITE-DIRECTED MUTAGENESIS AT LABILE  
   ASPARAGINE RESIDUES OF CYCLODEXTRIN  
   GLYCOSYLTRANSFERASE FROM *Paenibacillus* sp. RB01

By                                    Mr. Wanchai Yenpetch


Field of Study                    Biochemistry

Thesis Advisor                 Associate Professor Piamsook Pongsawasdi, Ph.D

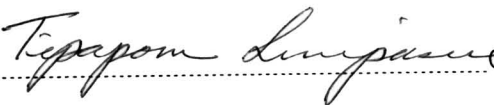
Thesis Co-Advisor             Assistant Professor Kanoktip Packdibamrung, Ph.D  
   Professor Wolfgang Zimmermann, Ph.D


---

Accepted by the Faculty of Science, Chulalongkorn University in Partial  
Fulfillment of the Requirements for the Doctoral Degree

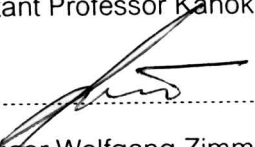
 ..... Dean of the Faculty of Science  
(Professor Supot Hannongbua, Dr.rer.nat)

THESIS COMMITTEE


 ..... Chairman  
(Associate Professor Tipaporn Limpaseni, Ph.D.)

 ..... Thesis Advisor  
(Associate Professor Piamsook Pongsawasdi, Ph.D.)

 ..... Thesis Co-Advisor  
(Assistant Professor Kanoktip Packdibamrung, Ph.D.)

 ..... Thesis Co-Advisor  
(Professor Wolfgang Zimmermann, Ph.D.)

 ..... Examiner  
(Associate Professor Siriporn Sitthipraneed, Ph.D.)

 ..... Examiner  
(Associate Professor Suganya Soontaros, Ph.D.)

 ..... External Examiner  
(Professor M.R. Jisnusan Svasti, Ph.D.)

วันชัย เย็นเพชร : การแสดงออกและการกลายพันธุ์เฉพาะตำแหน่งแอสปาราจีนไม่คงตัวของไซโคลเดกซ์ทรินไกลโคซิลทรานส์เฟอเรสจาก *Paenibacillus* sp. RB01. (EXPRESSION AND SITE-DIRECTED MUTAGENESIS AT LABILE ASPARAGINE RESIDUES OF CYCLODEXTRIN GLYCOSYLTRANSFERASE FROM *Paenibacillus* sp. RB01) อ.ที่ปรึกษาวิทยานิพนธ์หลัก : รศ.ดร. เปี่ยมสุข พงษ์สวัสดิ์, อ.ที่ปรึกษาวิทยานิพนธ์ร่วม : ผศ.ดร. กนกทิพย์ ภักดีบำรุง, Prof. Wolfgang Zimmermann 153 หน้า

ไซโคลเดกซ์ทรินไกลโคซิลทรานส์เฟอเรส (CGTase) จากแบคทีเรียทราน *Paenibacillus* sp. RB01 มี 3 รูปแบบ คือ ไอโซฟอร์ม I, II และ III ที่มีประจุต่างกันแต่มีขนาดเท่ากัน งานวิจัยนี้ มีวัตถุประสงค์ในการหาสาเหตุของการเกิดหลายรูปแบบของ เอนไซม์ โดยเริ่มจากการโคลนยีน *cgt* เข้าสู่เวกเตอร์ pET19b และแสดงออกใน *E. coli* BL21 (DE3) เอนไซม์โคลนมีหลายรูปแบบ เหมือนในสายพันธุ์เดิม เมื่อตรวจสอบค่า pI ของไอโซฟอร์ม I และ II บน IEF-PAGE พบว่าเท่ากับ 4.87 และ 4.75 ตามลำดับ จาก ข้อมูลเบื้องต้น เราตั้งสมมุติฐานว่าดิวเอมิเดชันของกรดอะมิโนแอสปาราจีนไปเป็นแอสปาร์เทต อาจเป็นสาเหตุของการเกิดไอโซ ฟอร์ม จึงได้ทำการทำนายอัตราการเกิดดิวเอมิเดชัน (Coefficient of deamidation, CD) ของแอสปาราจีนแต่ละตำแหน่งด้วย ขั้นตอนวิธีทางคอมพิวเตอร์ ที่มีอยู่ใน [www.deamidation.org](http://www.deamidation.org) โดยใช้โครงสร้างสามมิติของ CGTase จาก alkalophilic *Bacillus* sp. 1011 (PDB code 1PAM) ซึ่งมีค่าความเหมือนของลำดับกรดอะมิโนเมื่อเทียบกับ CGTase จาก *Paenibacillus* sp. RB01 ถึง 98% หลังจากนั้นได้เลือกกลายพันธุ์เฉพาะตำแหน่งแอสปาราจีนที่ไม่เสถียรซึ่งมีค่า CD ตั้งแต่ประมาณ 1 ถึง 158 โดยเปลี่ยนให้เป็น แอสปาร์เทต แล้วทำการแสดงออกใน *E. coli* ได้มีวแตนท์ 15 ตัว เป็นมีวแตนท์ 1 ตำแหน่ง 13 ตัว และมีวแตนท์ 2 และ 3 ตำแหน่ง อย่างละ 1 ตัว จากการติดตามรูปแบบการเคลื่อนที่เอนไซม์กลายบน native-PAGE พบว่าไอโซฟอร์ม II ของเอนไซม์โคลน เคลื่อนที่ ตรงกับแถบหลักของ N336D, N415D, N427D, และ N567D ส่วนเอนไซม์ที่ได้จากมีวแตนท์ 2 ตำแหน่ง (N336D/N415D) และ 3 ตำแหน่ง (N336D/N415D/N326D) มีรูปแบบการเคลื่อนที่เหมือนกับไอโซฟอร์ม III ของเอนไซม์โคลน ในงานวิจัยนี้สามารถแยก เอนไซม์แต่ละไอโซฟอร์มออกจากกันโดยใช้ preparative gel electrophoresis หรือ FPLC ด้วยคอลัมน์ Mono Q หรือ Mono P รวมทั้งการแยกบน IEF-PAGE จากนั้นใช้เทคนิคการเคลื่อนที่บนเจล 2 ทิศทาง เพื่อช่วยยืนยันว่าเอนไซม์กลายชนิดใดเหมือนไอโซ ฟอร์ม II ของเอนไซม์โคลนมากที่สุด โดยผสมเอนไซม์กลายกับไอโซฟอร์ม II ที่แยกได้ พบว่าเอนไซม์กลาย N336D, N427D และ N567D ไม่มีผลทำให้การเคลื่อนที่ของไอโซฟอร์ม II แตกต่างไปจากเดิม จากนั้นได้ทำการตรวจสอบผลของ pH และเวลาในการบ่ม ต่อการเพิ่มขึ้นของจำนวนไอโซฟอร์ม พบว่าการใช้ดิวเอมิเดชันบัฟเฟอร์ที่ pH 9.0 จะชักนำให้เกิดการเปลี่ยนไอโซฟอร์มเร็วกว่าที่ pH 6.0 ที่ 37°C และเมื่อตรวจวัดปริมาณ isoAsp ซึ่งเป็นสารตัวกลางของการเกิดปฏิกิริยาดิวเอมิเดชัน พบว่าปริมาณสารตัวกลางที่ pH 9.0 มีค่าสูงกว่าที่ pH 6.0 อย่างชัดเจนเมื่อทำการบ่มเอนไซม์ไว้ 15 วัน หลังจากนั้น ได้ทำการย่อยแต่ละไอโซฟอร์มด้วยทริปซิน แล้ว ตรวจสอบรูปแบบของเปปไทด์ด้วย reverse phase HPLC โดยใช้คอลัมน์ C<sub>18</sub> พบว่าไม่สามารถหาความแตกต่างของไอโซฟอร์ม I, II และเอนไซม์กลายได้ จึงได้ใช้เทคนิค MALDI-TOF เพื่อตรวจวัดขนาดของเปปไทด์ที่แตกต่าง พบว่าเอนไซม์กลาย N415D, N427D และ N567D มีขนาดของเปปไทด์ที่คาดว่าจะมี Asn ที่ถูกกลายอยู่ซึ่งมีมวลเพิ่มขึ้น 1 Da เมื่อ Asn เปลี่ยนเป็น Asp คือขนาด 1434.74, 1273.70, 2695.33 Da ตามลำดับ นอกจากนี้เอนไซม์กลายจากมีวแตนท์ 2 ตำแหน่ง (N336D/N415D) ก็พบการ เพิ่มขึ้น 1 Da ของมวลของเปปไทด์ขนาด 933.96 และ 1434.74 และเมื่อตรวจวัดขนาดของเปปไทด์ของไอโซฟอร์ม I และ II ของ เอนไซม์โคลน พบความแตกต่างที่ตำแหน่ง Asn 427 และจากการตรวจสอบการกระจายของไอโซพีนในเปปไทด์ พบความแตกต่าง ของไอโซฟอร์ม I และ II เพิ่มขึ้นที่ตำแหน่ง Asn 336 และ 567 จากนั้นได้ตรวจวัดอัตราส่วนผลิตภัณฑ์  $\alpha$ :  $\beta$ :  $\gamma$  CD ด้วยเทคนิค HPAEC-PAD พบว่าทั้งสองไอโซฟอร์มและเอนไซม์กลาย N415D, N427D และ N567D มีอัตราส่วนไม่ต่างกัน คือประมาณ 0.25 : 1.00 : 0.60 โดยทุกเอนไซม์คงมีผลผลิตหลักเป็น  $\beta$ -CD ผลการศึกษาค่าจลนพลศาสตร์ของปฏิกิริยาควบคุมสำหรับ  $\beta$ -CD พบว่าไอโซ ฟอร์ม I มีประสิทธิภาพในการเร่งปฏิกิริยา ( $k_{cat}/K_m$ ) และค่าจำนวนหมุนเวียน ( $k_{cat}$ ) สูงกว่าไอโซฟอร์ม II เล็กน้อย ส่วนเอนไซม์กลาย N336D และ N567D มีค่าทั้งสองใกล้เคียงกับไอโซฟอร์ม I ในขณะที่ N427D มีค่า  $k_{cat}/K_m$  ต่ำกว่าทั้งสองไอโซฟอร์ม จากผลงานวิจัย ทั้งหมด สนับสนุนว่าดิวเอมิเดชันที่แอสปาราจีนทำให้เกิดหลายรูปแบบของ CGTase และ Asn 336, Asn 427 และ Asn 567 เป็น กลุ่มไม่เสถียรที่มีผลต่อการเกิดไอโซฟอร์มของเอนไซม์

ภาควิชา.....ชีวเคมี.....ลายมือชื่อนิสิต *Jan* *Jan*  
 สาขาวิชา.....ชีวเคมี.....ลายมือชื่อ.ที่ปรึกษาวิทยานิพนธ์หลัก *Prof. Peemsook*  
 ปีการศึกษา.....2551.....ลายมือชื่อ.ที่ปรึกษาวิทยานิพนธ์ร่วม *Prof. Wangkarn*  
 ลายมือชื่อ.ที่ปรึกษาวิทยานิพนธ์ร่วม *Prof. Wangkarn*

# # 4773835523 : MAJOR BIOCHEMISTRY

KEYWORDS : CYCLODEXTRIN GLYCOSYLTRANSFERASE / ISOFORM / DEAMIDATION

WANCHAI YENPETCH : EXPRESSION AND SITE-DIRECTED MUTAGENESIS AT LABILE  
ASPARAGINE RESIDUES OF CYCLODEXTRIN GLYCOSYLTRANSFERASE FROM

*Paenibacillus* sp. RB01. THESIS ADVISOR : ASSOC. PROF. PIAMSOOK PONGSAWASDI,  
Ph. D., THESIS CO-ADVISOR : ASSIST. PROF. KANOKTIP PACKDIBAMRUNG, Ph.D., PROF.  
WOLFGANG ZIMMERMANN, Ph.D., 153 pp.

Cyclodextrin glycosyltransferase (CGTase) from a thermotolerant *Paenibacillus* sp. RB01 exhibits 3 isoforms (I, II, and III) with equal mass but different charge. The aim of this work is to determine the cause of formation of multiple forms of the enzyme. Starting with cloning of CGTase gene (*cgt*) into pET19b vector and expressed in *E. coli* BL21 (DE3), the cloned enzyme showed multiple forms as in the wild type. The pI of major isoform I and II from IEF-PAGE were 4.87 and 4.75. Preliminary investigation led us propose that deamidation of Asn to Asp may be the cause of isoform formation. Deamidation rate of each Asn (expressed as Coefficient of Deamidation, CD value) was predicted by the computer algorithm ([www.deamidation.org](http://www.deamidation.org)), by using the 3D-structure of CGTase from alkalophilic *Bacillus* sp. 1011 (PDB code 1PAM) which has 98% similarity in amino acid sequence with CGTase from *Paenibacillus* sp. RB01. Then, site-directed mutagenesis of labile Asn residues (with CD values of 1 to 158) into Asp and expression was performed, creating 13 single mutants, and one each of double and triple mutants. From native-PAGE, the isoform II of cloned showed the same migration with the major band of N336D, N415D, N427D, and N567D. While CGTase from double mutant (N336D/N415D) and triple mutant (N336D/N415D/N326D) moved similarly with the cloned isoform III. Separation of isoforms was carried out by preparative gel electrophoresis or FPLC with Mono Q or Mono P, or IEF-PAGE. Two-dimensional gel electrophoresis was then used to show which mutated enzyme most resembled to isoform II. By mixing mutated CGTase with isoform II, only the N336D, N427D, and N567D showed no effect on migration of isoform II. Then, the effect of pH and incubation time on the increase in number of isoforms was investigated. Deamidation buffer at pH 9.0 induced faster isoform formation than at pH 6.0, 37°C. And when the content of isoAsp, an intermediate of deamidation reaction, was determined, the value at pH 9.0 was clearly higher than at pH 6.0 after 15 days of incubation. Then, each isoform was digested with trypsin and separation pattern of peptide analyzed by reverse phase HPLC with C<sub>18</sub> column showed no difference between those of isoform I, II and mutated enzymes. MALDI-TOF was then used to investigate size difference in peptides. For mutated enzymes, N415D, N427D, and N567D showed the peptide fragments containing mutated Asn (each has an increase of 1 Da when Asn was mutated to Asp) of the size 1434.74, 1273.70, 2695.33 Da, respectively. N336D/N415D double mutant also showed a 1 Da increase of the fragment size 933.96 and 1434.74. And when compared the cloned isoform I and II, the difference in m/z of peptide containing Asn 427 was observed. Furthermore, from the analysis of isotopic distribution in other interesting peptides of isoform I and II, the difference was observed at two more positions, Asn 336 and Asn 567. Then, the product ratio  $\alpha:\beta:\gamma$  CD was determined by HPAEC-PAD. Isoform I, II, and mutated enzymes N415D, N427D, and N567D gave similar ratio around 0.25:1.00:0.60. All enzyme forms still produced  $\beta$ -CD as major product. From kinetics of coupling reaction with  $\beta$ -CD, catalytic efficiency ( $k_{cat}/K_m$ ) and turnover number ( $k_{cat}$ ) of isoform I was not much higher than those of isoform II. The mutated N336D and N567D showed similar values to those of isoform I, while  $k_{cat}/K_m$  of N427D was significantly lower than both isoforms. The overall results support that Asn deamidation is the cause of formation of multiple forms of CGTase, and Asn 336, Asn 427, and Asn 567 are among the susceptible residues responsible for the formation of CGTase isoforms.

Department : ..... Biochemistry ..... Student's Signature *Wanchai Yenpetch*

Field of Study : ..... Biochemistry ..... Advisor's Signature *P. Pongsaewasdi*

Academic Year : ..... 2008 ..... Co-Advisor's Signature *Kanoktip Packdibamrung*

Co-Advisor's Signature *Wolfgang Zimmermann*

## ACKNOWLEDGEMENTS

I would like to express my deepest gratitude to my great advisor, Associate Professor Piamsook Pongsawasdi, for her beautiful mind, excellent instruction, guidance, attention and support throughout this thesis. Without their kindness and understanding, this work could not be accomplished.

My gratitude is also extended to Associate Professor Tipaporn Limpaseni, Assistant Professor Kanoktip Packdibamrung, Professor Wolfgang Zimmermann, Professor M.R. Jisnusan Svasti, Associate Professor Siriporn Sitthipraneed, Associate Professor Suganya Soontaros for their valuable suggestion and comments and also dedicating valuable time for thesis examination.

The Department of Biochemistry, Faculty of Science gave a support for most of chemicals and instruments. My appreciate is also expressed to Professor Wolfgang Zimmermann, my co-advisor, and department of microbiology and bioprocess technology, institute of biochemistry, university of Leipzig, Germany for HPAEC support. All staff and student in starch and cyclodextrin research unit especially to Miss Wiraya Srisimarat, and Mr. Surachai Yaiyen.

Finally, the greatest gratitude is expressed to my parents and my family for their infinite love, encouragement, understanding and everything giving to my life.

This work was supported in part by the Grant from Thailand Research Fund, Royal Golden Jubilee, Ph. D. Program and 90<sup>th</sup> Anniversary Chulalongkorn University Fund.

## CONTENTS

	Pages
THAI ABSTRACT .....	iv
ENGLISH ABSTRACT .....	v
ACKNOWLEDGEMENTS .....	vi
CONTENTS .....	vii
LIST OF TABLES .....	xiii
LIST OF FIGURES .....	xv
LIST OF ABBREVIATIONS .....	xix
CHAPTER I INTRODUCTION .....	1
1.1 Cyclodextrin glycosyltransferases (CGTases) .....	1
1.2 Structure of CGTase .....	3
1.3 Physiological roles of CGTase .....	6
1.4 Application of CGTase .....	9
1.5 Cyclodextrins (CD) .....	9
1.6 CGTase from <i>Paenibacillus</i> sp. RB01 .....	9
1.7 Deamidation hypothesis on peptides and proteins .....	15
1.7.1 Effect of deamidation on proteins/enzymes .....	16
1.7.2 Effect of protein structure and other factors on nonenzymatic deamidation rate .....	17
1.7.2.1 Amino acid sequence and higher-order Structures .....	17
1.7.2.2 Other factors .....	17
1.7.3 Prediction of deamidation rate .....	17
1.7.4 Examples of deamidation in particular proteins .....	20
1.7.4.1 Cow heart muscle cytochrome c .....	20
1.7.4.2 Human Rhinovirus-14 3C Protease .....	20
1.7.4.3 Recombinant human phenylalanine hydroxylase ..	21
1.8 The objective of this study .....	21

	Pages
CHAPTER II MATERIALS AND METHODS.....	22
2.1 Equipments.....	22
2.2 Chemicals.....	23
2.3 Enzymes, Restriction enzymes and Bacterial stains.....	25
2.4 Cloning for overproduction of CGTase.....	26
2.4.1 Cultivation and genomic DNA extraction of <i>Paenibacillus</i> sp. RB01.....	26
2.4.2 Agarose gel electrophoresis.....	27
2.4.3 Amplification of CGTase gene ( <i>cgt</i> ) using PCR technique...	27
2.4.4 Restriction enzyme digestion.....	28
2.4.5 Ligation of PCR product with vector pET19b.....	28
2.4.6 Plasmid transformation.....	28
2.5 Colony selection and primary screening.....	29
2.5.1 Plasmid size screening.....	29
2.5.2 Plasmid extraction.....	29
2.5.3 Nucleotide sequencing.....	29
2.6 Prediction of Asn deamidation rate and site-directed mutagenesis on labile Asn residues.....	30
2.6.1 Prediction of Asn deamidation rate.....	30
2.6.2 Selection of labile Asn residues.....	30
2.7 Site-directed mutagenesis.....	31
2.7.1 Single mutation.....	31
2.7.2 Double and triple mutation.....	31
2.7.3 Transformation into <i>E. coli</i> BL21 (DE3).....	31
2.8 Purification of cyclodextrin glycosyltransferase.....	32
2.8.1 Bacterial cultivation.....	32
2.8.2 Partial purification of CGTase.....	32
2.9 CGTase isoforms separation.....	34
2.9.1 Preparative gel electrophoresis.....	34
2.9.2 Fast protein liquid chromatography (FPLC) with the anion column.....	34



	Pages
2.9.3 Fast protein liquid chromatography (FPLC) with isofocusing chromatography column.....	35
2.9.4 IEF-PAGE.....	35
2.10 Enzyme assay.....	35
2.10.1 Dextrinizing activity.....	35
2.10.2 Cyclizing activity assay.....	36
2.10.3 Coupling activity assay.....	36
2.11 Protein determination.....	36
2.12 Polyacrylamide Gel Electrophoresis (PAGE).....	37
2.12.1 Non-denaturing polyacrylamide gel electrophoresis (Native-PAGE).....	37
2.12.1.1 Protein staining.....	37
2.12.1.2 Dextrinizing activity staining.....	38
2.12.2 SDS-polyacrylamide gel electrophoresis.....	38
2.12.3 Isoelectric focusing-PAGE.....	38
2.13 Isoform pattern on native-PAGE of CGTase from <i>Paenibacillus</i> sp. RB01, cloned CGTase and mutated CGTase.....	39
2.14 Comparison of isoforms by analysis of tryptic digested pattern, peptide sequence and <i>iso</i> -Asp intermediate.....	39
2.14.1 In solution tryptic digestion.....	39
2.14.2 In gel tryptic digestion.....	39
2.14.3 Tryptic digested peptide separation by reverse phase HPLC.....	40
2.14.4 Mass analysis of peptides.....	40
2.14.5 Detection of <i>iso</i> -Aspartate content in CGTase.....	41
2.14.5.1 Sample preparation.....	41
2.14.5.2 Iso-aspartate detection.....	43
2.15 Comparison of properties of CGTase isoforms from the cloned and mutants.....	43
2.15.1 Optimum pH and Temperature.....	43
2.15.2 Kinetics parameters.....	43

	Pages
2.15.3 CD product ratio.....	44
2.15.4 Amino acid sequence.....	44
<b>CHAPTER III RESULTS.....</b>	<b>46</b>
3.1 Identification and expression of CGTase gene ( <i>cgt</i> ) from <i>Paenibacillus</i> sp. RB01.....	46
3.1.1 Cloning of <i>cgt</i> from <i>Paenibacillus</i> sp. RB01.....	46
3.1.2 Expression of cloned CGTase.....	54
3.2 Prediction of labile asparagines of CGTase from <i>Paenibacillus</i> sp. RB01.....	54
3.3 Site-directed mutagenesis at labile Asn residues of CGTase.....	57
3.4 Comparison of dextrinizing activity of CGTase from 3 sources: native, cloned, and mutated CGTase.....	62
3.5 Comparison of the isoform pattern of CGTases from 3 sources: native, cloned and mutated CGTase.....	65
3.5.1 Isoform formation of native CGTase from <i>Paenibacillus</i> sp. RB01.....	65
3.5.2 Isoform formation of cloned CGTase expressed by <i>E. coli</i> BL21 (DE3).....	65
3.5.3 Comparison of Isoform pattern between native CGTase and cloned CGTase.....	65
3.5.4 Comparison of isoform pattern between cloned and mutated CGTase expressed by <i>E. coli</i> BL21 (DE3).....	69
3.5.4.1 Isoform pattern of cloned vs. single mutated enzymes on native-PAGE.....	69
3.5.4.2 Isoform pattern of cloned vs. double and triple mutated enzymes on native-PAGE.....	69
3.5.4.3 isoform pattern of cloned vs. mutated CGTase on IEF-PAGE.....	72
3. 6 Separation of CGTase isoforms.....	75

	Pages
3.6.1 CGTase isoform separation by preparative gel electrophoresis.....	75
3.6.2 CGTase isoform separation by FPLC system with anion exchange column (MonoQ).....	75
3.6.3 CGTase isoform separation by FPLC system with chromatofocusing column (Mono P).....	79
3.6.4 CGTase isoform separation by IEF-PAGE.....	79
3.7 CGTase isoform pattern on two-dimensional gel electrophoresis.....	81
3.7.1 Isoform pattern of cloned CGTase.....	81
3.7.2 Comparison of isoform II of cloned CGTase and the mixture of isoform II with mutated CGTase.....	81
3.8 The effect of deamidation on isoform formation of cloned CGTase.....	85
3.8.1 The effect of pH and incubation time on isoform formation..	85
3.8.2 Determination of isoaspartate content in CGTase isoforms..	92
3.9 Tryptic digestion of isoforms of cloned and mutated CGTase.....	92
3.9.1 Separation of tryptic peptides by HPLC.....	92
3.9.2 Mass of tryptic peptides determined by matrix-assisted laser desorption/ionization time of flight-mass spectrometry (MALDI-TOF).....	94
3.10 Comparison of properties of CGTase isoforms from the cloned and mutants:.....	106
3.10.1 Optimum temperature.....	106
3.10.2 Optimum pH.....	106
3.10.3 Kinetic parameters of isoforms of cloned and mutated CGTase.....	109
3.10.4 Comparison of CD production by HPAEC-PAD.....	109
3.10.5 Amino acid sequence.....	121
CHAPTER IV DISCUSSION.....	122
4.1 Cloning of <i>cgt</i> from <i>Paenibacillus</i> sp. RB01.....	122
4.2 Isoforms of CGTase.....	122

	<b>Pages</b>
4.3 Evidences support Asn deamidation as the cause of formation of CGTase isoforms.....	123
4.3.1 Effect of pH, incubation time, and isoAspartate content.....	123
4.3.2 Prediction of labile Asn residues.....	124
4.3.3 Isolation of CGTase isoforms.....	127
4.3.4 Analysis of tryptic digested peptides.....	127
4.4 Enzyme characterization.....	129
4.4.1 CD production.....	129
4.4.2 Kinetic study.....	130
CHAPTER V CONCLUSION.....	132
REFERENCES.....	133
APPENDICES.....	142
BIOGRAPHY.....	153

## LIST OF TABLES

Table	Page
1.1 Some properties of bacterial CGTases (Tonkova, 1998).....	2
1.2 Approximate geometric dimensions and properties of $\alpha$ -, $\beta$ -, and $\gamma$ -CD molecules (Szejtli, 1998).....	11
1.3 Possible effects of the formation of inclusion complexes on properties of guest molecules (van der Veen, 2000).....	11
1.4 Isoform formation and pI values of CGTases from different CGTase-producing bacteria.....	14
2.1 List of selected asparagine residues and their primers for site-directed mutagenesis.....	33
3.1 Percent similarity of deduced amino acid sequence of CGTase from <i>Paenibacillus</i> sp. RB01 compared with other CGTases by pairwise alignment.....	53
3.2 Amino acid difference in CGTase of <i>Paenibacillus</i> sp. RB01 and <i>Bacillus</i> sp. 1011.....	58
3.3 An overview of the primary sequence of asparagine residues and coefficient of deamidation (CD value) and predicted by the program from www.deamidation.org using 3D structure information of alkalophilic <i>Bacillus</i> sp. 1011 (Protein Data Bank code 1PAM).....	59
3.4 The list of 12 asparagine residues selected for single mutation and the domain location.....	61
3.5 Activities of crude cloned and mutated CGTases expressed by <i>E.coli</i> BL21(DE3).....	64
3.6 Comparison of separation methods of CGTase isoforms.....	82
3.7 Theoretical and experimental monoisotopic mass ( $[M + H]^+$ ) of the tryptic digested peptide fragment at the mutated Asn residues determined by MALDI-TOF.....	98
3.8 Comparison of monoisotopic mass of tryptic digested fragments of cloned CGTase isoform I and isoform II from <i>Paenibacillus</i> sp. RB01.....	103

Table	Page
3.9 Kinetic parameters of CGTases from coupling reaction with various concentrations of $\beta$ -CD donor and fixed concentration of cellobiose acceptor.....	113
3.10 Cyclodextrin product with 3 Units activity of crude CGTase per reaction.....	117
3.11 Monoisotopic mass of tryptic digested peptides of isoform I from cloned CGTase analyzed and matching amino acid sequence predicted by the available program at <a href="http://www.matrixscience.com">www.matrixscience.com</a> .....	120
3.12 Monoisotopic mass of tryptic digested peptides of isoform I from cloned CGTase analyzed and matching amino acid sequence predicted by the available program at <a href="http://www.matrixscience.com">www.matrixscience.com</a> .....	121
4.1 Deamidation half-times in days at 37C, pH 7.4 vs. estimates by (100)(CD).....	126

## LIST OF FIGURES

Figure	Page
1.1 Schematic representation of the CGTase catalyzed reactions.....	4
1.2 Figure 8 Domain level organization of starch degrading enzymes.....	5
1.3 Structure of CGTase from alkalophilic <i>Bacillus</i> sp. 1011 (PDB number 1PAM).....	7
1.4 Roles of CGTase in glucan utilization by bacteria.....	8
1.5 (a) Chemical structure of three kinds of CDs (b) The molecular dimension structure of CDs (Szejtli, 1990).....	10
1.6 Structure of $\beta$ -cyclodextrin (Bender, 1986; Szejtli, 1990).....	12
1.7 Mechanism of isoAsp formation at Asn and Asp sites.....	18
2.1 Isoaspartate formation in protein deamidation at asparagine (A) and intrachain bond rearrangement at aspartic acid (B) and the detection of isoaspartic acid via PIMT-catalyzed reaction.....	42
3.1 Agarose gel electrophoresis of A) amplified <i>cgt</i> and genomic DNA of <i>Paenibacillus</i> sp.RB01, B) recombinant <i>cgt</i> inserted in pET19b vector.....	46
3.2 Selection of the transformant <i>E. coli</i> BL21 (DE3) containing pET19b inserted with <i>cgt</i> on LB agar plate containing 100 $\mu$ g/ml ampicillin and 1% soluble starch.....	47
3.3 Nucleotide and deduced amino acid sequences of <i>Paenibacillus</i> sp. RB01.....	49
3.4 Amino acid sequence alignment of CGTase from <i>Paenibacillus</i> sp. RB01 compared with other CGTases using ClustalX.....	51
3.5 Neighbor-joining tree based on amino acid similarity among CGTases.....	55
3.6 Optimization of IPTG induction of cloned CGTase in pET19b vector and expressed by <i>E. coli</i> BL21 (DE3).....	56
3.7 Location of selected asparagine residues for site-directed mutagenesis using 3D information of 1PAM.....	63
3.8 Non-denaturing PAGE of crude native CGTase of <i>Paenibacillus</i> sp. RB01 at different time of cultivation.....	66

Figure	Page
3.9 Non-denaturing PAGE of crude cloned CGTase expressed by <i>E. coli</i> BL21 (DE3) at different time after IPTG induction.....	67
3.10 Coomassie blue staining of isoform pattern of CGTase from <i>Paenibacillus</i> sp. RB01 compared with cloned CGTase expressed by <i>E.coli</i> BL21 (DE3) on A) native-PAGE and B) IEF-PAGE.....	68
3.11 Standard curve of pI and relative mobility on IEF-PAGE.....	70
3.12 Coomassie blue staining of non-denaturing PAGE of crude cloned and mutated CGTase.....	71
3.13 Coomassie blue staining of non-denaturing PAGE of cloned CGTase compared with N336D/N415D and N336D/N415D/N326D mutated CGTase expressed by <i>E. coli</i> BL21 (DE3).....	73
3.14 IEF-polyacrylamide gel electrophoresis of crude cloned CGTase from <i>Paenibacillus</i> sp. RB01 compared with mutated enzyme.....	74
3.15 IEF-polyacrylamide gel electrophoresis of crude cloned CGTase from <i>Paenibacillus</i> sp. RB01 compared with mutated enzyme.....	76
3.16 A) Preparative gel electrophoresis unit B) Separation pattern of CGTase isoforms by Preparative gel electrophoresis, as analyzed on non-denaturing PAGE with amylolytic activity staining.....	77
3.17 Chromatogram of CGTase isoform separation on a Mono Q FF column.....	78
3.18 Isoform pattern on native-PAGE of CGTase separated by Mono Q FF column.....	78
3.19 Chromatogram of CGTase isoform separation on a Mono P column.....	80
3.20 Isoform pattern on native-PAGE of cloned CGTase isolated by chromatofocusing column (Mono P).....	80
3.21 Separation on two-dimension gel electrophoresis of the crude cloned CGTase Isoforms.....	83
3.22 Coomassie blue staining of CGTase isoforms isolated by FPLC Mono Q column on A) non-denaturing PAGE and B) isolated isoform II on two-dimension gel electrophoresis.....	84



Figure	Page
3.23 Two-dimension gel electrophoresis of isoform II and isoform II mixed with mutated CGTases.....	86
3.24 Zoom-in of the two-dimension gel electrophoresis of isoform II and isoform II mixed with mutated CGTases.....	87
3.25 Dextrinizing activity staining (A and C) and coomassie blue staining (B and D) on non-denaturing PAGE of CGTase isoform I incubated in deamidation buffer (25 mM acetic acid, 25 mM Tris and 25 mM ethanolamine) of pH 6.0 (A and B) or pH 9.0 (C and D) at 37°C.....	89
3.26 IEF-PAGE of CGTase isoform I incubated in deamidation buffer (25 mM acetic acid, 25 mM Tris and 25 mM ethanolamine).....	90
3.27 Coomassie blue stain of SDS-PAGE of CGTase isoform I incubated in deamidation buffer (25 mM acetic acid, 25 mM Tris and 25 mM ethanolamine) of pH 6.0 (Lane 2-5) or pH 9.0 (Lane 6-9) at 37°C.....	91
3.28 Isoaspartate content in CGTase after the isoform I was incubated in deamidation buffer at pH 6.0 and 9.0 for various incubation time.....	95
3.29 HPLC profile of the in gel tryptic peptides of isoform I (A) and II (B) of cloned CGTase separated by C <sub>18</sub> column.....	95
3.30 HPLC Profile of the in the gel tryptic peptides of mutated CGTase from N415D (A), N336D/N415D (B) and N336D/N415D/N326D separated by HPLC using C <sub>18</sub> column (C).....	96
3.31 Mass spectra of tryptic digested peptide of N567D.....	99
3.32 Mass spectra of tryptic digested peptide of isoform I.....	100
3.33 Mass spectra of tryptic digested peptide of isoform II.....	101
3.34 The percentage of isotopic distribution of tryptic digested peptides containing interested asparagine residues in CGTase.....	104
3.35 Analysis of the charge in isoform pattern and tryptic peptides upon incubation of isoform I.....	105
3.36 Optimum temperature for dextrinizing activity (A) and cyclizing activity (B) of the isoform I and II of cloned CGTase from <i>Paenibacillus</i> sp. RB01.....	107

Figure	Page
3.37 Optimum pH for dextrinizing activity (A) and cyclizing activity (B) of the isoform I and II of cloned CGTase from <i>Paenibacillus</i> sp. RB01 in the universal buffer.....	108
3.38 Optimum pH for dextrinizing activity (A) and cyclizing activity (B) of the isoform I of cloned CGTase from <i>Paenibacillus</i> sp. RB01 in various buffers.....	110
3.39 Optimum pH for dextrinizing activity (A) and cyclizing activity (B) of the isoform II of cloned CGTase from <i>Paenibacillus</i> sp. RB01 in various buffers.....	111
3.40 Lineweaver-Burk plot of CGTase on coupling reaction with $\beta$ -cyclodextrin as donor and cellobiose as acceptor.....	112
3.41 Example of elution profile of HPAEC the CDs produced by CGTase from <i>Paenibacillus</i> sp. RB01.....	115
3.42 CDs production of isoform I and II of cloned CGTase.....	116
3.43 Ratio of $\alpha$ -CD ( <span style="color: blue;">■</span> ), $\beta$ -CD ( <span style="color: red;">■</span> ) and $\gamma$ -CD ( <span style="color: yellow;">■</span> ) by crude CGTase 3 Units per reaction.....	118

## LIST OF ABBREVIATIONS

A	absorbance
Asn	asparagine
Asp	aspartic acid
BSA	bovine serum albumin
CDs	cyclodextrins
CD value	coefficient of deamidation
CGTase	cyclodextrin glycosyltransferase
cm	centrimeter
°C	degree Celsius
g	gram
Gln	glutamine
Glu	glutamic acid
hr	hour
IPTG	<b>Isopropyl <math>\beta</math>-D-1-thiogalactopyranoside</b>
l	litre
mA	milliampere
min	minute
$\mu$ l	microlitre
ml	millilitre
mM	millimolar
M	molar
PAGE	polyacrylamide gel electrophoresis
rpm	revolution per minute
$\mu$ g	microgram

# CHAPTER I

## INTRODUCTION

### 1.1 Cyclodextrin glycosyltransferases (CGTases)

Starch is a source of energy of many (micro) organisms in nature. In order for organisms to use the glucose monomer unit of the starch granule as a growth substrate, the starch degradation process requires a whole range of enzymes. The starch molecules need to be converted extracellularly into molecules suitable for uptake and further conversion by the cells. Starch degrading enzymes can be roughly divided into amylases, hydrolyzing  $\alpha(1-4)$  linkages, and debranching enzymes, hydrolyzing  $\alpha(1-6)$  linkages.

Cyclodextrin glycosyltransferase (CGTase, 4- $\alpha$ -D-glucan:1,4- $\alpha$ -glucanotransferase, EC 2.4.1.19), a transferase, is a member of the  $\alpha$ -amylase family of glycosylase with a low hydrolytic activity. The enzyme has functional properties related to  $\alpha$ -amylase, which hydrolyzes starch into linear products. In addition, this enzyme is responsible for the conversion of starch and related  $\alpha$ -1,4-glucans into cyclodextrins (CDs), a group of cyclic oligosaccharide (Nagamura *et al.*, 1993; van der Veen *et al.*, 2000). The CGTase may be divided into three categories depending on the kind of CD mainly produced ( $\alpha$ - or  $\beta$ -  $\gamma$ -CGTase). The CGTase is an extracellular enzyme produced by a large number of microorganisms (Tonkova, 1998). The enzymes produced from different sources show different properties, such as working pH, temperature, molecular weight, and yield different ratio of CD products. (Table 1.1).

The CGTase is known to catalyze four different transferase reactions: cyclization, coupling, disproportionation, and hydrolysis (Bender, 1986). The size of substrate determines which reaction is going to occur. The enzyme catalyzes the intramolecular transglycosylation, called *cyclization* reaction, in which the part of the donor that has been cleaved off also acts as the acceptor, resulting in formation of CDs product. The reverse reaction is referred to *coupling* reaction in which CD rings are opened and act as glycosyl donor while malto-oligosaccharide or glucose residues act as an acceptor. If chain

Table 1.1 Some properties of bacterial CGTases (Tonkova, 1998)

Producer	Optimum pH	Optimum Temp(°C)	Molecular mass	Main CD produced	Reference
<i>Bacillus macerans</i> ATCC 8514	6.1-6.2	60 °C	139,000	-	De Pinto, 1968
<i>Bacillus macerans</i> IFO 3490	5.0-5.7	55 °C	-	$\alpha$ -CD	Kitahata, 1974
<i>Bacillus macerans</i> IAM 1243	-	-	74,000	$\alpha$ -CD	Takano, 1986
<i>Bacillus megaterrium</i> No5	5.0-5.7	55 °C	-	$\beta$ -CD	Kitahata, 1974
<i>Bacillus circuitans</i> var. <i>alkalophilus</i> ATCC 21783	4.5-4.7	45 °C	88,000	$\beta$ -CD	Nakamura, 1976
<i>Bacillus</i> sp. AL-6 (alkalophilic strain)	7.0-10.0	60 °C	74,000	$\gamma$ -CD	Fujita, 1990
<i>Bacillus cereus</i> NCIMB	5.0	40 °C	-	$\alpha$ -CD	Jamuna, 1993
<i>Bacillus</i> sp. INMIA T6 (thermophilic strain)	6.5	55 °C	38,000	$\alpha$ -CD	Abelian, 1995
<i>Bacillus</i> sp. INMIA T42 (thermophilic strain)	6.5	55 °C	35,000	$\beta$ -CD	Abelian, 1995
<i>Bacillus</i> sp. INMIA A7/1 (alkalophilic strain)	6.0	50 °C	44,000	$\beta$ -CD	Abelian, 1995
<i>Bacillus</i> sp. INMIA 1919	4.0	50 °C	42,000	$\alpha$ -CD	Abelian, 1995
<i>Bacillus halophilus</i> INMIA 3849	7.0	60-62 °C	71,000	$\beta$ -CD	Abelian, 1995
<i>Thermoanaerobacterium thermosulfurigenes</i> EM1	4.5-7.0	80-85 °C	68,000	$\beta$ -CD	Wind, 1995
<i>Bacillus ohbensis</i> sp. nov. C-1400	5.0	55 °C	80,000	$\beta$ -CD	Sin, 1991

length of substrates is containing 16-80 glucopyranosyl residues, the *disproportionation* (the transfer of glycosyl group from a linear oligosaccharide to another oligosaccharide) reaction dominates. The enzyme also catalyzes the *hydrolysis* reaction where water is an acceptor, in a low activity. Coupling, disproportionation, and hydrolysis can be classified as intermolecular transglycosylation reaction. All these reactions can be summarized as shown in Figure 1.1.

## 1.2 Structure of CGTase

In contrast to the limited similarity in primary structure (<30%), the enzyme in  $\alpha$ -amylase family showed the high similarity in secondary-tertiary structures. The domains of CGTase were comparable with the general  $\alpha$ -amylase family which the  $(\beta/\alpha)_8$ -chain fold and four conserved regions of  $\alpha$ -amylase were found. CGTase has two extra domain (domain D and E) (Figure 1.2) where  $\alpha$ -amylase has only three (A to C) (Schmid, 1989; Jespersen *et al.*, 1991 with modified by van der Veen, 2000). The CGTase structure and domain of alkalophilic *Bacillus* sp. 1011 are shown in Figure 1.3. The function of each domain is clarified as follows:

**Domain A:** the catalytic and substrate binding residues conserved in the  $\alpha$ -amylase family are located in loops at the C-termini of  $\beta$ -strands

**Domain B:** consists of 44-133 amino acid residues and contributes to substrate binding.

**Domain C:** approximately 100 amino acids long and has an antiparallel  $\beta$ -sandwich fold. Domain C of the CGTase from *B.circulans* strain 251 contains one of the maltose binding sites observed in the structure derived from maltose dependent crystals (Lawson *et al.*, 1994). This maltose binding site was found to be involved in raw starch binding (Peninga *et al.*, 1996), suggesting a role of the C-domain in substrate binding. Some authors suggest that this domain is involved in bond specificity, in hydrolyzing or forming  $\alpha$ -1,6-bonds (e.g. pullulanase, isoamylase, branching enzyme).

**Domain D:** consisting of approximately 90 amino acids with an immunoglobulin fold, is almost exclusively found in CGTase and has an unknown function.

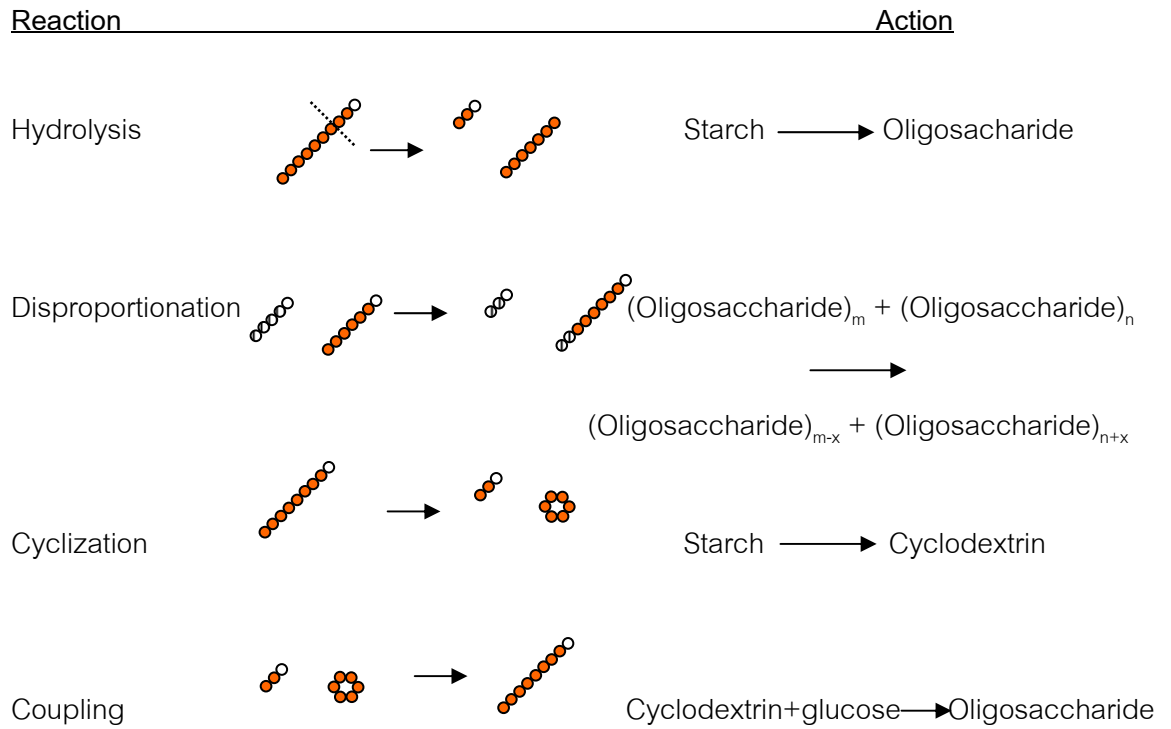


Figure 1.1 Schematic representation of the CGTase catalyzed reactions The circles represent glucose residues; the white circles indicate the reducing end sugars. (a): hydrolysis, (b): disproportionation, (c): cyclization, (d): coupling (van der Veen *et al.*, 2000)

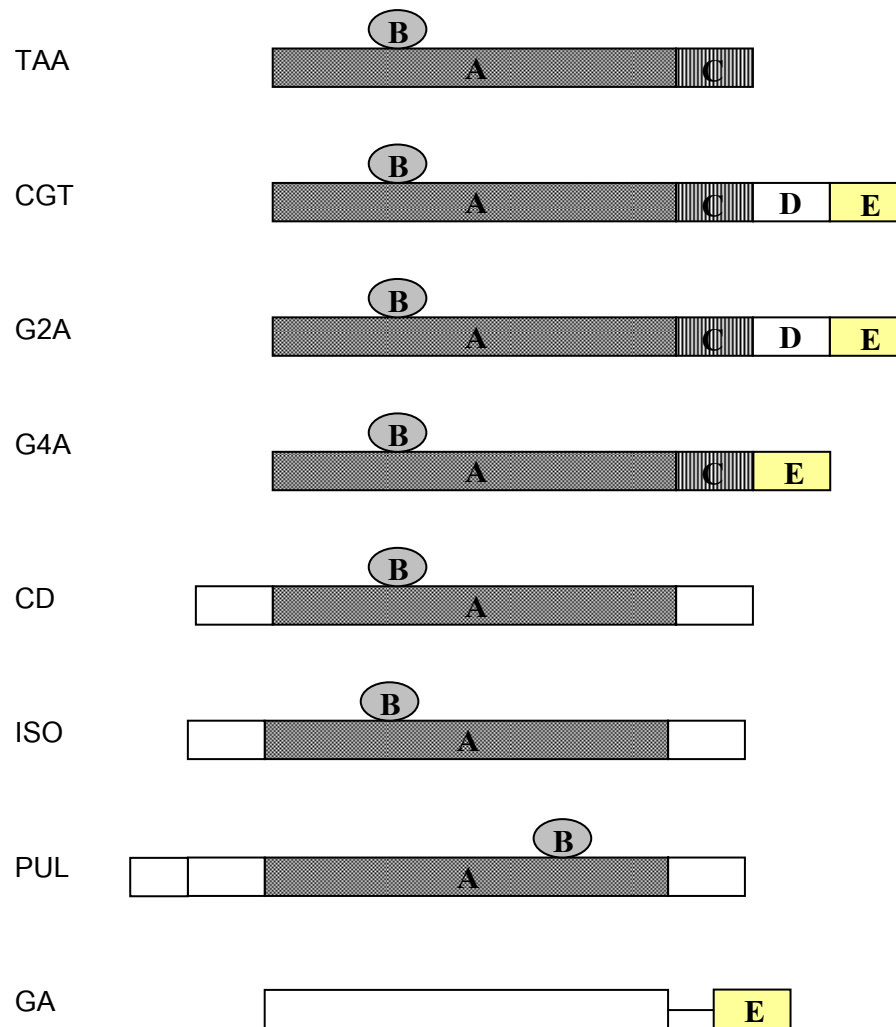


Figure 1.2 Figure 8 Domain level organization of starch degrading enzymes

TAA:  $\alpha$ -amylase from *Aspergillus oryzae* (Taka-amylase A); CGT: CGTase from *Bacillus circulans*; G2A: maltogenic  $\alpha$ -amylase from *Bacillus stearothermophilus*; G4A: maltotetraose forming  $\alpha$ -amylase from *Pseudomonas stutzeri*; CD: cyclodextrinase from *Klebsiella ozytoca*; ISO: isoamylase from *Pseudomonas amyloclavata*; PUL: pullulanase from *Klebsiella aerogenes*; GA: glucoamylase (family 15 of glycosylases) from *Aspergillus niger* (Jespersen *et al.*, 1991 with modified by van der Veen, 2000)



**Domain E:** approximately 110 amino acids and is found to be responsible for the adsorption onto granular starch. It is also found in some other starch degrading enzymes.

The active site of CGTase has been intensively studied. Three carboxylic acid groups, one glutamic acid and two aspartic acid residues, are essential for catalytic activity in CGTases; Asp229, Glu257 and Asp328 in CGTase from *B. circulans* (Klein *et al.*, 1992; Strokopytov *et al.*, 1996). These amino acids are equivalent to Asp206, Glu230, and Asp297 in  $\alpha$ -amylase from *Aspergillus oryzae* (Matsuura *et al.*, 1984). Roles of the three important amino acid residues in CGTase are investigated. The Glu257 (CGTase *B. circulans* numbering) is the general acid catalyst, acting as proton donor. Asp229 serves as the nucleophile, stabilizing the intermediate and Asp328 has an important role in substrate binding. Moreover, the two conserved histidine residues, His140 and His327, are involved in substrate binding and transition state stabilization (Nakamura *et al.*, 1993; Uitdehaag *et al.*, 1999b). A third histidine, present only in some  $\alpha$ -amylases and CGTase (His233, CGTase numbering), is involved in substrate binding and acts as a calcium-ligand with its carbonyl oxygen (Lawson *et al.*, 1994; Strokopytov *et al.*, 1996).

### 1.3 Physiological roles of CGTase

Breakdown of starch or other glucan is initiated by extracellular starch-degrading enzyme such as amylase (a hydrolase) or CGTase (a transferase), depending upon the species of bacteria (Takaha and Smith, 1999). Maltooligosaccharides (MOS) or CDs are then imported by specific transporter proteins (Figure 1.4) into the cells. A specific CD uptake system has been reported (Fiedler *et al.*, 1996). Inside the cells, a cytoplasmic cyclodextrinase (CDase) hydrolyzes CD into MOS (Kaulpiboon and Pongsawasdi, 2005) which is further metabolized by a phosphorylase-dependent pathway found in many bacteria. A  $4\alpha$ GTase (type II, called amylomaltase) helps catalyze disproportionation reaction to create larger MOS and release glucose for metabolic use. The evolution of such a CD synthesis and uptake mechanism provides a competitive advantage over other bacteria which do not have CGTase enzyme.



Figure 1.3 Structure of CGTase from alkalophilic *Bacillus* sp. 1011 (PDB number 1PAM). Purple color represents domain A-B; blue color, domain C; brown color, domain D; and green color, domain E.

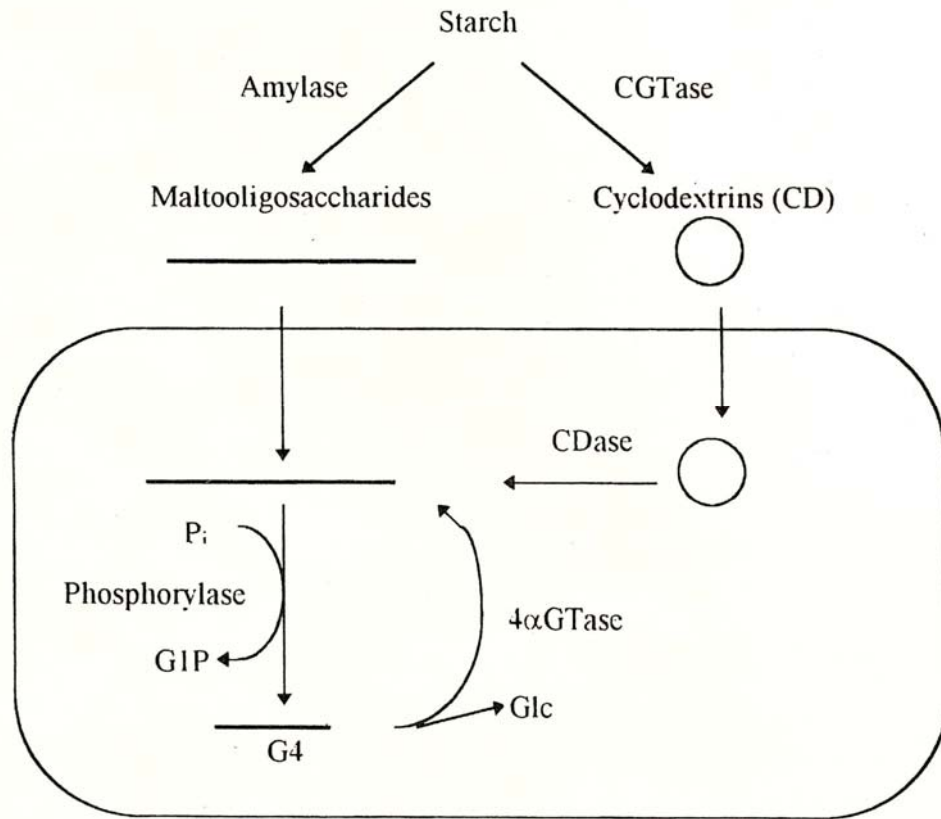


Figure 1.4 Roles of CGTase in glucan utilization by bacteria (Takaha and Smith, 1999)

#### 1.4 Application of CGTase

CGTase presently known as the only one glycosyltransferase used as industrial enzyme. Mostly, CGTase is used for synthesis of cyclodextrins which are widely required as stabilizer or solubilizer in various types of industry (see section 1.5). In addition, CGTase is presently used in the production of oligosaccharides and glucosides. Immobilized CGTase is used in the synthesis of MOS or coupling sugar, an anticariogenic sweetener, from starch hydrolysate and sucrose. The amount of this sugar produced is 5,000 tons/year in Japan (Buchholz *et al.*, 2005). In the field of useful flavonoid, stevioside glucoside, a sweetener with improved water solubility and less better taste, was produced via transglucosylation activity of CGTase and was commercially available (Pongsawasdi, 2008).

#### 1.5 Cyclodextrins (CD)

Cyclodextrins (Schardinger dextrans, Cycloamylose, Cyclomaltose or Cycloglucans) are the oligomers of anhydroglucose units join to form a ring structure with  $\alpha$ -1,4 glycosidic bonds. The main CDs synthesized naturally by the cyclodextrin glycosyltransferase (CGTase) are composed of 6, 7 and 8 glucose units called  $\alpha$ -(alpha) or CD6,  $\beta$ -(beta) or CD7 and  $\gamma$ -(gamma) cyclodextrin or CD8 (Figure 1.5) (Pulley and French, 1961). They have different physical properties as summarized in Table 1.2 (Saenger, 1982; Szejtli, T. 1988). This molecule shows a hydrophilic outside, thus dissolves in water, and an apolar cavity, which provides a hydrophobic matrix, enabling cyclodextrins to form "inclusion complexes" with appropriate hydrophobic "guest" molecules (Figure 1.6). Result of the complexation between cyclodextrins and guests includes alteration of the solubility of the guest compound, stabilization against the effects of light, heat, and oxidation, masking of unwanted physiological effects, reduction of volatility, and others (van der Veen, 2000) (Table 1.3). The applications of cyclodextrins have been increased rapidly in food, cosmetics, pharmaceutical, agrochemical, and plastic industries.

#### 1.6 CGTase from *Paenibacillus* sp. RB01

A thermotolerant *Paenibacillus* sp. RB01 was isolated from hot spring area of Ratchaburi province, Thailand (Tesana, 2001). The bacteria produced CGTase at temperature range of 30-45 °C.

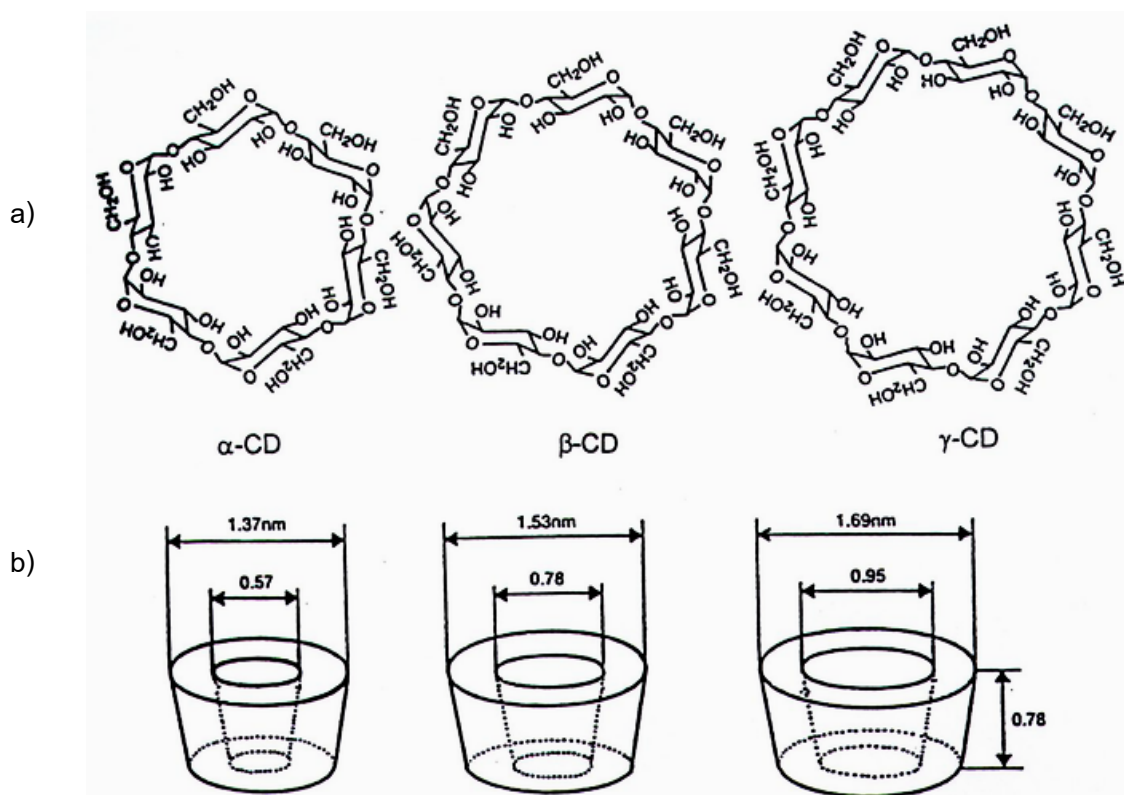


Figure 1.5 (a) Chemical structure of three kinds of CDs  
(b) The molecular dimension structure of CDs (Szejtli, 1990)

Table 1.2 Approximate geometric dimensions and properties of  $\alpha$ -,  $\beta$ -, and  $\gamma$ -CD molecules (Szejtli, 1998)

	$\alpha$ -CD	$\beta$ -CD	$\gamma$ -CD
Number of glucopyranose units	6	7	8
Molecular weight (g/mole)	972	1,135	1,297
Solubility in water at 25°C (%w/v)	14.5	1.85	23.2
Outer diameter (°A)	14.6	15.4	17.5
Inner diameter (°A)	4.7-5.3	6.0-6.5	7.5-8.3
Height of torus (°A <sup>3</sup> )	7.9	7.9	7.9
Approx. cavity volume 1 mol CD (ml)	174	262	427

Table 1.3 Possible effects of the formation of inclusion complexes on properties of guest molecules (van der Veen, 2000)

Stabilization of light- or oxygen-sensitive compounds
Stabilization of volatile compounds
Alteration of chemical reactivity
Improvement of solubility
Improvement of smell and taste
Modification of liquid compounds to powders

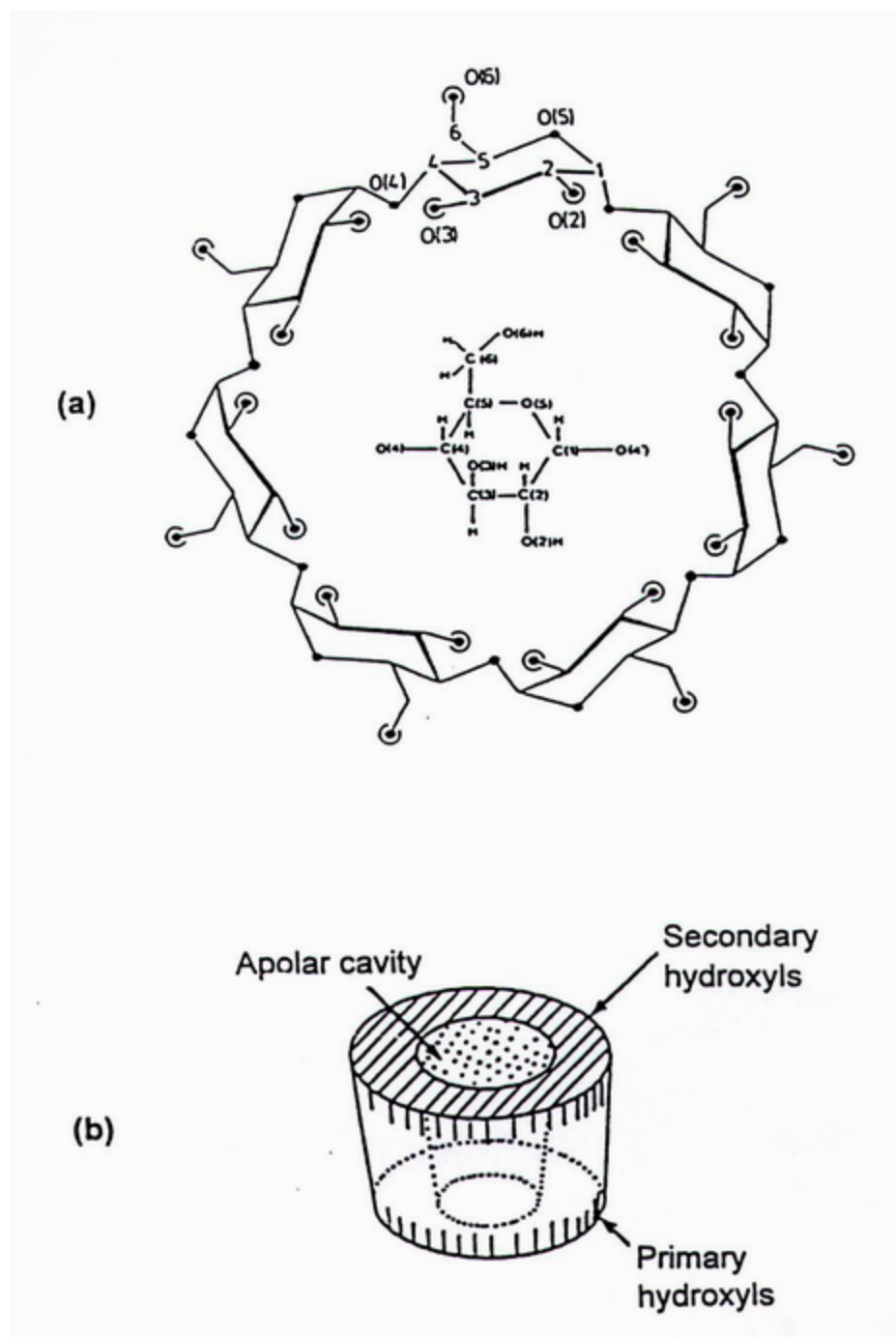


Figure 1.6 Structure of  $\beta$ -cyclodextrin (Bender, 1986; Szejtli, 1990)

(a) Chemical structure; ● = oxygen atoms, ○ = hydroxyl groups

(b) Functional structure scheme

It can grow best at 37°C, but exerted highest CGTase activity at 40°C. The enzyme was purified and biochemically characterized (Yenpetch, 2002). Optimum pH and temperature of the enzyme were 6.0 and 55°C, while the pH and temperature stability were 7.0 and 40°C, respectively. This CGTase showed a single band on SDS-PAGE with the molecular weight about 65 kDa, while on native PAGE the enzyme showed one major with two minor protein bands which were corresponded to bands obtained from dextrinizing activity. In addition, the analysis by IEF-PAGE in which the enzyme showed 3 protein bands supports that this enzyme had the isoforms. These results suggest the existence of 3 isoforms of the same size of this CGTase. However, they showed small difference in net charge as evidenced by their closed relative mobilities on native PAGE and IEF-PAGE.

The CGTase enzyme from *Paenibacillus* sp. A11 which was isolated from South-East Asian soil (Pongsawasdi and Yagisawa, 1988) was purified and characterized. The isoform existence of this enzyme was proved, 3-4 isoforms with different pI values but the same size (72 kDa) were reported. Preparative cell electrophoresis was developed for isoform preparation (Kaskangam, 1998). The existence of CGTase isoforms was also reported by other research group (Table 1.4), the pI values of those reported isoforms were slightly different, usually within 0.1-0.2 pH units. The isoforms of some bacteria e.g. *Bacillus* INMIA (Abelyan *et al.*, 1994) had different size. Some studies suggested that the amino acid compositions among isoforms were shown to be different e.g. *Bacillus circulans* E192 (Bovetto *et al.*, 1992)

Previous study by our research group suggests that the cause of isoform formation was by post-translational modification, not by the existence of multiple genes for CGTase from *Paenibacillus* sp. A11 (Prasong, 2002). Phosphorylation, glycosylation and disulfide bond formation were proved not to be the cause. While modification of carboxyl residues resulted in the change of electrophoretic mobility of the isoforms, the deamidation hypothesis is then raised. However, not much more information is known due to difficulty in isoform separation and the small amounts obtained.



Table 1.4 Isoform formation and pI values of CGTases from different CGTase-producing bacteria.

Bacteria	Isoform formation and pI value	Molecular weight	Reference
<i>Alkalophilic Bacillus</i> ATCC 21783	6 isoforms with pI range of 4.75-4.99	72 kDa	(Mattsson <i>et al.</i> , 1990)
<i>Bacillus circulans</i> E192	2 isoforms with pI 6.7 and 6.9	78 kDa	(Bovetto <i>et al.</i> , 1992)
<i>Bacillus circulans</i> 251	More than 7 isoforms with pI 4.78-5.22	75 kDa	(Lawson <i>et al.</i> , 1994)
<i>Bacillus circulans</i> A11	A few isoforms with pI 4.4-4.9	72 kDa	(Rojtinnakorn <i>et al.</i> , 2001)
<i>Bacillus</i> INMIA-T6, -T42, -A7/1	Each strain contained 2, 4 and 2 isoforms (no reported pI values), respectively.	38, 35 and 44 kDa respectively	(Abelyan <i>et al.</i> , 1994)
<i>Bacillus</i> sp. 1070	2 isoforms with pI 5.1 and 5.3	≅ 70 kDa	(Volkova <i>et al.</i> , 2001)
<i>Thermoanaerobacterium thermosulfurigenes</i> EM1	1 major isoform with pI 5.0 and 3 minor isoforms with pI 4.3, 4.4, and 4.6.	68 kDa	(Wind <i>et al.</i> , 1995)

## 1.7 Deamidation hypothesis on peptides and proteins

Hypothesis of deamidation was proposed since 1966 by Robinson (Robinson *et al.*, 1970) that deamidation is a major source of spontaneous protein damage such as degradation or aging of proteins. Deamidation is one of many common mechanisms on post-translational modification of protein: chain cleavage, acetylation, methylation, oxidation, glycosylation, and phosphorylation. The deamidation reaction can occur both enzymatically and non-enzymatically, by changing the Asn to Asp or Gln to Glu residue resulting to the change of net charge and possibly migration of a polypeptide in a gel matrix (Webb, 1964). The deamidation of Gln proceeds both enzymatically and nonenzymatically in physiological systems, while only the nonenzymatic deamidation of Asn has been reported. The Asn deamidation occurs much more rapidly than that of Gln (up to ten times faster) because the formation of a six-membered cyclic amide (Figure 1.7) is entropically less favorable (Bischoff and Kolbe, 1994). Labile residues of Asn/Gln are prone to deamidation. Deamidation may occur via two different pathways depending on the pH of the solution (Li *et al.*, 2008). In an acidic solution ( $\text{pH} < 5$ ), the acid-catalyzed pathway, where direct hydrolysis of amide side-chain of Asn results in Asp as the only product. At  $\text{pH} > 5$ , deamidation primarily occurs via a base-catalyzed pathway, in which Asn is converted to a succinimide intermediate which subsequently hydrolyzes to generate a mixture of isoAsp-Xaa and Asp-Xaa (Xaa = aminoacid) linkages in a typical ratio of 2:1 to 3:1 (Figure 1.7). This reaction is reversible in aqueous solution. A small amount of direct hydrolysis may also occur at  $\text{pH} > 5$  (Aswad *et al.*, 2000). Similarly, Gln deamidation proceeds through a glutarimide, but, since this reaction is relatively slow, direct hydrolysis is more significant.

Between 1967 and 1974, it was discovered that deamidation occurs *in vivo* and that genetic control of deamidation provides *in vivo* deamidation rates over a very wide physiologically relevant range. *In vitro* deamidation was later shown to occur resulting in instability and change in biological activity of several proteins (Solstad *et al.*, 2003; Zomber *et al.*, 2005). Moreover, in addition to protein sequence, the rate of deamidation is also determined by the protein secondary and tertiary structures because the necessary flexibility for the formation of the cyclic intermediate may be limited in proteins (Bischoff and

Kolbe, 1994). Other factor such as pH, temperature, ionic strength, buffer ions, protein turnover, and other solution properties can also influence deamidation rate (Li *et al.*, 2008).

### 1.7.1 Effect of deamidation on proteins/enzymes

Deamidation hypothesis has been supported by studies in several proteins or enzymes showing that non-enzymatic deamidation spontaneously occurred resulting in multiple molecular forms with changes in function, as seen in the following examples:

<u>Effect of deamidation on the protein/enzyme</u>	<u>Example of protein/enzyme and reference</u>
1. Conformation change and catalytic efficiency	human phenylalanine hydroxylase (Carvalho <i>et al.</i> , 2003)
2. Turnover rate	rat kidney cytochrome c (Flatmark and Sletten, 1968), rabbit muscle aldolase (Koida <i>et al.</i> , 1969)
3. Conformation change and biological activity	Cow heart muscle cytochrome c (Flatmark, 1966)
4. Apoptosis regulation	Bcl-x <sub>L</sub> (Deverman, 2002)
5. Reduction in cytotoxicity	Protective antigen from <i>Bacillus anthracis</i> (Zomber <i>et al.</i> , 2005)

### 1.7.2 Effect of protein structure and other factors on nonenzymatic deamidation rate

#### 1.7.2.1 Amino acid sequence and higher-order structures

One of the factors influenced deamidation rate is the primary structure of the proteins, by the nearest neighbor effect (Robinson and Robinson, 2001). Robinson and Rudd (1974) earlier reported that bulky residues in the n-1 position (N-terminal side of Asn) decrease the rate of deamidation. However, later studies showed that the importance of amino acid at n-1 position was less than at n+1 position. The series of synthetic pentapeptides with the sequence VSNXV and VXNSV, where X is one of 10 different amino acids, were investigated at neutral, alkaline and acid pH values (Tyler-Cross and Schirch,

1991). They found that at the position n+1 residue (C-terminal side of Asn), the degree of side chain branching at this position affected the rate of deamidation while charge did not show much effect. Gly or Ser greatly accelerates Asn deamidation. While Ser and, to a lesser extent, Thr and Lys at the n-1 position may also facilitate Asn deamidation. The small side chains of Gly and Ser allow extensive conformational changes, while amino acids with branched, bulky, hydrophobic side chains reduce the conformational flexibility necessary for the intermediate formation. In addition, intramolecular disulfide bonds closed to Asn/Gln also reduce deamidation rate (Bischoff and Kolbe, 1994). Furthermore, the structural change induced by one deamidation site may further influence deamidation rates at other sites. And higher-order (secondary and tertiary) structures also take part on determining the occurrence of deamidation since hydrogen bonding and other types of interaction may result in conformational restrictions of the target residues.

#### **1.7.2.2 Other factors**

Usually it is stated that pH has a marked effect to deamidation rates, while buffer effects have been reported to be both important and not important (Robinson and Robinson, 2001). In acidic pH the peptide might not play a role in the rate of deamidation. While alkaline pH increases deamidation rate, the effect are probably the result of increased general base catalysis by the buffer. It is also found that ionic strength and temperature have also an effect on deamidation rate. Since the ionic strength significantly affects protein conformation, in neutral or alkaline solution, the effect is through a succinimide intermediate, regardless of the sequence of the peptide and buffer (Tyler-Cross and Schirch, 1991).

#### **1.7.3 Prediction of deamidation rate**

Recently a computational method had been designed by Robinson and Robinson, 2001 to estimate the probability of deamidation within a folded protein. This calculation method, based on the sequence-controlled deamidation rates of Asn model peptides and simple aspects of the Asn 3D environment in proteins, permits a useful estimation of the

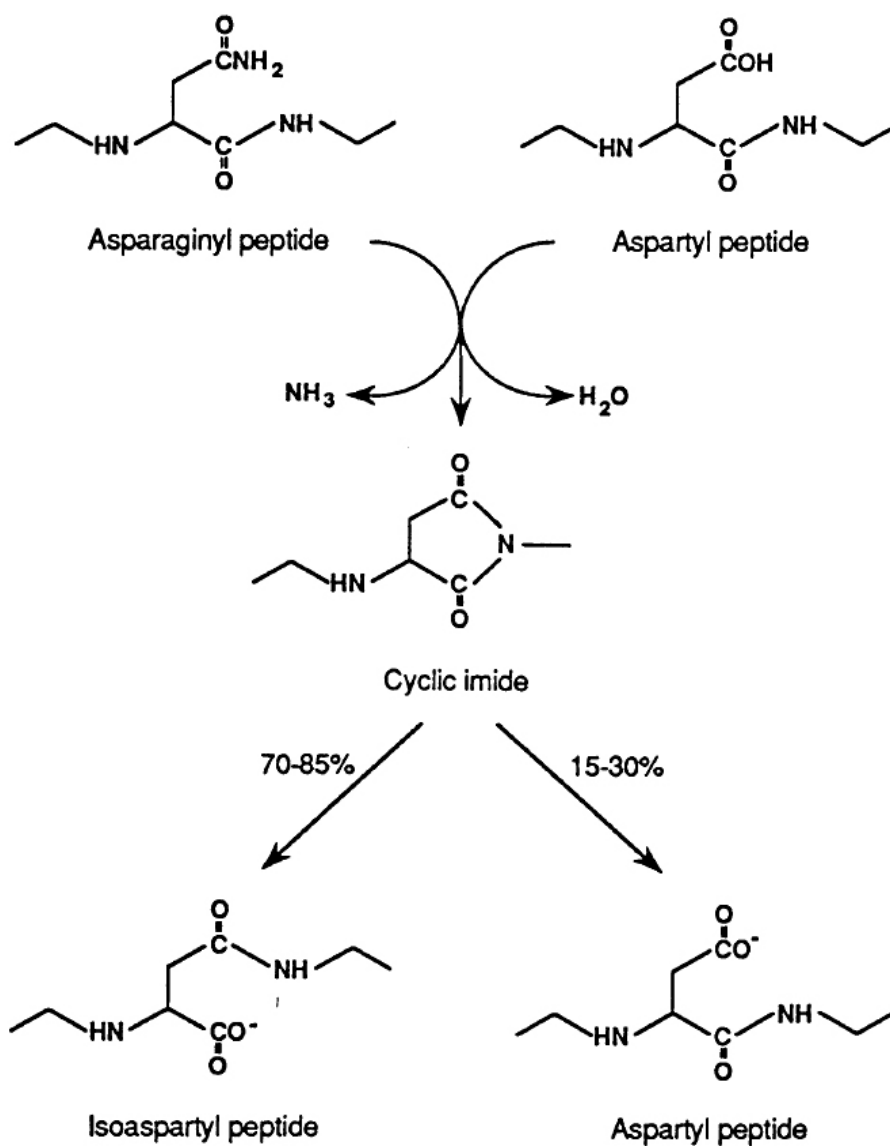


Figure 1.7 Mechanism of isoAsp formation at Asn and Asp sites. The  $\alpha$ -amino of the residue  $n+1$  (C-side) flanking to the Asn or Asp makes a nucleophilic attack on the Asx side chain to form a cyclic imide (succinimide) intermediate. This hydrolyzes to a mixture of isoAsp and Asp in a ratio that ranges from 60:40 to 85:15 (Capasso, *et al.*, 1989).

instability with respect to deamidation of Asn in proteins. The Asn deamidation in proteins is, on average, determined approximately 60% by primary structure and 40% by 3D structure. These percentages apply to 3D effects that diminish deamidation rates below those of primary structure alone. In 2 cases out of 36—about 6% of deamidating Asn and 1% of all Asn examined here—3D structure is reported to actually accelerate deamidation. These calculations demonstrate that most deamidation rates of Asn residues in proteins are approximately equal to the sequence-controlled rates modulated through slowing by 3D structure.

#### Deamidation coefficient (CD) and deamidation index (ID)

The deamidation coefficient value (CD value) and the deamidation index (ID value) have been proposed to be used to compare deamidation rate of each Asn and of all Asn in the protein. To obtain these values, 3D-structure of the protein has to be put into the program available at [www.deamidation.org](http://www.deamidation.org). For the deamidation half-time ( $T_{1/2}$ ) of each Asn, of which primary sequence is significantly governed, the theoretical values based on synthetic peptides have been determined and used by several research groups. The half-time ( $t_{1/2}$ ) of several synthetic peptides with different sequence were available at [www.deamidation.org](http://www.deamidation.org).

#### Calculation of CD and ID values

$CD = (\text{deamidation half-time})/100$  in days for a single amide.  $ID = [(\sum CD_n)^{-1}]^{-1}$ , where  $CD_n$  is the  $n^{\text{th}}$  amide residue. ID is therefore the single-residue deamidation half-time/100 for the whole protein molecule with all amide residues considered. For example, that the three Asn in a particular protein have  $CD1 = 1.0$ ,  $CD2 = 6.0$ , and  $CD3 = 100$ , then  $ID = 1/(1 + 1/6 + 1/100) = 0.85$ . Thus, the fastest amide in this protein would then have a deamidation half-time of 100 days, while a net half-time deamidation of the protein with all three Asn considered would require 85 days.

Current values for CD and ID for asparagines that have been experimentally measured or computed in more than 18,000 peptides and proteins are available at [www.deamidation.org](http://www.deamidation.org). Computation of values can be obtained with the proteins which three-dimensional structures are available.

#### 1.7.4 Examples of deamidation in particular proteins

##### 1.7.4.1 Cow heart muscle cytochrome c

In 1966, Flatmark reported that cow heart cytochrome c deamidates sequentially from molecular form I to II to III. The deamidation half-times of I and II in 37°C, borate buffer pH 7.4 were 12 days and 5 days, respectively. These deamidations increase in rate with increasing ionic strength, pH, and temperature. The amino acid sequence AlaThrAsn(103)GluCOOH at the C-terminus end of cytochrome c was identified with conversion of I to II. Using isoelectric focusing, Flatmark and Vesterberg (1966) resolved cytochrome II into two components with one component present in much greater amount than the other. Isoelectric focusing showed a 0.23 pH unit change in isoelectric point per deamidation. Flatmark (1967) found that cytochromes I, II, and III showed different spectroscopic optical rotation properties and that biological activity decreases with successive deamidations.

##### 1.7.4.2 Human Rhinovirus-14 3C Protease

Cox *et al.*, 1999, reported that the purified 3C protein by isoelectric focusing showed differently charged 3C isoforms that had isoelectric points (pI) of 8.3 (55%) and 9.0 (45%). The protein with pI 8.3 was the deamidated form of 3C, and it displayed 10-fold reduced cleavage activity relative to the original 3C protease sample. Peptide mapping followed by sequence analysis revealed that a single asparagine, Asn-164, was deamidated to aspartic acid in the pI 8.3 isoform. They suggested that 3C protein deamidation plays a role in the regulation of its enzymatic activity.

##### 1.7.4.3 Recombinant human phenylalanine hydroxylase (Carvalho *et al.*, 2003)

The enzyme was shown to exist as 4 to 5 molecular forms (differing in pI about 0.1 pH unit, with the same molecular mass) as a result of nonenzymatic deamidation of labile Asn residues. Microheterogeneity pattern was dependent on induction time with IPTG, and the nondeamidated form was the newly synthesized and most native form of the enzyme. Asn 32, followed by a Gly, as well as Asn 28 and Asn 30 in a loop region of the N-terminal

part are among the susceptible residues verified. Deamidation at Asn 32 resulted in a 1.7 folds increase in catalytic efficiency of the enzyme.

### 1.8 The objective of this study

As the existence of isoforms of CGTase from *Paenibacillus* sp. RB01 has been reported but the cause of isoform formation is still unknown. On the basis of preliminary data on CGTase and the works in deamidation of several proteins/enzyme as reviewed, we here propose to examine the effect of deamidation of Asn residues of CGTase from *Paenibacillus* sp. strain RB01 on microheterogeneity and functional properties of the enzyme.

#### Objectives

1. To express CGTase gene from a thermotolerant *Paenibacillus* sp. RB01 in *E. coli*.
2. To predict deamidation rates of Asn residues in CGTase and to perform site-directed mutagenesis at selected labile Asn residues.
3. To analyze isoform pattern and functional properties of native, cloned and mutated CGTases.
4. To prove cause of isoform formation of CGTase by detection of *iso*-Asp in wild type and cloned CGTases.



## CHAPTER II

### MATERIALS AND METHODS

#### 2.1 Equipments

Autoclave: Model H-88LL, Kokusan Ensinki Co., Ltd., Japan

Autopipette: Pipetman, Gilson, France

Centrifuge, refrigerated centrifuge: Model J2-21, Beckman Instrument  
Inc., U.S.A.

Electrophoresis unit:

- Mini protein, Bio-Rad, U.S.A. and
- Submarine agarose gel electrophoresis unit, Bio-Rad, U.S.A.
- Mini IEF-CELL Model 111, Bio-Rad, USA

FPLC AKLA Amersham Pharmacia Biotech unit

Column: Amersham Biosciences Mono Q<sup>TM</sup> HR 5/5 and Mono P<sup>TM</sup> HR 5/5

Detector: UPC-900

Pump: P-920

Fraction collector: Frac-900

Gene Pulser<sup>R</sup>/*E. coli* Pulser<sup>TM</sup> Cuvettes: Bio-Rad, U.S.A.

Gel Document: SYNGEND, England

Gel support film for polyacrylamide, Bio-Rad, U.S.A.

HPAEC DX-600: Dionex Corp., Sunnydale, USA

Column: Carbopac<sup>TM</sup> PA-100 4 x 250 mm

Pulsed amperometry detector:

Autosample: DIONEX AS40

Column oven: DIONEX ICS-3000 SP

HPLC Shimadzu unit

Column: C<sub>18</sub> intersil<sup>®</sup> ODS-3, 4.5 x 250 mm

UV Detector: Shimadzu SPD-20A

Pump: Shimadzu LC-20AT

Autosampler: Shimadzu SIL-20A

Column oven: Shimadzu CTO-10AS

Incubator, waterbath: Model M20S, Lauda, Germany and BioChiller  
2000, FOTODYNE Inc., U.S.A. and ISOTEMP 210, Fisher Scientific, U.S.A.

Incubator shaker: Innova<sup>TM</sup> 4080, New Brunswick Scientific, U.S.A.

Light box: 2859 SHANDON, Shandon Scientific Co., Ltd., England

Laminar flow: HT123, ISSCO, U.S.A.

Magnetic stirrer: Model Fisherbrand, Fisher Scientific, U.S.A.

Membrane filter: cellulose nitrate, pore size 0.45  $\mu\text{m}$ , Whatman, England

Microcentrifuge: Model 5417C, Eppendorf, Germany

Microwave oven: Model TRX1500, Turbora International Co., Ltd., Korea

Orbital incubator: Model 1H-100, Gallenkamp, England

Orbital shaker: Orbital shaker 03, Stuart Scientific, England

pH meter: Model PHM95, Radiometer Copenhagen, Denmark

Power supply: Model POWER PAC 300, Bio-Rad, U.S.A.

Shaking waterbath: Model G-76, New Brunswick Scientific Co., Inc., U.S.A.

Spectrophotometer: DU Series 650, Beckman, U.S.A.

Ultrafilter: Suprec<sup>Tm-01, Tm-02</sup>, pore size 0.20  $\mu\text{m}$  and 0.22  $\mu\text{m}$ ,  
Takara Shuzo Co, Ltd., Japan

Vortex: Model K-550-GE, Scientific Industries, Inc, U.S.A.

## 2.2 Chemicals

Acetonitrile: Labscan, Thailand

Acrylamide: Merck, Germany

Agar: Merck, Germany

Agarose: SEKEM LE Agarose, FMC Bioproducts, U.S.A.

Ammonium persulphate: Sigma, U.S.A.

Ammonium sulphate: Carlo Erba Reagent, Italy

Ampicillin: Sigma, U.S.A.

Ampholyte 46 : Pharmacia, Sweden

BIS-TRIS, minimum 98% titration: Sigma, U.S.A

Bovine serum albumin: Sigma, U.S.A.

Bromphenol blue: Merck, Germany

Casein hydrolysate: Merck, Germany

Chloroform: BDH, England

Coomassie brilliant blue R-250: Sigma, U.S.A.

Copper sulfate: Merck, Germany

di-Potassium hydrogen phosphate anhydrous: Carlo Erba Reagenti, Italy

di-Sodium ethylene diamine tetra acetic acid: M&B, England

100 base pair DNA ladder, Promega Co., U.S.A.

dNTP: Stratagene, U.S.A.

Endoproteinase Asp-N, sequencing grade, Wako, Japan

Ethidium bromide: Sigma, U.S.A.

Ethyl alcohol absolute: Carlo Erba Reagenti, Italy

Ethylene diamine tetraacetic acid (EDTA): Merck, Germany

Ficoll type 400: Sigma, U.S.A.

Glacial acetic acid: Carlo Erba Reagenti, Italy

Glucose: BDH, England

Glycerol: Merck, Germany

Glycine: Sigma, U.S.A.

Hydrochloric acid: Carlo Erba Reagenti, Italy

8-Hydroxyquinolin: Merck, Germany

Isoamyl alcohol: Merck, Germany

ISOQUANT Isoaspartate detection kit: Promega, USA

Isopropanol: Merck, Germany

Isopropylthio- $\beta$ -D-galactoside (IPTG): Sigma, U.S.A.

Magnesium sulphate: BDH, England

Maltose: BDH, England

2- Mercaptoethanol: Fluka, Switzerland

Methylalcohol: Merck, Germany

*N,N*-Dimethyl-formamide: Fluka, Switzerland

*N,N'*-Methylene-bis-acrylamide: Sigma, U.S.A.

*N,N,N',N'*-Tetramethyl-1, 2-diaminoethane (TEMED): Carlo Erba Reagent, Italy

Peptone from casein pancreatically digested: Merck, Germany

Phenol: BDH, England  
Phenylmethylsulfonyl fluoride (PMSF): Sigma, U.S.A.  
Plasmid Mini Kit: Bio-Rad, U.S.A.  
Polybuffer<sup>®</sup>74: Pharmacia, Sweden  
Potassium acetate: Merck, Germany  
Potassium chloride: Merck, Germany  
Potassium hydroxide: Carlo Erba Reagenti, Italy  
Potassium phosphate monobasic: Carlo Erba Reagenti, Italy  
QIA quick Gel Extraction Kit: QIAGEN, Germany  
Riboflavin (Lactoflavine); BDH, England  
5-Sulfosalicylic acid: Mallin Krodl, USA  
Sodium acetate: Merck, Germany  
Sodium carbonate anhydrous: Carlo Erba Reagenti, Italy  
Sodium chloride: Carlo Erba Reagenti, Italy  
Sodium citrate: Carlo Erba Reagenti, Italy  
Sodium dodecyl sulfate: Sigma, U.S.A.  
Sodium hydroxide: Merck, Germany  
Soluble starch: Sigma, U.S.A.  
Standard protein marker: Amersham Pharmacia Biotech Inc., U.S.A.  
Sucrose: Sigma, U.S.A.  
Tris (hydroxymethyl)-aminomethane: Carlo Erba Reagenti, Italy  
Yeast extract: Scharlau microbiology, Spain

### 2.3 Enzymes, Restriction enzymes and Bacterial stains

Amyloglucosidase from *Aspergillus niger*: Fluka, Switzerland.  
*E. coli* BL21 (DE3): Novagen, Germany  
*Paenibacillus sp.* RB01 (screened from Ratchburi province, Thailand: Tesana, 2001)  
*PfuTurbo*<sup>®</sup> DNA polymerase: Promega, U.S.A.  
Plasmid pET19b: Novagen, Germany  
Restriction enzymes: GIBCOBRL, U.S.A., Amersham Pharmacia Biotech Inc., U.S.A.,

New England BioLabs Inc., U.S.A. and Zibenzyme, Sweden.

RNaseA: Sigma, U.S.A.

T<sub>4</sub> DNA ligase: New England BioLabs, Inc, U.S.A.

## 2.4 Cloning for overproduction of CGTase

### 2.4.1 Cultivation and genomic DNA extraction of *Paenibacillus* sp. RB01

The thermotolerant *Paenibacillus* sp. RB01 was cultivated in medium I (beef extract 0.5 g%, peptone 1.0 g%, NaCl 0.2 g%, yeast extract 0.2 g%, pH 7.2) at 40°C, with rotary shaking at 250 rpm overnight. The cells were collected by centrifugation at 4°C with speed 5,000 rpm for 15 minutes. Then genomic DNA extraction was performed. The cells were washed with TE buffer (10 mM Tris-HCl and 1 mM EDTA, pH 8.0) then centrifuged and resuspended with 10 ml of TE buffer in the clean tube. After that, the cells were frozen at -20°C for 10 minutes then thawed at 65°C. TE buffer 30 ml was added (total volume should be 40 ml), followed by 7 ml of 10% SDS and 200 µl proteinase K. The sample was gently mixed and then incubated at 37°C for 1 hour. To the reaction mixture, 7.2 ml of 5 M NaCl was added and mixed, followed by the addition of 5.7 ml of CTAB solution. The mixture was then incubated at 65°C for 20 minutes. Phenol-chloroform extraction was performed by addition of an equal volume of phenol-chloroform to the mixture, mixed thoroughly and centrifuged at 12,000 rpm for 10 minutes. The upper solution was collected and extracted again with equal volume of chloroform solution. The upper solution was collected. After that, 2 volume of ethanol or 0.6 volume of isopropanol was added. Genomic DNA was collected, washed with 70% ethanol and resuspended in TE buffer. Amount of genomic DNA was quantitated by measuring absorbance at 260 nm.

$$\text{Concentration of original DNA solution in } \mu\text{g/ml} = \text{Abs} \times \text{dilution factor} \times 50 \mu\text{g/ml}$$

The purity of this DNA was checked by the ratio of spectrophotometry  $A_{260/280}$  values and by 1% agarose gel electrophoresis.

### 2.4.2 Agarose gel electrophoresis

Electrophoresis through agarose is the standard method used to separate, identify, and purify DNA fragments. The 1% of agarose powder was added to 100 ml electrophoresis buffer (89 mM Tris-HCl, 8.9 mM boric acid and 2.5 mM EDTA, pH 8.0) in an Erlenmeyer flask and heated until complete solubilization in a microwave oven. The agarose solution was cooled down below to 60°C until all air bubbles were completely eliminated. The solution was then poured into an electrophoresis mould. After the gel was completely set, the comb and seal of the mould was carefully removed. When ready, the DNA samples were mixed with one-fifth volume of the desired gel-loading buffer (0.025% bromphenol blue, 40% ficoll 400 and 0.5% SDS) and slowly loaded the mixture into an appropriate percentage of agarose gel. Electrophoresis had been performed at constant voltage of 10 volt/cm until the faster migration dye (bromphenol blue) migrated to approximately 1 cm from the bottom of the gel. The gel was stained with 2.5 µg/ml ethidium bromide solution for 5 minutes and destained to remove unbound ethidium bromide in distilled water for 10 minutes. DNA fragments on agarose gel were visualized under a long wavelength UV light and photographed through gel document. The molecular weight of DNA sample was compared with the relative mobility of the standard 1 kDa DNA fragment.

### 2.4.3 Amplification of CGTase gene (*cgt*) using PCR technique

The extracted genomic DNA from *Paenibacillus* sp. RB01 was used as template to amplify the *cgt*. The forward and reverse primers were designed from the start to stop codons and contained a restriction site of *Nco* I and *Xho* I, respectively as shown below.

**Forward Primer:** CATGCCATGGAAAGATTTATGAAACTAACAGCCGTA

**Reverse Primer:** CCGCTCGAGTTAAGGCTGCCAGTTCACATTCATC

\* Note: The bold letters are start and stop codon respectively. The underlined letters were designed for the restriction site of *Nco* I and *Xho* I.

PCR was performed in a 25 µl reaction mixture containing 50 ng of chromosomal DNA from *Paenibacillus* sp. RB01, 1x *Pfu* buffer with MgSO<sub>4</sub>, 0.2 mM each dNTPs, 10 pmole of each primer and 1U of *Pfu* DNA polymerase. PCR condition consisted of predenaturation at 94°C for 10 minutes, denaturation at 94°C for 1 minute, annealing at

45°C for 1 minute, extension at 72°C for 5 minutes and final extension at 72°C for 10 minutes. The cycle was repeated for 20 times. PCR products were detected by 1% agarose gel electrophoresis. The desired DNA band of *cgt* was extracted from agarose gel by the gel extraction kit (QIAGEN).

#### 2.4.4 Restriction enzyme digestion

The PCR product and plasmid vector pET19b were separately double digested with *Nco* I and *Xho* I in reaction mixture 20 µl containing 1X NEB buffer, 1 µg BSA, 10 U of *Nco* I, 20 U of *Xho* I and 50 µg of DNA template. The reaction was performed at 37°C for 16 hours.

#### 2.4.5 Ligation of PCR product with vector pET19b

The purified digested PCR product and vector pET19b were then ligated at 16°C overnight in the 10 µl reaction mixture that composed of 10X ligation buffer, 5 U of T4 DNA ligase, 30 µg of PCR product and 50 µg of pET19b.

#### 2.4.6 Plasmid transformation

The recombinant plasmids from section 2.4.4 were introduced into a competent of *E. coli* strain BL21 (DE3) by electroporation. In the electroporation step, 0.2 cm cuvettes and sliding cuvette holder were chilled on ice. The Gene Pulser apparatus was set to the 25 µF capacitor, 2.5 kV, and the pulse controller unit was set to 200Ω. Competent cells, which were prepared by the method of Sambrook (2001) (see Appendix 5), were gently thawed on ice. One to five microliter of recombinant plasmid from section 2.4.4 was mixed with 40 µl of the competent cells and then placed on ice for 1 minute. This mixture was transferred to a cold cuvette. The cuvette was applied one pulse at the above settings. Subsequently, one milliliter of LB medium was added immediately to the cuvette. The cells were quickly resuspended with a Pasteur pipette. Then the cell suspension was transferred to new tube and incubated at 37°C for 1 hour with shaking. Finally, this suspension was spread onto the LB agar plates containing 100 µg/ml ampicillin and 1% soluble starch. After incubation at 37°C for 16 hours, the clear zone forming colonies, which contained the recombinant plasmids, were replicated and iodine solution was poured over the original plate.

## 2.5 Colony selection and primary screening

### 2.5.1 Plasmid size screening

The colonies containing *cgt* that showed clear zone from the starch degradation reaction were picked and resuspended in 40  $\mu$ l of the size screening buffer 20  $\mu$ l of lysis buffer (0.05 mM Tris-HCl, pH 8.0 Lysozyme 1%(w/v), Heat Treated RNase A 0.1%(w/v), 50% (v/v) Glycerol) which was pre-warmed at 37°C for 10 minutes. Then, the solution was incubated at 40°C for 5 minutes. The viscous sample was centrifuged at 12,000 rpm for 10 minutes. To estimate the size of plasmid, the twenty microliters of the supernatant were loaded onto 1% agarose gel and compared with relative mobility of DNA markers.

### 2.5.2 Plasmid extraction

The recombinant *E. coli* BL21 (DE3) was grown in LB-medium (1% peptone, 0.5% NaCl and 0.5% yeast extract, pH 7.2) containing 100  $\mu$ g/ml ampicillin overnight at 37°C with rotary shaking. The cell culture was collected by centrifugation at 10,000 rpm for 5 minutes. The recombinant plasmid pET19b vector harboring *cgt* was extracted by QIAquick Plasmid Extraction kit (QIAGEN, Germany). The concentration of plasmid was determined by spectrophotometric method ( $A_{260/280}$ ) and agarose gel electrophoresis.

### 2.5.3 Nucleotide sequencing

About 50-100 ng of the extracted recombinant plasmid pET19b harboring *cgt* from section 2.5.2 was subjected to automated DNA sequence (Macrogen, Korea). The first sequencing was performed using primers of T7 promotor and T7 terminator which located at upstream of the 5'-terminus and downstream of 3'-terminus of the inserted *cgt*, respectively. The obtained DNA sequences were extended using primers pBT\_590\_F and pBT\_1480\_R which located in the middle of the gene. The sequences of both later primers were shown below. The sequence results were analyzed using GENETYX-WIN software.

pBT\_590\_F: 5' GCGGATACACCAACGATACC 3'

pBT\_1480\_R: 5' GCCGAGCACATCGTTATAGC 3'



## 2.6 Prediction of Asn deamidation rate and site-directed mutagenesis on labile Asn residues

### 2.6.1 Prediction of Asn deamidation rate

Deamidation rate means the relative rate of deamidation reaction from Asn/Gln residues to Asp/Glu residues in protein/enzyme. In this work, the Asn residues were considered because deamidation of Asn can occur with/without enzyme catalysis. Deamidation of Gln is similar to Asn, but, as a result of the longer deamidation half-times of Gln residues in peptides and proteins, little quantitative information about deamidation of Gln in proteins is, as yet, available (Robinson and Robinson, 2001). The rate of deamidation of CGTase from *Paenibacillus* sp. RB01 was predicted using the program from [www.deamidation.org](http://www.deamidation.org) based on the primary sequence and three dimensional structure of the enzyme, The Asn deamidation in proteins is determined approximately 60% by primary structure and 40% by 3D structure. The available 3D structure information of cyclodextrin glucanotransferase from alkalophilic *Bacillus* sp. 1011 (PDB number 1PAM) which shared 98% amino acid similarity with the CGTase from *Paenibacillus* sp. RB01 was feeded to the program and the coefficient of deamidation (CD value) of each Asn residue was predicted. The predicted half-life in days of the amide (Asn residue) at 37 °C, pH 7.4, 0.15 M Tris-HCl buffer is given by  $(100 \cdot CD)$ .

### 2.6.2 Selection of labile Asn residues

According to the CD values obtained, Asn residues were selected. The position to be mutated was classified into 4 groups;

1) Asn residues with low CD values: Asn336, Asn415, Asn326, Asn567 and Asn188 which has CD value of 1.004, 1.067, 1.347 and 1.902, respectively.

2) Asn residues with intermediate CD values: Asn370 and Asn620 which has CD values of 3.854 and 10.516, respectively.

3) Asn residues with high CD values: Asn427, Asn428 and Asn435 which had CD values of 53.416, 105.027 and 158.306, respectively.

4) Asn residues which are close to the active site: Asn263, Asn274 which has CD values 68.124 and 306.815, respectively.

## 2.7 Site-directed mutagenesis

Mutagenesis was carried out by PCR amplification using a pair of oligonucleotide with a desired point mutation as primers and the recombinant plasmid as a template. The PCR product was digested with *Dpn* I endonuclease (target sequence: 5'-GA<sub>CH<sub>3</sub></sub><sup>^</sup>TC-3') which specific for methylated as well as hemimethylated DNA. This enzyme is used to digest the parental DNA template to select for mutation-containing synthesized DNA. DNA isolated from almost all *E. coli* strains is dam methylated and therefore susceptible to *Dpn* I digestion. The nicked plasmid of the *Dpn* I-treated was then transformed into the host *E. coli* competent cells.

### 2.7.1 Single mutation

The recombinant plasmid pET19b containing *cgt* was extracted as described in section 2.5.2 to use as a template. The list of selected Asn residues and sequences of their mutagenesis primers are shown in Table 2.1. The primers were designed for substitution of Asn residue by Asp residue. PCR was performed in a 50  $\mu$ l reaction mixture containing 50-100 ng of the recombinant plasmid, 1x *Pfu* buffer with MgSO<sub>4</sub>, 20 each dNTPs, 10 pmole of each primer and 1 U of *Pfu* DNA polymerase. PCR condition consisted of predenaturation at 95°C for 5 minutes, denaturation at 95°C for 1 minute, annealing at 50/55°C for 1 minute, extension at 68°C for 8 minutes and final extension at 68°C for 16 minutes. The cycle was repeated for 12 times. Afterward, 30  $\mu$ l of PCR product was transferred to a new tube and incubated with 1 $\mu$ l (10 U) of *Dpn* I for 1 hour at 37°C. In the mean time, five  $\mu$ l from the rest of PCR tube was taken to run on agarose gel.

### 2.7.2 Double and triple mutation

The reaction was performed as same as single mutation except the template which a recombinant plasmid from single mutant was used for double mutation. The plasmid from the double mutant also used as a template of triple mutation experiment.

### 2.7.3 Transformation into *E. coli* BL21 (DE3)

The *Dpn* I digested PCR product from section 2.7.1 was prepared for transformation by gently mixed with competent *E. coli* BL21 (DE3) cell and incubated on

ice for 30 minutes. The transformation reaction was heated at 42°C for 45 seconds and then placed on ice for 2 minutes. The transformed reaction was added to 0.5 ml of LB broth which was preheated at 42°C and incubated at 37°C for 1 hour with shaking at 250 rpm. Finally, this transformed culture was spread onto the LB agar plate containing 100 µg/ml ampicillin and then incubated at 37°C for 16 hours. Cells containing the recombinant plasmids, which formed clear zone, were picked and the plasmids were further extracted. To confirm the mutation, the plasmids were extracted and checked their size by agarose gel electrophoresis as described in section 2.5.2 and 2.4.2. The point of mutation was further confirmed by nucleotide sequencing and blast with the parent *cgt*.

## 2.8 Purification of cyclodextrin glycosyltransferase

### 2.8.1 Bacterial cultivation

One colony of *E. coli* BL21(DE3) containing *cgt* gene in pET19b from agar plate was grown in 50 ml LB-medium supplemented with 100 µg/ml ampicillin, at 37°C with 250 rpm shaking overnight, then the culture was inoculated into 300 ml LB-medium containing 100 µg/ml ampicillin. Cell culture was grown at 37°C until the  $A_{600}$  was about 0.4-0.6 then the IPTG was added at the final concentration of 20 µM. The bacteria were continuously grown for 24 hours of cultivation. The cells were harvested by centrifugation at 8,000 g for 15 minutes at 4°C. The crude enzyme in the medium was collected for the next experiments.

### 2.8.2 Partial purification of CGTase

The crude enzyme from section 2.8.1 was partially purified by starch adsorption (Kato and Horikoshi, 1985, modified by Kuttiarcheewa, 1994). Corn starch was oven dried at 120°C for 30 minutes and cooled to room temperature. It was then gradually sprinkled into stirring crude CGTase broth to make 10 g% concentration. After 3 hours of continuous stirring at 4°C, the starch cake was collected by centrifugation at 5,000 rpm for 30 minutes and washed twice with TB (25 mM Tris-HCl, pH 8.5). The adsorbed CGTase was eluted from the starch cake with TB buffer containing 0.2 M maltose (2 x 125 ml for starting broth of 1 l), by stirring for 30 minutes. CGTase eluted was recovered

Table 2.1 List of selected asparagine residues and their primers for site-directed mutagenesis.

Asn position	CD value	Name	Sequence
Asn336	1.004	pRB336F pRB336R	GAGCGTTTCCACACCAGCGATGGCGACAGACGGAAGC GCTTCCGTCTGTGCCATCGCTGGTGTGGAACGCTC
Asn415	1.067	pRB415F pRB415R	CACAGGAGCGCTGGATCGACAACGATGTGATCATCCAG GATGATCACATCGTTGTCGATCCAGCGCTCCTGTG
Asn326	1.347	pRB326F pRB326R	GACCAGGTGACCTTCATCGACGATCATGACATGGAGCGT TTCC GGAACGCTCCATGTCATGATCGTCCGATGAAGGTCACCT GGTC
Asn567	1.703	pRB567F pRB567R	CTATGATATCAGAGTTGCCGACGCGCCGAGCAGCCAG CTGGCTGCTCCGGCTGCGTCGGCAACTCTGATATCATAG
Asn188	1.901	pRB188F pRB188R	GCACGGATTCTCCACCATTGAGGACGGCATTATAAAA ACCTGTAC GTACAGTTTTTATAAATGCCGTCCTCAATGGTGGAGAA ATCCGTGC
Asn370	3.854	pRB370F pRB370R	GTATATGTCTGGCGGGGATGATCCGGACAACCG CGGTTGTCCGGATCAICCCCGCCAGACATATAC
Asn620	10.516	pRB620F pRB620R	GCAACTGGGATCCGAACGACGCGATCGGCCCGATG CATCGGGCCGATCGCGTCGTTCCGATCCCAGTTGC
Asn427	53.416	pRB427F pRB427R	CTATGAACGCAAATTCGGCGATAACGTGGCCGTTGTTGC GCAACAACGGCCACGTTATCGCCGAATTTGCGTTCATAG
Asn263	68.124	pRB263F pRB263R	CGGAATACCATCAATTCGCTGACGAGTCCGGGATGAGCCTG CAGGCTCATCCCGACTCGTCAGCGAATTGATGGTATTCCG
Asn428	105.027	pRB428F pRB428R	CGCAAATTCGGCAATGACGTGGCCGTTGTTG CAACAACGGCCACGTCATTGCCGAATTTGCG
Asn435	158.306	pRB435F pRB435R	CGTGGCCGTTGTTGCCATTGACCGCAATATGAACACACC GGTGTGTTTCATATTGCGGTCATGGCAACAACGGCCACG
Asn274	306.815	pRB274F pRB274R	GCGAATGGTTCCTTGGCGTCGATGAGATTAGTCCGGAATAC GTATTCCGACTAATCTCATCGACGCCAAGGAACCATTTCGC
**Asn336	1.004	pRB336N-QF pRB336N-QR	CATGGAGCGTTTCCACACCAGCCAGGGCGACAGACGGAAGCTGGAGC GCTCCAGCTTCCGTCTGTCGCCCTGGCTGGTGTGGAACGCTCCATG

\*Underlined letters were mutated positions

\*\*Primers were designed for substitution of Asn residue by Glu residue.

by centrifugation at 3,000 rpm for 30 minutes. The solution was dialyzed against water at 4°C with three changes of water.

## 2.9 CGTase isoforms separation

The isoforms of cloned CGTase were separated by four methods; preparative gel electrophoresis, Ion-exchange chromatography (Mono Q), Isofocusing chromatography (Mono P), and IEF-PAGE as described below.

### 2.9.1 Preparative gel electrophoresis

The concentrated partially purified CGTase was loaded to a discontinuous preparative polyacrylamide gel electrophoresis, performed on Model 491 Prep cell (diameter 38 mm), using 10% separating gel and 5% stacking gel. Tris-glycine buffer, pH 8.3 was used as electrode buffer. The electrophoresis was run at constant power of 12 W until the dye reached the bottom of the gel. Protein was eluted from the gel with electrode buffer at a flow rate of 1 ml/min. Fractions of 3 ml was collected and measured for dextrinizing activity. To identify the CGTase isoform, every 5 fractions which contained dextrinizing activity was run on slab gels and observed by dextrinizing activity staining. Each isoform was pooled and collected at -80 °C for further studies.

### 2.9.2 Fast protein liquid chromatography (FPLC) with the anion column

The anion exchanger Mono Q<sup>TM</sup> HR 5/5 (5 cm x 5 mm) which had a column volume of 1 ml was used to isolate the isoform of the partially purified cloned CGTase. The column was pre-equilibrated with 10 mM phosphate buffer pH 6.5, flow rate 1 ml/min for 30 minutes. The concentrated of partially purified CGTase (2 ml) was loaded onto the column. The column was eluted with equilibrating buffer until  $A_{280}$  was nil. The gradient of 0.5 M NaCl was increased from 0-100% within 30 minutes to separate the isoforms. The fractions 0.5 ml were collected and the isoform pattern of the enzyme was followed by 7% native-PAGE.

### 2.9.3 Fast protein liquid chromatography (FPLC) with isofocusing chromatography column

Mono P column was also used to separate the isoforms of CGTase. The column was equilibrated with 25 mM Bis-Tris-HCl pH 6.5. The partially purified CGTase was mixed with equilibrating buffer and loaded into the column. The column was eluted with 20X polybuffer pH 4.2. The fractions were collected and measured for pH. The active fractions were taken to detect the isoform pattern of the enzyme by 7% native-PAGE.

### 2.9.4 IEF-PAGE

The isoform was separated by IEF-PAGE as described in section 2.12.3. After the gel was stained with coomassie, the isoform band was cut and collected at -20°C for use in the next experiments.

## 2.10 Enzyme assay

CGTase activity was determined by starch degrading (dextrinizing) activity assay, cyclizing activity assay, and coupling activity assay.

### 2.10.1 Dextrinizing activity

Dextrinizing activity of CGTase was measured by the method of Fuwa (1954) with slight modification (Techaiyakul, 1991).

Sample (10-100  $\mu$ l) was incubated with 0.3 ml starch substrate (0.2 g% soluble starch (potato) in 0.2 M phosphate buffer pH 6.0) at 40°C for 10 minutes. The reaction was stopped with 4 ml of 0.2 M HCl. Then 0.5 ml of iodine reagent (0.02% I<sub>2</sub> in 0.2% KI) was added. The mixture was adjusted to a final volume of 10 ml with distilled water and its absorbance at 600 nm was measured. For a control tube, HCl was added before the enzyme sample.

One unit of enzyme was defined as the amount of enzyme which produces 10% reduction in the intensity of the blue color of the starch-iodine complex per minute under the described conditions.

### 2.10.2 Cyclizing activity assay

Cyclization activity was determined by the phenolphthalein method of Goel and Nene (1995). Soluble starch 6.0% 1.25 ml of was added to 0.25 ml of purified CGTase. The reaction mixture was incubated for 30 minutes under 70°C. Reaction was stopped by boiling 5 minutes. The sample 1.0 ml of was incubated with 4.0 ml of phenolphthalein solution at 70°C for 10 minutes. Absorption was measured at 550 nm and  $\beta$ -CD formed was calculated using the calibration curve. One unit of activity was defined as the amount of enzyme able to produce 1  $\mu$ mole of CD per minute under the corresponding condition.

Phenolphthalein stock (1 mg/ml in ethanol) 1 ml was added to 100 ml of 100 mM  $\text{Na}_2\text{CO}_3$  solution in distilled water just before starting the experiment.  $\beta$ -CD standard (0-5 mM) was prepared.

### 2.10.3 Coupling activity assay

The coupling reaction was determined by incubating various concentrations of  $\beta$ -cyclodextrin as donor (0.5-15 mM) with 10 mM cellobiose as glucosyl acceptor at 55 °C in 50 mM acetate buffer, pH 6.0. Cyclodextrin and cellobiose was pre-incubated for 5 minutes at indicated temperature. The reaction was started with addition of partially purified CGTases. The reaction was incubated for 5 minutes and stopped by boiling 5 minutes. Subsequently, 4 units of *Aspergillus niger* glucoamylase was then added to convert linearized oligosaccharides to glucose by incubated at 55 °C for 1 hr. The reaction was stopped by boiling for 5 minutes. The amount of cyclodextrins degraded was monitored by measuring the released reducing sugar using the dinitrosalicylic acid method (Miller, 1959). The amount of reducing sugar was determined by comparing with standard glucose.

Dinitrosalicylic acid reagent was consisted of dinitrosalicylic acid (2-hydroxy-3,5-dinitrobenzoic acid) 5 g, 2 N NaOH 100 ml, potassium sodium tartrate 150 g and adjusted volume to 500 ml with distilled water.

### 2.11 Protein determination

Protein concentration was determined by the method of Bradford (1976) with bovine serum albumin as the standard.

## 2.12 Polyacrylamide gel electrophoresis (PAGE)

Three types of PAGE, non-denaturing, denaturing and isoelectric focusing gels, were employed for analysis of the purified protein and detection of the isoform pattern.

### 2.12.1 Non-denaturing polyacrylamide gel electrophoresis (Native-PAGE)

The gel was prepared as followed: for 2 slab gels, separating gel 7.0%, 0.67 ml of solution A (30 % (w/v) acrylamide, 0.8 % (w/v) bis-acrylamide and 2.5 ml of solution B (1.5 M Tris-HCl, pH 8.8) were mixed with 5.17 ml of distilled water. Fifty microlitter of 10% ammonium persulfate and 10  $\mu$ l of TEMED were added and mixed rapidly by swirling or inverting gently. The stacking gel (5 % acrylamide) consisted of 0.67 ml of solution A (30 % (w/v) acrylamide, 0.8 % (w/v) bis-acrylamide) mixed with 1.0 ml of solution C (0.5 M Tris, pH 6.8) and 2.3 ml of distilled water. Thirty microlitter of 10 % ammonium persulfate and 5  $\mu$ l of TEMED were then added. The electrophoresis buffer (25 mM Tris, 192 mM glycine, pH 8.8) was added into the inner and outer reservoir. The protein sample was mixed with 5 x sample buffer (0.3 mM Tris-HCl, 50% glycerol and 0.05% bromophenol blue). Then the sample solution was introduced into well by using syringe. The gel was running at constant current (30 mA). Electrophoresis was continued until the dye front reached the bottom of the gel.

#### 2.12.1.1 Protein staining

The gel was stained with coomassie solution composed of 1% Coomassie Blue R-250, 45% methanol, and 10% glacial acetic acid. Destaining was performed in 10% methanol, 10% glacial acetic acid solution.

**2.12.1.2 Dextrinizing activity staining** (slightly modified from the method of Kobayashi, et al., 1978),

The running gel was soaked in 10 ml of substrate solution, containing 2% (w/v) potato starch in 0.2 M phosphate buffer pH 6.0, at 40°C for 10 minutes. The gel was then quickly rinsed several times with distilled water and 10 ml of I<sub>2</sub> staining reagent (0.2% I<sub>2</sub> in 2% KI) was added for color development at room temperature. The clear zone on the blue background represents starch degrading activity of the protein.



### 2.12.2 SDS-polyacrylamide gel electrophoresis

The SDS-polyacrylamide system was performed. For 2 slab gels, separating gel (7.5 % acrylamide) consisted of 3.0 ml of solution A (30 % (w/v) acrylamide, 0.8 % (w/v) bis-acrylamide, 2.5 ml of solution B (1.5 M Tris-HCl, pH 8.8, 4% SDS) and 1.89 ml of distilled water. Stacking gel (5 % acrylamide) consisted of 0.67 ml of solution A (30 % (w/v) acrylamide, 0.8 % (w/v) bis-acrylamide, 1.0 ml of solution C (0.5 M Tris, pH 6.8, 4% SDS) and 3.27 ml of distilled water. Protein sample was mixed with 5 x sample buffer (0.3 mM Tris-HCl, 50 % glycerol, 20% SDS, 5% 2-mercaptoethanol and 0.05 % bromophenol blue) in an Eppendorf tube and was boiled 10 min at 95°C and cooled at room temperature. Then the sample solution was introduced into gel by using syringe. The electrophoresis buffer (25 mM Tris, 192 mM glycine and 0.1% SDS, pH 8.8) was used for gel running. After electrophoresis, proteins in the gel were visualized by protein staining as described in section 2.12.1.5.

### 2.12.3 Isoelectric focusing-PAGE

The monomer-ampholyte solution was composed of distilled water 2.2 ml, acrylamide monomer concentrate (25% T, 3% C) 0.8 ml, 25% (w/v) glycerol 0.8 ml and ampholyte 4/6 0.2 ml. The catalyst solution was consisted of 10% (w/v) ammonium persulphate 12  $\mu$ l, 0.1% (w/v) riboflavin (FMN) 40  $\mu$ l and TEMED (neat) 4  $\mu$ l. The gel dimension was 125 x 65 x 0.4 mm. The gel was set exposed to the light at room temperature for 4-6 hrs. The enzyme sample was prepared by dialyzed against distilled water to remove the salt. After sample loading, the run condition for focusing was carried out under constant voltage in a stepped fashion (100 V for 20 minutes, then 200 V for 20 minutes, and finally, increase the voltage to 450 V for an additional of 90 minutes).

Note: Step increases of voltage are necessary to prevent overheating and subsequent dehydration of the gel. Failure to follow this procedure will result in poor resolution. To visualize, the gel was immersed in the fixative solution for 30 minutes, then staining solution for 30 minutes (see appendix 4). The pI's of sample proteins were determined by the standard curve constructed from the pI's of the standard proteins and their migrating distance from cathode.

### 2.13 Isoform pattern on native-PAGE of CGTase from *Paenibacillus* sp. RB01, cloned CGTase and mutated CGTase

The *Paenibacillus* sp. RB01 was cultivated in Horikoshi's medium for 3 days and the cloned and the mutated enzymes from *E.coli* BL21 (DE3) were cultured in LB broth for 24 hrs (see Appendix 1 for the broth composition). The crude enzyme was prepared by centrifuged at 5,000 rpm and the supernatant (crude enzyme) was measured for enzyme activity and protein content. The sample was loaded onto the 7% native-PAGE and the isoform pattern was compared by observing the bands stained by coomassie solution or dextrinizing activity as described above.

### 2.14 Comparison of isoforms by analysis of tryptic digested pattern, peptide sequence and iso-Asp intermediate.

In this experiment, isoforms I and II of cloned CGTase were separated by IEF-PAGE as described in 2.12.3

#### 2.14.1 In solution tryptic digestion

The CGTase isoforms I and II (1 mg/ml, 15.4  $\mu$ M) was prepared for the detection of iso-aspartate content. The sample in Microcon YM-10 (cut-off 10 kDa) tube was centrifuged at 5,000 rpm for 1 hr and then ultrapure water was added and centrifuged again. These steps were repeated 3 times. The desalted sample was digested by trypsin at a ratio of 1:20 (w/w) in 200 mM  $\text{NH}_4\text{HCO}_3$  for 2 hrs at room temperature. To stop the reaction, 100 mM PMSF was added (final concentration 1 mM).

#### 2.14.2 In gel tryptic digestion

The protein band (isoform I or II on IEF-PAGE) was cut with clean scalpel and washed with 200  $\mu$ l of solution B for 30 minutes, repeat until the gel was no longer blue color then removed solution. Acetonitrile (200  $\mu$ l) was added for 10 minutes and removed. The gel was dried by speedvac for 10 minutes, after that 10 mM DTT was added for 10 minutes at 37°C and removed. Wash the gel twice with solution B. Iodoacetamide (55 mM) was added for 10 minutes in the dark and discarded. Wash the gel with 200  $\mu$ l of solution B twice and acetonitrile was added for 10 minutes and removed. After the gel was dried, add 0.1 mg/ml trypsin solution until the gel was

submerged. Incubate at 37°C for 2 hrs. The reaction was stopped by adding 1 ml formic acid. The solution was collected and the peptide was extracted from the gel by incubating the gel in 50/50 ultrapure water : acetonitrile for 30 minutes.

Solution B composed of 10 ml of 25 mM  $\text{NH}_4\text{HCO}_3$  and 10 ml of acetonitrile.

### 2.14.3 Tryptic digested peptide separation by reverse phase HPLC

Peptides resulting from in gel tryptic digested were then separated by reversed phase HPLC on a  $\text{C}_{18}$  column intersil<sup>®</sup> ODS-3 (size 4.5 x 250 mm) previously equilibrated with solvent A. Solvent A was 0.1% (v/v) trifluoroacetic acid in water. Elution was made by mixing solvent A and B at the indicate proportion and time as shown below. Solvent B was the mixture of 0.1% (v/v) trifluoroacetic acid in water and acetonitrile in the ratio of 1:3.

<u>Time (min)</u>	<u>Solvent A (%)</u>	<u>Solvent B (%)</u>
0.0	100	0.0
5.0	90.0	10.0
20.0	80.0	20.0
60.0	50.0	50.0
90.0	0.0	100.0
120.0	0.0	100.0
140.0	100.0	0.0

Elution of HPLC was carried out at a flow rate of 1 ml/min. Detection of peptide was performed at 210 and 246 nm. Injecting the ultrapure water alone under the same chromatographic conditions was also performed as control.

### 2.14.4 Mass analysis of peptides

Peptides from in gel tryptic digested were analyzed by mass spectrometry (MALDI-TOF). A mass spectrometer is an analytical device that determines the molecular mass of chemical compounds by separating molecular ions according to their mass-to-charge ratio (m/z). The molecular mass was calculated by (Siuzdak G., 1996)

$$(\text{molecular mass} + \text{number of protons}) / \text{charge} = \text{mass-to-charge ratio (m/z)}$$

## 2.14.5 Detection of *iso*-Aspartate content in CGTase

### 2.14.5.1 Sample preparation

The isoform I (2.5 mg/ml) of cloned CGTase separated by Mono Q column was incubated in deamidation buffer (25 mM acetic acid, 25 mM Tris, and 50 mM ethanolamine, pH 9, (DeLuna, 2005) at 37°C. The sample at time intervals of 0, 3 and 7 days was kept at -80°C until analyzed at the same time. The alteration of isoform I was followed by native-PAGE, SDS-PAGE and slab IEF-PAGE as described above.

### 2.14.5.2 Iso-aspartate detection

The ISOQUANT Isoaspartate detection kit was used. The kit contained the enzyme Protein Isoaspartyl Methyltransferase (PIMT) which specifically detect the presence of isoaspartic acid residues in a target protein (Aswad, 1994). PIMT catalyzes the transfer of a methyl group from S-adenosyl-L-methionine (SAM) to isoaspartic acid at the  $\alpha$ -carboxyl position, generating S-adenosyl homocysteine (SAH) in the process (Figure 2.1). The SAH was quantitated by reverse phase HPLC using C<sub>18</sub> column (Intersil<sup>®</sup> ODS-3, 4.5x250 mm). Reagent preparation: The reaction reagents were diluted with ultrapure water to give a concentration as followed;

The amount of SAH was determined quantitatively following the instruction. Then the pmole of isoaspartate per pmole of CGTase was calculated by comparing with standard SAH provided in the kit.

The HPLC program was performed as follows to detect the amount of the SAH:

<u>Time</u>	<u>Unit</u>	<u>Command</u>	<u>Value</u>
0.01	Pump	B concentration	80
0.01	Pump	C concentration	20
0.01	Controller	start	
7.50	Pump	B concentration	70
7.50	Pump	C concentration	30
8.50	Pump	B concentration	80
8.50	Pump	C concentration	20
15.01	Controller	stop	

Time - in minutes

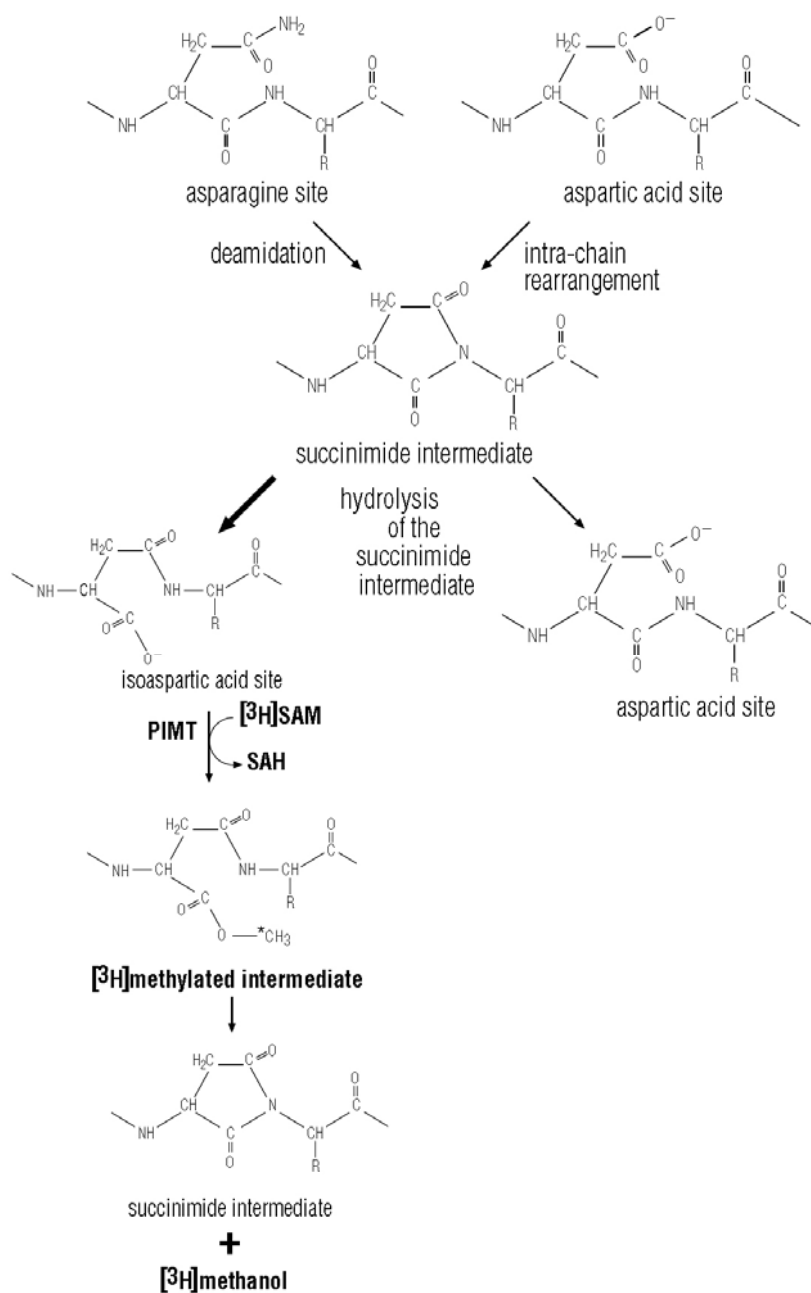


Figure 2.1 Isoaspartate formation in protein deamidation at asparagine (A) and intrachain bond rearrangement at aspartic acid (B) and the detection of isoaspartic acid via PIMT-catalyzed reaction. The side chains of asparagine or aspartic acid residues can spontaneously form a succinimide ring intermediate with the peptide backbone, which rearranges to form isoaspartic acid (70.85%) and aspartic acid (15.30%). The detection of isoaspartic acid is by the PIMT-catalyzed generation of SAH. Quantitation of isoaspartate can be by using [<sup>3</sup>H]SAM and following [<sup>3</sup>H] methanol as shown or by using non-labeled SAM and monitoring SAH by HPLC (modified from ISOQUANT<sup>®</sup> kit, Promega).

Pump B = 50 mM potassium phosphate, pH 6.2

Pump C = 100% methanol HPLC grade

Flow rate = 1 ml/min

UV Detector =  $A_{260}$  was measured

## 2.15 Comparison of properties of CGTase isoforms from the cloned and mutants.

Isoform I and isoform II of cloned CGTase were separated by Mono P FF column. For mutated CGTases, crude enzyme was used.

### 2.15.1 Optimum pH and Temperature

The isoform I and II of cloned CGTases and some selected mutated CGTase were determined for their optimum pH and temperature. The dextrinizing and cyclization activity was assayed as mentioned above. Optimum pH was performed by using 50 mM buffer solution in the pH range from 3.0 to 11.0. The buffers used were potassium acetate (pH 3.0-5.0), phosphate (pH 5.0-7.0), Tris-HCl (pH 7.0-9.0) and Tris-glycine NaOH (pH 9.0-11.0) and also using universal buffer pH 3.0-11.0. For optimization of temperature, activities were determined in the range from 30 to 80°C

### 2.15.2 Kinetics parameters

Kinetic parameters of the coupling reaction were determined by incubating various concentrations of  $\beta$ -cyclodextrin as donor (0.5-15 mM) with 10 mM cellobiose as glucosyl acceptor at 55°C in acetate buffer, pH 6.0 for 5 minutes. Cyclodextrin and cellobiose were mixed and pre-incubated for 5 minutes at indicated temperature. The reaction was started with addition of the enzyme sample and stopped after 5 minutes of incubation by boiling for 5 min. Subsequently, 4 units of Amyloglucosidase from *Aspergillus niger* (67 U/mg) was then added. The reaction was performed at 55°C for 90 minutes to convert linearized oligosaccharides to glucose. Measuring the released reducing sugars was monitored as described in section 2.10.3. The kinetic parameters,  $K_m$ ,  $V_{max}$ , and  $k_{cat}/K_m$  was calculated from the Michealis-Menten equation using nonlinear least square regression analysis.

### 2.15.3 Cyclodextrin product ratio

The enzyme 3 Units of dextrinizing activity was incubated with 10 ml of 2% soluble starch at 60°C. The sample (1 ml) was taken at the time 6, 12, 24 hrs. The reaction was stopped by boiling for 10 minutes. Amyloglucosidase 20 µl (0.4 U) was added to degrade the linear oligosaccharides for 6 hrs and the reaction was stopped by boiling for 10 minutes then centrifuged at 12,000 rpm for 30 minutes. The cyclodextrin product was analyzed by high performance anion exchange chromatography with pulsed amperometric detection (HPAEC-PAD). The main eluent, 150 mM NaOH (1 liter distilled water + 7.92 ml 50% NaOH) was prepared and for gradient eluent, 150 mM NaOH with 200 mM NaNO<sub>3</sub> (1 liter of distilled water + 7.92 ml 50% NaOH + 17.2 g NaNO<sub>3</sub>) was also prepared. Ultrasonic bath USR 30 (Merck Eurolab N.V., Belgium) was used for ultrasonication of eluent. To analyze the CD sample, 25 µl was automatically injected onto a column. The CD product was identified and quantitated by comparing with standard CDs. CDs were eluted with a linear gradient of NaNO<sub>3</sub> as below

Time (min)	% NaNO <sub>3</sub>
-15-0	0
0-10	4
10-12	4
12-32	8
32-48	9
48-59	18
59-79	28
79-85	100

### 2.15.4 Amino acid sequence

The amino acid sequence of tryptic peptide was predicted by using program Mascot from [www.matrixscience.com](http://www.matrixscience.com). The experimental monoisotopic mass of peptide from MALDI-TOF was input into the program, then the primary sequence of amino acid was predicted by homology scoring algorithm with the closest match from the available database.

## CHAPTER III

### RESULTS

#### 3.1 Identification and expression of CGTase gene (*cgt*) from *Paenibacillus* sp. RB01

##### 3.1.1 Cloning of *cgt* from *Paenibacillus* sp. RB01

###### Genomic DNA extraction

The genomic DNA was extracted and checked by agarose gel electrophoresis (Figure 3.1A Lane 1). The result showed that the size of DNA template was larger than 10 kb. The ratio of  $A_{260/280}$  values was 1.8 indicated that the purity of this extracted DNA was sufficient to be used as template for PCR amplification.

###### *cgt* amplification and preparation

The product from the PCR amplification was found as a single band on agarose gel electrophoresis shown in Figure 3.1A Lane 2. The size of PCR product was 2.1 kb as expected for *cgt*. This product was then subjected to digestion with the restriction enzymes *Nco* I and *Xho* I.

###### Plasmid vector preparation

The extracted plasmid pET19b was shown by agarose gel electrophoresis in Figure 3.1B Lane 1. The plasmid was subjected to digestion with *Nco* I and *Xho* I, the same restriction enzymes as the PCR product, and the size of the linear form of this plasmid vector was shown to be 5.7 kb (Figure 3.1B Lane 3).

###### Transformation and colony selection

The digested PCR product and the linear form of plasmid vector were ligated by T4 DNA ligase. The recombinant plasmid was constructed and transformed into the competent cell of *E. coli* BL21 (DE3). One hundred  $\mu$ l of the transformant was spread on LB agar plate containing 100  $\mu$ g/ml ampicillin and 1% soluble starch and incubated at 37°C for overnight. The *E. coli* BL21 (DE3) containing pET19b vector harboring *cgt* was grown on the plate as shown in Figure 3.2A. The plate was then replicated and the iodine solution was overlaid. Only the colonies contained pET19b vector harboring *cgt* showed a clear zone as shown in Figure 3.2B. The selected colonies were cultured in LB broth containing 100  $\mu$ g/ml ampicillin at 37°C overnight and the cultures were subjected



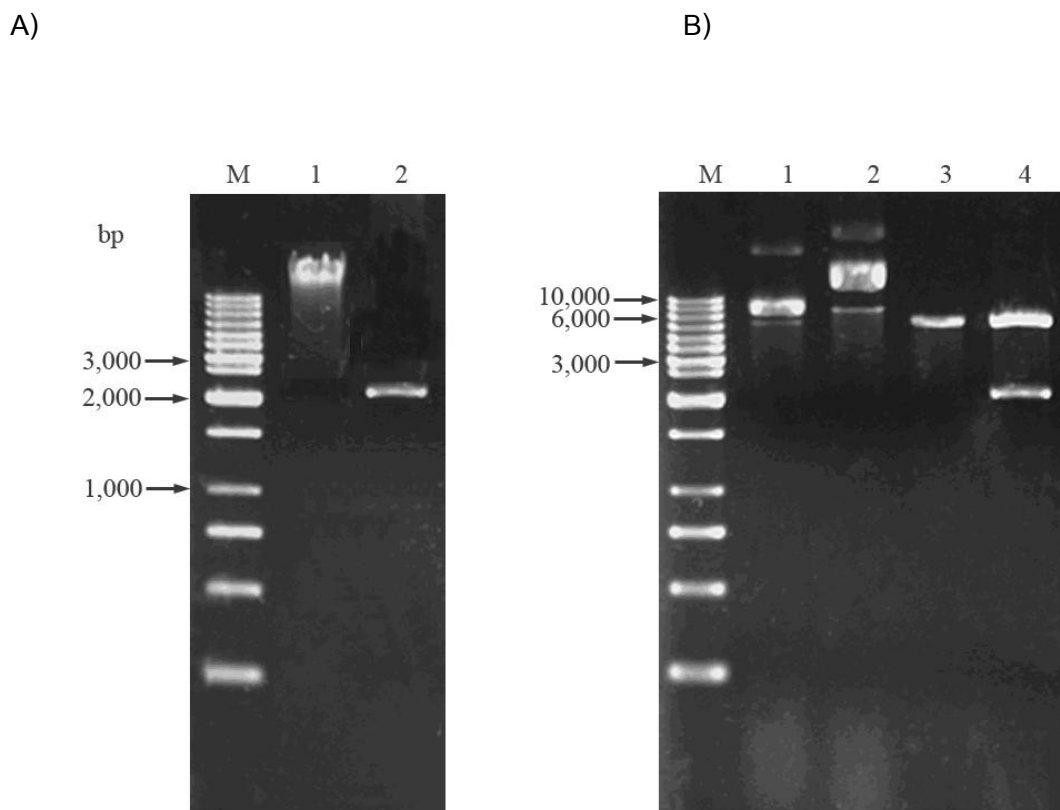


Figure 3.1 Agarose gel electrophoresis of A) amplified *cgf* and genomic DNA of *Paenibacillus* sp.RB01, B) recombinant *cgf* inserted in pET19b vector. The DNA samples were separated on 1% agarose gel and visualized by ethidium bromide staining

A)

Lane M = 1 kb marker

Lane 1 = Genomic DNA of  
*Paenibacillus* sp. RB01

Lane 2 = Amplification product of *cgf*

B)

Lane M = 1 kb marker

Lane 1 = pET19b vector

Lane 2 = pET19b vector inserted with *cgf*

Lane 3 = pET19b vector digested with *NcoI*  
and *XhoI*

Lane 4 = pET19b vector harboring *cgf*,  
digested with *NcoI* and *XhoI*

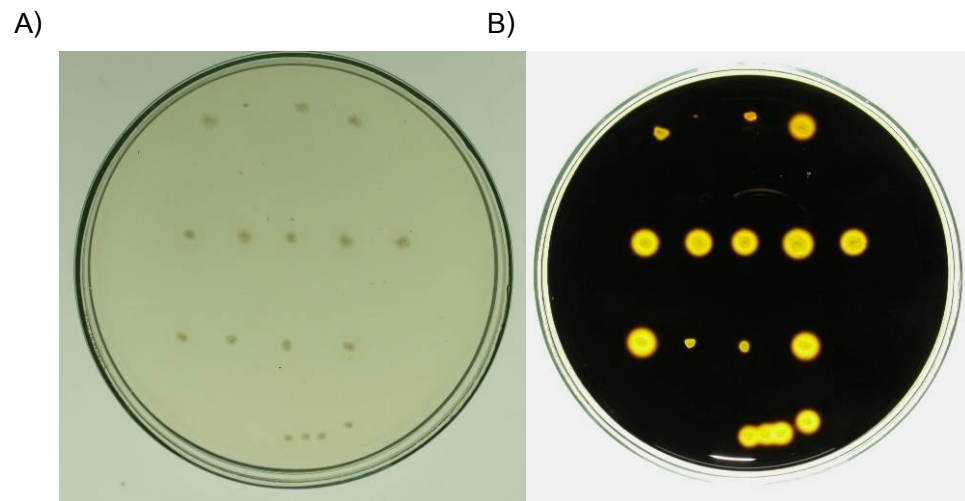


Figure 3.2 Selection of the transformant *E. coli* BL21 (DE3) containing pET19b inserted with *cgt* on LB agar plate containing 100 µg/ml ampicillin and 1% soluble starch.

A) Grown colonies before overlaid with iodine solution and B) Colonies after overlaid with iodine solution.

to plasmid extraction and checked for plasmid on agarose gel electrophoresis (Figure 3.1B Lane 2). To verify the insertion of PCR product into pET19b, the agarose gel electrophoresis pattern of the recombinant plasmid containing *cgt* was also checked. The relaxed form of recombinant plasmid moved slower than that of the original plasmid, pET 19b (Figure 3.1B Lane 2). Lane 4 comprised of two bands, at 5.7 kb: the size of linear form of the recombinant plasmid and 2.1 kb corresponded to the expected size for the PCR product of *cgt*.

#### **Nucleotide sequencing**

To confirm whether the inserted fragment was indeed *cgt*, the recombinant plasmid was subjected to DNA sequencing by using the primers of T7 promotor and T7 terminator which can sequence through the 5'-terminus and 3'-terminus of the inserted *cgt* in plasmid, respectively. The sequence was extended by using primer pBT590F and pBT1480R as described in section 2.5.3 and searched for overlapping regions. The nucleotide sequence of *cgt* and deduced amino acid sequence were shown in Figure 3.3. The 713 amino acid residues was deduced from the *cgt* which had an open reading frame of 2,142 bp in length. The nucleotide sequence of this gene had very high similarity (98-99%) with those from *Bacillus* sp. N-227, *Bacillus circulans* A11 and *Bacillus* sp. strain 1011 (Table 3.1). However, the sequence was relatively not similar (60-66%) to those of *Paenibacillus macerans* and *Geobacillus stearothermophilus*.

From the nucleotide sequence, the amino acid sequence was deduced. The first 27 amino acid residues were predicted as a signal peptide which was cut off when the enzyme was secreted to the medium as an extracellular enzyme.

#### **Amino acid alignment and phylogenetic analysis**

The alignment of the obtained deduced amino acid sequence with other published CGTases in NCBI amino acid database was performed (Figure 3.4). The result of the alignment was shown in Table 3.1. The result revealed that the deduced amino acid sequence of the recombinant plasmid shared 100% similarity with the CGTases from *Bacillus* sp. N-227 (ABG02281) and *Paenibacillus* sp. A11 (AAG31622.1). When compared with CGTases from *Paenibacillus* sp. BL11 and *Bacillus* sp. 1011, 98% similarity were obtained. The difference in Asn residue in these enzymes was found at Asn93 in BL11 and 1011 (numbering without signal sequence) which was replaced by

```

      10          20          30          40          50          60
AGGAGATATACCAATGGAAAAGATTTATGAAACTAACAGCCGTATGGACACTCTGGTTATCC
      M E R F M K L T A V W T L W L S
      70          80          90          100         110         120
CTCACGCTGGGCCTCTTGAGCCCGGTCCACGCAGCCCCGGATACCTCGGTATCCAACAAG
L T L G L L S P V H A A P D T S V S N K
      130         140         150         160         170         180
CAGAATTTTCAGCACGGATGTCATATATCAGATCTTACCGACCGGTTCTCGGACGGCAAT
Q N F S T D V I Y Q I F T D R F S D G N
      190         200         210         220         230         240
CCGGCCAACAATCCGACCGGCGCGGCATTTGACGGATCATGTACGAATCTTCGCTTATAC
P A N N P T G A A F D G S C T N L R L Y
      250         260         270         280         290         300
TGCGGCGGCGACTGGCAAGGCATCATCAACAAAATCAACGACGGTTATTTGACCGGCATG
C G G D W Q G I I N K I N D G Y L T G M
      310         320         330         340         350         360
GGCATTACGGCCATCTGGATTTACAGCCTGTCGAGAATATCTACAGCGTGATCAACTAC
G I T A I W I S Q P V E N I Y S V I N Y
      370         380         390         400         410         420
TCCGGCGTCCATAATACGGCTTATCACGGCTACTGGGCGCGGGACTTCAAGAAGACCAAT
S G V H N T A Y H G Y W A R D F K K T N
      430         440         450         460         470         480
CCGGCCTACGGAACGATGCAGGACTTCAAAAACCTGATCGACACCGCGCATGCGCATAAC
P A Y G T M Q D F K N L I D T A H A H N
      490         500         510         520         530         540
ATAAAAGTCATCATCGACTTTGCACCGAACCATACATCTCCGGCTTCTTCGGATGATCCT
I K V I I D F A P N H T S P A S S D D P
      550         560         570         580         590         600
TCCTTTGCAGAGAACGGCCGCTTGTACGATAACGGCAACCTGCTCGGCGGATACACCAAC
S F A E N G R L Y D N G N L L G G Y T N
      610         620         630         640         650         660
GATACCCAAAATCTGTTCCACCATTATGGCGGCACGGATTTCTCCACCATTGAGAACGGC
D T Q N L F H H Y G G T D F S T I E N G
      670         680         690         700         710         720
ATTTATAAAAACCTGTACGATCTGGCTGACCTGAATCATAACAACAGCAGCGTCGATGTG
I Y K N L Y D L A D L N H N N S S V D V
      730         740         750         760         770         780
TATCTGAAGGATGCCATCAAAAATGTGGCTCGACCTCGGGGTTGACGGCATTCGCGTGGAC
Y L K D A I K M W L D L G V D G I R V D
      790         800         810         820         830         840
GCGGTCAAGCATATGCCATTCGGCTGGCAGAAGAGCTTTATGTCCACCATTAACAACACTAC
A V K H M P F G W Q K S F M S T I N N Y
      850         860         870         880         890         900
AAGCCGGTCTTACCTTCGGCGAATGGTTTCCCTTGGCGTCAATGAGATTAGTCCGGAATAC
K P V F T F G E W F L G V N E I S P E Y
      910         920         930         940         950         960
CATCAATTCGCTAACGAGTCCGGGATGAGCCTGCTCGATTTCCGCTTTGCCCAGAAGGCC
H Q F A N E S G M S L L D F R F A Q K A
      970         980         990         1000        1010        1020
CGGCAAGTGTTCAGGGACAACACCGACAATATGTACGGCCTGAAAGCGATGCTGGAGGGC
R Q V F R D N T D N M Y G L K A M L E G
      1030        1040        1050        1060        1070        1080
TCTGAAGTAGACTATGCCCAGGTGAATGACCAGGTGACCTTCATCGACAATCATGACATG
S E V D Y A Q V N D Q V T F I D N H D M

```

Figure 3.3 Nucleotide and deduced amino acid sequences of *Paenibacillus* sp. RB01. The bold letters indicate start and stop codons. The underlined letters indicate signal sequence.

```

1090      1100      1110      1120      1130      1140
GAGCGTTTTCCACACCAGCAATGGCGACAGACGGAAGCTGGAGCAGGCGCTGGCCTTTACC
E R F H T S N G D R R K L E Q A L A F T
      1150      1160      1170      1180      1190      1200
CTGACTTCACGCGGTGTGCCTGCCATCTATTACGGCAGCGAGCAGTATATGTCTGGCGGG
L T S R G V P A I Y Y G S E Q Y M S G G
      1210      1220      1230      1240      1250      1260
AATGATCCGGACAACCGTGCTCGGATTCCTTCTCCACGACGACGACCGCATATCAA
N D P D N R A R I P S F S T T T T A Y Q
      1270      1280      1290      1300      1310      1320
GTCATCCAAAAGCTCGCTCCGCTCCGCAAATCCAACCCGGCCATCGCTTACGGTTCCACA
V I Q K L A P L R K S N P A I A Y G S T
      1330      1340      1350      1360      1370      1380
CAGGAGCGCTGGATCAACAACGATGTGATCATCTATGAACGCAAATTCGGCAATAACGTG
Q E R W I N N D V I I Y E R K F G N N V
      1390      1400      1410      1420      1430      1440
GCCGTTGTTGCCATTAACCGCAATATGAACACACCCGGCTTCGATTACCGGCCTTGCTACT
A V V A I N R N M N T P A S I T G L V T
      1450      1460      1470      1480      1490      1500
TCCCTCCCGCAGGGCAGCTATAACGATGTGCTCGGCGGAATTCTGAACGGCAATACGCTA
S L P Q G S Y N D V L G G I L N G N T L
      1510      1520      1530      1540      1550      1560
ACCGTGGGTGCTGGCGGTGCAGCTTCCAACCTTTACTTTGGCTCCTGGCGGCACTGCTGTA
T V G A G G A A S N F T L A P G G T A V
      1570      1580      1590      1600      1610      1620
TGGCAGTACACAACCGATGCCACAGCTCCGATCATCGGCAATGTCGGCCCCGATGATGGCC
W Q Y T T D A T A P I I G N V G P M M A
      1630      1640      1650      1660      1670      1680
AAGCCAGGGGTCACGATTACGATTGACGGCCGCGCTTCGGCTCCGGCAAGGGAACGGTT
K P G V T I T I D G R G F G S G K G T V
      1690      1700      1710      1720      1730      1740
TACTTCGGTACAACGGCAGTCACTGGCGCGGACATCGTAGCTTGGGAAGATAACAAAATC
Y F G T T A V T G A D I V A W E D T Q I
      1750      1760      1770      1780      1790      1800
CAGGTGAAAATCCCTGCGGTCCCTGGCGGCATCTATGATATCAGAGTTGCCAACGCAGCC
Q V K I P A V P G G I Y D I R V A N A A
      1810      1820      1830      1840      1850      1860
GGAGCAGCCAGCAACATCTACGACAATTTTCGAGGTGCTGACCGGAGACCAGGTCACCGTT
G A A S N I Y D N F E V L T G D Q V T V
      1870      1880      1890      1900      1910      1920
CGGTTTCGTAATCAACAATGCCACAACGGCGCTGGGACAGAATGTGTTCCCTCACGGGCAAT
R F V I N N A T T A L G Q N V F L T G N
      1930      1940      1950      1960      1970      1980
GTCAGCGAGCTGGGCAACTGGGATCCGAACAACGCGATCGGCCCGATGTATAATCAGGTC
V S E L G N W D P N N A I G P M Y N Q V
      1990      2000      2010      2020      2030      2040
GTCTACCAATACCCGACTTGGTATTATGATGTCAGCGTTCCGGCAGGCCAAACGATTGAA
V Y Q Y P T W Y Y D V S V P A G Q T I E
      2050      2060      2070      2080      2090      2100
TTTAAATTCCTGAAAAAGCAAGGCTCCACCGTCACATGGGAAGGCGGCGGAATCGCACC
F K F L K K Q G S T V T W E G G A N R T
      2110      2120      2130      2140      2150      2160
TTCACCACCCCAACCAGCGGCACGGCAACGATGAATGTGAACTGGCAGCCTTAACTCGAG
F T T P T S G T A T M N V N W Q P *
      2170
GATCC

```

Figure 3.3 (continued) Nucleotide and deduced amino acid sequences of *Paenibacillus* sp. RB01. The bold letters indicate start and stop codons. The underlined letters indicate signal sequence.

pRB01	MKRFMKLTAVWTLWLSLTLGLLSPVHAAPDTS-VSNKQNFSTDVYQIFTRDFSDGNPAN	59
N-227	MKRFMKLTAVWTLWLSLTLGLLSPVHAAPDTS-VSNKQNFSTDVYQIFTRDFSDGNPAN	59
A11	MKRFMKLTAVWTLWLSLTLGLLSPVHAAPDTS-VSNKQNFSTDVYQIFTRDFSDGNPAN	59
1011	MKRFMKLTAVWTLWLSLTLGLLSPVHAAPDTS-VSNKQNFSTDVYQIFTRDFSDGNPAN	59
I-5	MKRFMKLTAVWTLWLSLTLGLLSPVHAAPDTS-VSNKQNFSTDVYQIFTRDFSDGNPAN	59
38-2	MKRFMKLTAVWTLWLSLTLGLLSPVHAAPDTS-VSNKQNFSTDVYQIFTRDFSDGNPAN	59
BL11	MKRFMKLTAVWTLWLSLTLGLLSPVHAAPDTS-VSNKQNFSTDVYQIFTRDFSDGNPAN	59
STEAROTHERMOPHILUS	MKSRYKRLTSLALSLSMALGSLPAWASPDTS-VDNKVNFSSTDVYQIVTDRFADGDRTN	59
MACERANS	MKSRYKRLTSLALSLSMALGSLPAWASPDTS-VDNKVNFSSTDVYQIVTDRFADGDRTN	59
THERMOSULFURIGENES	MKTKFKLILVLMLSLTLVFLGTAPIQAASDTA-VSNVVNYSTDVYQIVTDRFVDGNTSN	59
	*: . : : : . : : : * * : : * : * : * : * : * : *	
pRB01	NPTGAAFDGSCTNLRLYCGGDWQGIINKINDGYLTGMGITAIWISQFVENIYSVINYSVG	119
N-227	NPTGAAFDGSCTNLRLYCGGDWQGIINKINDGYLTGMGITAIWISQFVENIYSVINYSVG	119
A11	NPTGAAFDGSCTNLRLYCGGDWQGIINKINDGYLTGMGITAIWISQFVENIYSVINYSVG	119
1011	NPTGAAFDGSCTNLRLYCGGDWQGIINKINDGYLTGMGITAIWISQFVENIYSVINYSVG	119
I-5	NPTGAAFDGSCTNLRLYCGGDWQGIINKINDGYLTGMGITAIWISQFVENIYSVINYSVG	119
38-2	NPTGAAFDGSCTNLRLYCGGDWQGIINKINDGYLTGMGITAIWISQFVENIYSVINYSVG	119
BL11	NPTGAAFDGSCTNLRLYCGGDWQGIINKINDGYLTGMGITAIWISQFVENIYSVINYSVG	119
STEAROTHERMOPHILUS	NPAGDAFSGDRSNLKLKLYFGGDWQGIIDKINDGYLTGMGVTALWISQFVENITSVIKYSVG	119
MACERANS	NPAGDAFSGDRSNLKLKLYFGGDWQGIIDKINDGYLTGMGVTALWISQFVENITSVIKYSVG	119
THERMOSULFURIGENES	NPTGDLYDPTHTSLKKYFGGDWQGIINKINDGYLTGMGVTAIWISQFVENIYAVLPDSTF	119
	** : * : . : : * : * : * : * : * : * : * : * : * : * : * : * : * : *	
pRB01	H-NTAYHGYWARDFKKTNPAYGTMQDFKNLIDTAHAHNKVIIDFAPNHTSPASSDDPSF	178
N-227	H-NTAYHGYWARDFKKTNPAYGTMQDFKNLIDTAHAHNKVIIDFAPNHTSPASSDDPSF	178
A11	H-NTAYHGYWARDFKKTNPAYGTMQDFKNLIDTAHAHNKVIIDFAPNHTSPASSDDPSF	178
1011	N-NTAYHGYWARDFKKTNPAYGTMQDFKNLIDTAHAHNKVIIDFAPNHTSPASSDDPSF	178
I-5	H-NTAYHGYWARDFKKTNPAYGTMQDFKNLIDTAHAHNKVIIDFAPNHTSPASSDDPSF	178
38-2	H-NTAYHGYWARDFKKTNPAYGTMQDFKNLIDTAHAHNKVIIDFAPNHTSPASSDDPSF	178
BL11	N-NTAYHGYWARDFKKTNPAYGTMQDFKNLIDTAHAHNKVIIDFAPNHTSPASSDDPSF	178
STEAROTHERMOPHILUS	N-NTSYHGYWARDFKQTNDAFGDFADFNQNLIDTAHAHNKVIIDFAPNHTSPADRNPGF	178
MACERANS	N-NTSYHGYWARDFKQTNDAFGDFADFNQNLIDTAHAHNKVIIDFAPNHTSPADRNPGF	178
THERMOSULFURIGENES	GGSTSYHGYWARDFKRTNPFYGSFTDFQNLINTAHAHNKVIIDFAPNHTSPASSETDPT	179
	: : * : * : * : * : * : * : * : * : * : * : * : * : * : * : * : *	
pRB01	AENGRLYDNGNLLGGYTNDTQNLFFHHYGGTDFSTIENGIYKNLYDLADLNHNNSVVDVYL	238
N-227	AENGRLYDNGNLLGGYTNDTQNLFFHHYGGTDFSTIENGIYKNLYDLADLNHNNSVVDVYL	238
A11	AENGRLYDNGNLLGGYTNDTQNLFFHHYGGTDFSTIENGIYKNLYDLADLNHNNSVVDVYL	238
1011	AENGRLYDNGNLLGGYTNDTQNLFFHHYGGTDFSTIENGIYKNLYDLADLNHNNSVVDVYL	238
I-5	AENGRLYDNGNLLGGYTNDTQNLFFHHYGGTDFSTIENGIYKNLYDLADLNHNNSVVDVYL	238
38-2	AENGRLYDNGNLLGGYTNDTQNLFFHHYGGTDFSTIENGIYKNLYDLADLNHNNSVVDVYL	238
BL11	AENGRLYDNGNLLGGYTNDTQNLFFHHYGGTDFSTIENGIYKNLYDLADLNHNNSVVDVYL	238
STEAROTHERMOPHILUS	AENGMVDNLSLLGAYSNDTAGLFHHNGGTFDFSTIEDGIYKNLYDLADLNHNNSVVDVYL	238
MACERANS	AENGMVDNLSLLGAYSNDTAGLFHHNGGTFDFSTIEDGIYKNLYDLADLNHNNSVVDVYL	238
THERMOSULFURIGENES	AENGRLYDNGTLLGGYTNDTNGYFHHYGGTDFSSYEDGIYRNLFDLADLNQNSTIDSYL	239
	* : * : * : * : * : * : * : * : * : * : * : * : * : * : * : * : *	
pRB01	KDAIKMWLDLGVGDIRVDAVKHMPFGWQKSFMSFINN-YKPVFTFGWEFLGVNEISPEYH	297
N-227	KDAIKMWLDLGVGDIRVDAVKHMPFGWQKSFMSFINN-YKPVFTFGWEFLGVNEISPEYH	297
A11	KDAIKMWLDLGVGDIRVDAVKHMPFGWQKSFMSFINN-YKPVFTFGWEFLGVNEISPEYH	297
1011	KDAIKMWLDLGVGDIRVDAVKHMPFGWQKSFMSFINN-YKPVFTFGWEFLGVNEISPEYH	297
I-5	KDAIKMWLDLGVGDIRVDAVKHMPFGWQKSFMSFINN-YKPVFTFGWEFLGVNEISPEYH	297
38-2	KDAIKMWLDLGVGDIRVDAVKHMPFGWQKSFMSFINN-YKPVFTFGWEFLGVNEISPEYH	297
BL11	KDAIKMWLDLGVGDIRVDAVKHMPFGWQKSFMSFINN-YKPVFTFGWEFLGVNEISPEYH	297
STEAROTHERMOPHILUS	KSAIDLWLGMDGIRFDVAVKHMPFGWQKSFVSSYGGDHPVFTFGEWYLGADQTDGDNI	298
MACERANS	KSAIDLWLGMDGIRFDVAVKHMPFGWQKSFVSSYGGDHPVFTFGEWYLGADQTDGDNI	298
THERMOSULFURIGENES	KSAIKVWLDMDGIRLDVAVKHMPFGWQKSFMSFINN-YRVPVFTFGWEFLGTNEIDVNT	298
	* : * : * : * : * : * : * : * : * : * : * : * : * : * : * : * : *	
pRB01	QFANESGMSLLDFRFAQKARQVFRDNTDNMYGLKAMLEGSEVDYAQVNDQVTFIDNHME	357
N-227	QFANESGMSLLDFRFAQKARQVFRDNTDNMYGLKAMLEGSEVDYAQVNDQVTFIDNHME	357
A11	QFANESGMSLLDFRFAQKARQVFRDNTDNMYGLKAMLEGSEVDYAQVNDQVTFIDNHME	357
1011	QFANESGMSLLDFRFAQKARQVFRDNTDNMYGLKAMLEGSEVDYAQVNDQVTFIDNHME	357
I-5	QFANESGMSLLDFRFAQKARQVFRDNTDNMYGLKAMLEGSEVDYAQVNDQVTFIDNHME	357
38-2	QFANESGMSLLDFRFAQKARQVFRDNTDNMYGLKAMLEGSEVDYAQVNDQVTFIDNHME	357
BL11	QFANESGMSLLDFRFAQKARQVFRDNTDNMYGLKAMLEGSEVDYAQVNDQVTFIDNHME	357
STEAROTHERMOPHILUS	KFANESGMNLLDFEYAEVREVRDKTETMKDLYEVLASTESQYDYINNMTVTFIDNHDM	358
MACERANS	KFANESGMNLLDFEYAEVREVRDKTETMKDLYEVLASTESQYDYINNMTVTFIDNHDM	358
THERMOSULFURIGENES	YFANESGMSLLDFRFSQKVRQVFRDNTDMYGLDSMIQSTASDYNFINDMVTFIDNHDM	358
	* : * : * : * : * : * : * : * : * : * : * : * : * : * : * : * : *	

Figure 3.4 Amino acid sequence alignment of CGTase from *Paenibacillus* sp. RB01 compared with other CGTases using ClustalX.

pRB01 = <i>Paenibacillus</i> sp. RB01	38-2 = <i>Bacillus</i> sp. 38-2
N-227 = <i>Bacillus</i> sp. N-227	BL11 = <i>Paenibacillus</i> sp. BL11
A11 = <i>Bacillus circulans</i> A11	STEAROTHERMOPHILUS = <i>Geobacillus</i> <i>stearothermophilus</i>
1011 = <i>Bacillus</i> sp. strain 1011	MACERANS = <i>Paenibacillus</i> <i>macerans</i>
I-5 = <i>Bacillus</i> sp. I-5	THERMOSULFURIGENES = <i>Thermoanaerobacterium</i> <i>thermosulfurigenes</i>

pRB01	RFHTSNGDRRKLEQALAFLLTSRQVPAIYYGSEQYMSGGNDPDNRARI	PSFSTTTTAYQV	417
N-227	RFHTSNGDRRKLEQALAFLLTSRQVPAIYYGSEQYMSGGNDPDNRARI	PSFSTTTTAYQV	417
A11	RFHTSNGDRRKLEQALAFLLTSRQVPAIYYGSEQYMSGGNDPDNRARI	PSFSTTTTAYQV	417
1011	RFHTSNGDRRKLEQALAFLLTSRQVPAIYYGSEQYMSGGNDPDNRARI	PSFSTTTTAYQV	417
I-5	RFHTSNGDRRKLEQALAFLLTSRQVPAIYYGSEQYMSGGNDPDNRARI	PSFSTTTTAYQV	417
38-2	RFHTSNGDRRKLEQALAFLLTSRQVPAIYYGSEQYMSGGNDPDNRARI	PSFSTTTTAYQV	417
BL11	RFHTSNGDRRKLEQALAFLLTSRQVPAIYYGSEQYMSGGNDPDNRARI	PSFSTTTTAYQV	417
STEAROTHERMOPHILUS	RFQVAGSGTRATEQALALTLTSRQVPAIYYGTEQYMTGDGDPPNRRAMMTS	FNTGTTAYKV	418
MACERANS	RFQVAGSGTRATEQALALTLTSRQVPAIYYGTEQYMTGDGDPPNRRAMMTS	FNTGTTAYKV	418
THERMOSULFURIGENES	RFYN-GGSTRPVEQALAFLLTSRQVPAIYYGTEQYMTGNDYVRRAMMTS	FNTSTTAYNV	417
	** ... * : ***.***** ***:***:..... * * : :*. . * **:		
pRB01	IQKLAPLRKSNPAIAYGSTQERWINNDV I IYERKFGNNVAVVA	INRNMNTPASITGLVTS	477
N-227	IQKLAPLRKSNPAIAYGSTQERWINNDV I IYERKFGNNVAVVA	INRNMNTPASITGLVTS	477
A11	IQKLAPLRKSNPAIAYGSTQERWINNDV I IYERKFGNNVAVVA	INRNMNTPASITGLVTS	477
1011	IQKLAPLRKSNPAIAYGSTQERWINNDV I IYERKFGNNVAVVA	INRNMNTPASITGLVTS	477
I-5	IQKLAPLRKSNPAIAYGSTQERWINNDV I IYERKFGNNVAVVA	INRNMNTPASITGLVTS	477
38-2	IQKLAPLRKSNPAIAYGSTQERWINNDV I IYERKFGNNVAVVA	INRNMNTPASITGLVTS	477
BL11	IQKLAPLRKSNPAIAYGSTQERWINNDV I IYERKFGNNVAVVA	INRNMNTPASITGLVTS	477
STEAROTHERMOPHILUS	IQALAPLRKSNPAIAYGTTTTERVWVNDVLI IERKFGSSAALVA	INRNSAAYPISGLLS	478
MACERANS	IQALAPLRKSNPAIAYGTTTTERVWVNDVLI IERKFGSSAALVA	INRNSAAYPISGLLS	478
THERMOSULFURIGENES	IKKLAPLRKSNPAIAYGTTQQRWINNDV I IYERKFGNNVALVA	INRNLTSYNI TGLYTA	477
	* :*.***:***:*** * **:*. ** : ***:.....*:***. . : **:* :		
pRB01	LPQGSYNDVLGGILNGNTLTVGAGGAASNFTLAPGGTAVWQYTTDATAPI	IGNVGPMMAK	537
N-227	LPQGSYNDVLGGILNGNTLTVGAGGAASNFTLAPGGTAVWQYTTDATAPI	IGNVGPMMAK	537
A11	LPQGSYNDVLGGILNGNTLTVGAGGAASNFTLAPGGTAVWQYTTDATAPI	IGNVGPMMAK	537
1011	LPQGSYNDVLGGILNGNTLTVGAGGAASNFTLAPGGTAVWQYTTDATAPI	IGNVGPMMAK	537
I-5	LPQGSYNDVLGGILNGNTLTVGAGGAASNFTLAPGGTAVWQYTTDATAPI	IGNVGPMMAK	537
38-2	LPQGSYNDVLGGILNGNTLTVGAGGAASNFTLAPGGTAVWQYTTDATAPI	IGNVGPMMAK	537
BL11	LPQGSYNDVLGGILNGNTLTVGAGGAASNFTLAPGGTAVWQYTTDATAPI	IGNVGPMMAK	537
STEAROTHERMOPHILUS	LPAGTYSVDVLLNGLLNGNSITVSGGAVTNFTLAAGGTAVWQYTAPETS	PAIGNVGTMTGQ	538
MACERANS	LPAGTYSVDVLLNGLLNGNSITVSGGAVTNFTLAAGGTAVWQYTAPETS	PAIGNVGTMTGQ	538
THERMOSULFURIGENES	LPAGTYTDVLLNGLLNGNSISVASDGSVTFTLSAGEVAWQYVSSNS	PLIGHVGTMTK	537
	* :*.***. . * **:* ** . :*.***: . : . * . ** * : . : * **:* :		
pRB01	PGVTTITIDGRGFGSGKGTVYFGTTAVTGADIVAWEDTQIQVKIPAV	PGGIYDIRVANAAG	597
N-227	PGVTTITIDGRGFGSGKGTVYFGTTAVTGADIVAWEDTQIQVKIPAV	PGGIYDIRVANAAG	597
A11	PGVTTITIDGRGFGSGKGTVYFGTTAVTGADIVAWEDTQIQVKIPAV	PGGIYDIRVANAAG	597
1011	PGVTTITIDGRGFGSGKGTVYFGTTAVTGADIVAWEDTQIQVKIPAV	PGGIYDIRVANAAG	597
I-5	PGVTTITIDGRGFGSGKGTVYFGTTAVTGADIVAWEDTQIQVKIPAV	PGGIYDIRVANAAG	597
38-2	PGVTTITIDGRGFGSGKGTVYFGTTAVTGADIVAWEDTQIQVKIPAV	PGGIYDIRVANAAG	597
BL11	PGVTTITIDGRGFGSGKGTVYFGTTAVTGADIVAWEDTQIQVKIPAV	PGGIYDIRVANAAG	597
STEAROTHERMOPHILUS	PGNIVTIDGRGFGGTAGTVYFGTTAVTGSGIVSWEDTQIKAVIPKVA	AGKTVGSVKTSSG	598
MACERANS	PGNIVTIDGRGFGGTAGTVYFGTTAVTGSGIVSWEDTQIKAVIPKVA	AGKTVGSVKTSSG	598
THERMOSULFURIGENES	AGQTITIDGRGFGTTSGVLFVGSTAGT---IVSWDDTEVKVVP	SVTPGKYNISLKTSSG	594
	* :***. . * **:* ** . :*.***: . : . * . ** * : . : * **:* :		
pRB01	AASNIYDNFEVLTGQVTVRFINNATTALGQNVFLTGNVSELGNWDPNNA	I GPMYNQVV	657
N-227	AASNIYDNFEVLTGQVTVRFINNATTALGQNVFLTGNVSELGNWDPNNA	I GPMYNQVV	657
A11	AASNIYDNFEVLTGQVTVRFINNATTALGQNVFLTGNVSELGNWDPNNA	I GPMYNQVV	657
1011	AASNIYDNFEVLTGQVTVRFINNATTALGQNVFLTGNVSELGNWDPNNA	I GPMYNQVV	657
I-5	AASNIYDNFEVLTGQVTVRFINNATTALGQNVFLTGNVSELGNWDPNNA	I GPMYNQVV	657
38-2	AASNIYDNFEVLTGQVTVRFINNATTALGQNVFLTGNVSELGNWDPNNA	I GPMYNQVV	657
BL11	AASNIYDNFEVLTGQVTVRFINNATTALGQNVFLTGNVSELGNWDPNNA	I GPMYNQVV	657
STEAROTHERMOPHILUS	TASNTFKSFNVLTVRFLVQANTNYGTVYLVGNAAELGSDPNKAI	GPMYNQVI	658
MACERANS	TASNTFKSFNVLTVRFLVQANTNYGTVYLVGNAAELGSDPNKAI	GPMYNQVI	658
THERMOSULFURIGENES	ATSNNTNNINLTGNQICVRFVNNASTVYGENVYLTGNVAELGNWD	TSKAIGPMFNQVV	654
	* :.***:***:*** * **:*. ** . :*.***: . : . * . ** * : . : * **:* :		
pRB01	YQYPTWYDVSVPAGQTIEFKFLKKQG-STVWTEGGANRTFTTPTSGTAT	MNVNWQP	713
N-227	YQYPTWYDVSVPAGQTIEFKFLKKQG-STVWTEGGANRTFTTPTSGTAT	MNVNWQP	713
A11	YQYPTWYDVSVPAGQTIEFKFLKKQG-STVWTEGGANRTFTTPTSGTAT	MNVNWQP	713
1011	YQYPTWYDVSVPAGQTIEFKFLKKQG-STVWTEGGANRTFTTPTSGTAT	MNVNWQP	713
I-5	YQYPTWYDVSVPAGQTIEFKFLKKQG-STVWTEGGANRTFTTPTSGTAT	MNVNWQP	712
38-2	YQYPTWYDVSVPAGQTIEFKFLKKQG-STVWTEGGANRTFTTPTSGTAT	MNVNWQP	712
BL11	YQYPTWYDVSVPAGQTIEFKF-----	679	
STEAROTHERMOPHILUS	AKYPSWYDVSVPAGTKLDFKIKKGG-GTVWTEGGNHTYTPASGVGT	VTVDWQN	714
MACERANS	AKYPSWYDVSVPAGTKLDFKIKKGG-GTVWTEGGNHTYTPASGVGT	VTVDWQN	714
THERMOSULFURIGENES	YQYPTWYDVSVPAGTIIQFKFKKNG-NITWTEGGSNHTYTPSSSTG	TVINWQQ	710
	.*** ** ***** * ..:***		

Figure 3.4 (continues) Amino acid sequence alignment of CGTase from *Paenibacillus* sp. RB01 compared with other CGTases using ClustalX.

- |  |   |
|--|---|
| pRB01 = <i>Paenibacillus</i> sp. RB01  | 38-2 = <i>Bacillus</i> sp. 38-2   |
| N-227 = <i>Bacillus</i> sp. N-227      | BL11 = <i>Paenibacillus</i> sp. BL11  |
| A11 = <i>Bacillus circulans</i> A11    | STEAROTHERMOPHILUS = <i>Geobacillus</i> <i>stearothermophilus</i>           |
| 1011 = <i>Bacillus</i> sp. strain 1011 | MACERANS = <i>Paenibacillus</i> <i>macerans</i>                             |
| I-5 = <i>Bacillus</i> sp. I-5          | THERMOSULFURIGENES = <i>Thermoanaerobacterium</i> <i>thermosulfurigenes</i> |

Table 3.1 Percent similarity of deduced amino acid sequence of CGTase from *Paenibacillus* sp. RB01 compared with other CGTases by pairwise alignment. The accession number and source of CGTase were from NCBI database.

Accession number	Organism	Number of amino acid	% Similarity
	<i>Paenibacillus</i> sp. RB01	713	100
ABG02281	<i>Bacillus</i> sp. N-227	713	100
AAG31622.1	<i>Bacillus circulans</i> A11	713	100
DQ243816	<i>Paenibacillus</i> sp. BL11	679	99
AAA22308	<i>Bacillus</i> sp. strain 1011	713	98
AY478421	<i>Bacillus</i> sp. I-5	712	98
M19880	<i>Bacillus</i> sp. 38-2	712	98
AAB00845	<i>Thermoanaerobacterium thermosulfurigenes</i>	710	68
AF047363	<i>Paenibacillus macerans</i>	714	66
AAA22298	<i>Geobacillus stearothermophilus</i>	714	64
CAA41770	<i>Geobacillus stearothermophilus</i>	711	60



His93 in pRB01 (Figure 3.4). The phylogenetic tree (Figure 3.5) was constructed and the result showed that the *cgt* in recombinant plasmid occupied the phylogenetic position very close to those in *Bacillus* sp. N-227 (ABG02281) and *Paenibacillus* sp. A11 (AAG31622.1).

These results confirmed that the recombinant plasmid contained the *cgt* of *Paenibacillus* sp. RB01.

### 3.1.2 Expression of cloned CGTase

The *E.coli* BL21 (DE3) containing *ctg* was cultivated in LB broth containing ampicillin antibiotic. The enzyme production was induced with IPTG at final concentration of 0-20  $\mu\text{M}$ . The growth rate was followed by  $A_{600}$ , the result showed a rapid growth rate of the *E. coli* from 0-6 hrs after induction (Figure 3.6A). The growth rate at 5 and 20  $\mu\text{M}$  IPTG induction was similar. The enzyme activity was found in the supernatant after 6 hrs of induction and the enzyme production increased until 24 hrs after induction. Without IPTG induction the recombinant cells did not show dextrinizing activity (Figure 3.6B). The enzyme activity was increased correlated with the concentration of IPTG. However, the enzyme activity obtained by induction with 5 and 20  $\mu\text{M}$  IPTG was not different. The specific dextrinizing activity significantly increased between 6-12 hrs of induction (Figure 3.6C) with all IPTG concentrations. After 12 hrs of induction, the specific activity was slightly increased. However, at low IPTG, the specific activity of the enzyme was level off after 24 hrs. From the result, the IPTG final concentration of 5  $\mu\text{M}$  was selected for enzyme induction in further experiment.

### 3.2 Prediction of labile asparagines of CGTase from *Paenibacillus* sp. RB01

Labile asparagine residues which are prone to deamidation in the CGTase was predicted by using available 3D-structure information from Protein Data Bank. There are many factors affected to deamidation reaction of asparagine residue e.g. primary sequence, secondary structure, and 3D-structure, of the protein. (Chazin and Kossiakov, 1995) Since 3D-structure of RB01 CGTase is unknown, the prediction by using provided 3D information of the CGTase from alkalophilic *Bacillus* sp. 1011 (PDB code 1PAM), which had 98% similarity in amino acid sequence with the CGTase from *Paenibacillus*

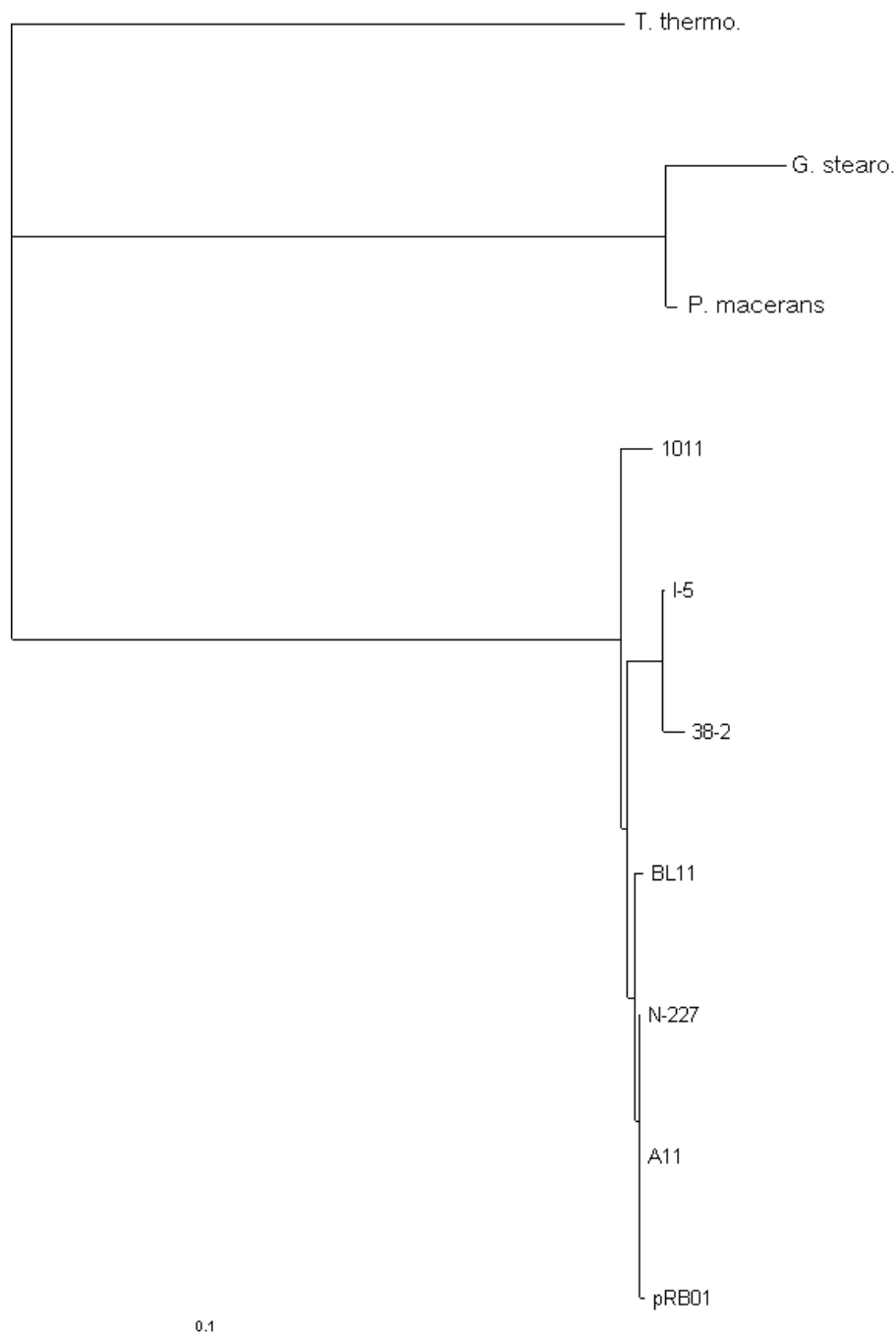


Figure 3.5 Neighbor-joining tree based on amino acid similarity among CGTases. Tree construction using the neighbor-joining method and bootstrap analysis was performed with ClustalX.

pRB01 = *Paenibacillus* sp. RB01

N-227 = *Bacillus* sp. N-227

A11 = *Bacillus circulans* A11

BL11 = *Paenibacillus* sp. BL11

1011 = *Bacillus* sp. strain 1011

I-5 = *Bacillus* sp. I-5

38-2 = *Bacillus* sp. 38-2

*P. macerans* = *Paenibacillus macerans*

*G. stearotherm* = *Geobacillus stearothermophilus*

*T. thermo* = *Thermoanaerobacterium thermosulfurigenes*

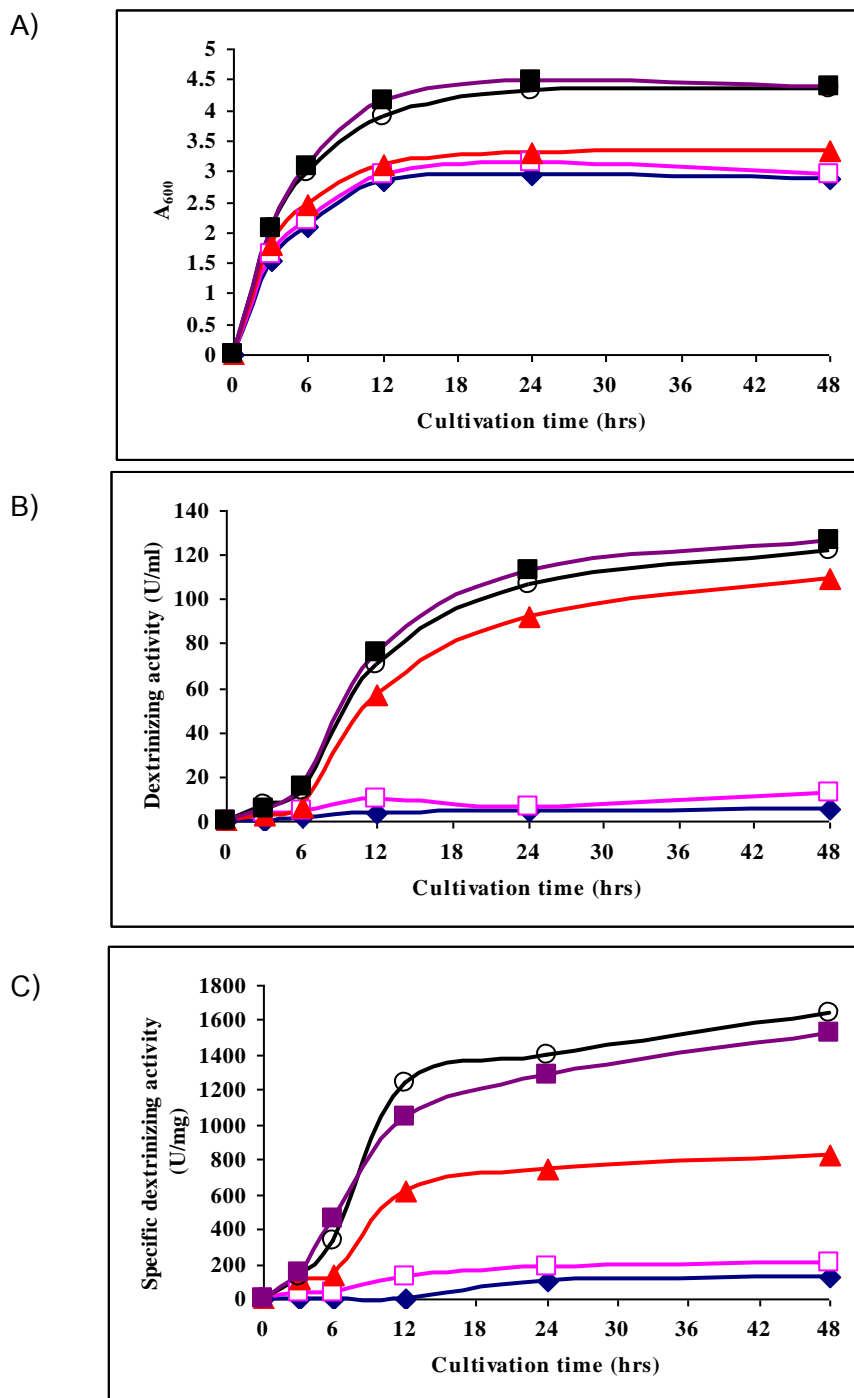
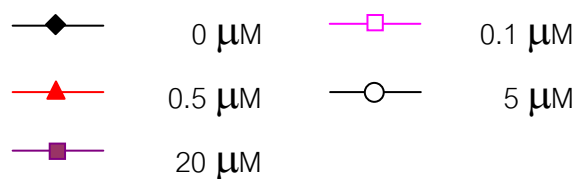


Figure 3.6 Optimization of IPTG induction of cloned CGTase in pET19b vector and expressed by *E. coli* BL21 (DE3). A) Growth profile B) Dextrinizing activity

C) Specific dextrinizing activity.



sp. RB01 was performed. Both CGTases had 713 amino acid residues. However, 7 positions showed different amino acids (Table 3.2, see also Figure 3.4). Among the amino acid difference between 1PAM and RB01, the amino acid position 93 is noticeable because this position in 1PAM is Asn while in RB01 this amino acid position is His. Thus, the CGTase from RB01 contained only 63 Asn residues while 1PAM contained 64 Asn residues.

By using the program from [www.deamidation.com](http://www.deamidation.com), the predicted deamidation index (ID value) of CGTase and coefficient of deamidation (CD value) of 64 Asn residues in CGTase were calculated. The ID value indicates net deamidation half-life for protein with all Asn residues considered. 1PAM had ID value of 0.15834 which means the predicted half-life of this enzyme was 15.834 days ( $ID \times 100$ ). The CD value indicates the relative rate of deamidation of each Asn residue based on the nearest neighbor amino acids and the 3D-structure. From Table 3.3, the most labile Asn residue in 1PAM is Asn 336 which had a CD value of 1.004 and the most stable Asn173 had CD value of 26,445.997. Asn93 in 1PAM, which is replaced by His in RB01, was relatively labile since the CD value was 25.121.

### 3.3 Site-directed mutagenesis at labile Asn residues of CGTase

The selected 12 Asn residues according to the CD values and X-ray crystallographic structure of 1PAM were listed in Table 3.4. The half-life ( $T_{1/2}$ ) days was calculated based on the primary sequence of GlyXxxAsnYyyGly synthetic peptide (Robinson and Robinson, 2001). The exception for this synthetic peptide is the double amide peptide half-times of which the half-life days cannot be calculated from the straight forward formula. They are in the range of about 20, 40, 5,000, and 5,000 days for the third residues in GlyXxxAsnAsnGly, GlyXxxAsnGlnGly, GlyXxxGlnAsnGly, and GlyXxxGlnGlnGly, respectively. Appendix 8 for the example of computed  $T_{1/2}$  and CD value on human phenylalanine hydroxylase.

The selected Asn residues can be divided into 4 groups as follows:

- Asn residues which have low CD values (from 1-100): Asn336, Asn370, Asn326, Asn620 and Asn427 which have CD values of 1.004, 3.854, 10.516, and 53.416.

Table 3.2 Amino acid difference in CGTase of *Paenibacillus* sp. RB01 and *Bacillus* sp. 1011

Amino acid position (numbering without 27 signal amino acid sequence)	Domain	Amino acid residue in RB01	Amino acid residue in 1PAM
93	A-B	His	Asn
244	A-B	Ser	Ala
378	A-B	Ile	Leu
410	C	Glu	His
453	C	Glu	Arg
498	D	Ala	Tyr
680	E	Met	Val

Table 3.3 An overview of the primary sequence of asparagine residues and coefficient of deamidation (CD value) and predicted by the program from [www.deamidation.org](http://www.deamidation.org) using 3D structure information of alkalophilic *Bacillus* sp. 1011 (Protein Data Bank code 1PAM).

Number	Primary Sequence	CD Value
1	SER-ASN336-GLY	1.004
2	ILE-ASN415-ASN	1.067
3	ASP-ASN326-HIS	1.347
4	ALA-ASN567-ALA	1.703
5	GLU-ASN188-GLY	1.901
6	LEU-ASN465-GLY	2.006
7	TYR-ASN457-ASP	2.727
8	GLY-ASN467-THR	2.744
9	GLY-ASN370-ASP	3.854
10	ASN-ASN620-ALA	10.516
11	ILE-ASN594-ASN	13.193
12	PRO-ASN619-ASN	18.888
13	ILE-ASN247-ASN	19.062
14	GLN-ASN603-VAL	19.148
15	GLU-ASN154-GLY	19.492
16	GLN-ASN11-PHE	20.037
17	LEU-ASN201-HIS	20.269
18	GLU-ASN82-ILE	21.116
19	VAL-ASN93*-ASN	25.121
20	ASP-ASN160-GLY	31.403
21	ASP-ASN299-MET	32.823

Number	Primary Sequence	CD Value
22	ASN-ASN595-ALA	37.777
23	ALA-ASN667-ARG	45.404
24	ASN-ASN94-THR	46.260
25	ILE-ASN62-ASP	47.698
26	MET-ASN439-THR	48.438
27	SER-ASN574-ILE	52.171
28	SER-ASN8-LYS	52.731
29	GLY-ASN427-ASN	53.416
30	VAL-ASN683-TRP	55.832
31	THR-ASN169-ASP	62.945
32	GLY-ASN162-LEU	65.315
33	VAL-ASN263-GLU	68.124
34	ASN-ASN248-TYR	72.338
35	VAL-ASN681-VAL	76.260
36	TYR-ASN627-GLN	90.303
37	GLY-ASN503-VAL	92.989
38	SER-ASN479-PHE	103.535
39	ASN-ASN428-VAL	105.027
40	ASN-ASN33-PRO	114.141
41	PRO-ASN139-HIS	114.141
42	VAL-ASN318-ASP	117.540

Number	Primary Sequence	CD Value
43	ASN-ASN416-ASP	129.605
44	ASP-ASN578-PHE	136.504
45	ILE-ASN435-ARG	158.306
46	GLY-ASN29-PRO	172.680
47	ARG-ASN437-MET	179.018
48	LYS-ASN193-LEU	187.533
49	ILE-ASN88-TYR	189.061
50	ALA-ASN32-ASN	207.564
51	ASP-ASN374-ARG	207.895
52	THR-ASN109-PRO	217.335
53	ASN-ASN204-SER	225.868
54	LYS-ASN120-LEU	297.066
55	ALA-ASN274-GLU	306.815
56	GLY-ASN609-VAL	337.132
57	THR-ASN45-LEU	355.281
58	HIS-ASN203-ASN	382.569
59	ASP-ASN296-THR	478.634
60	HIS-ASN129-ILE	1,036.899
61	SER-ASN401-PRO	1,057.685
62	ILE-ASN59-LYS	1,531.409
63	GLY-ASN615-TRP	2,010.087
64	GLN-ASN173-LEU	26,445.997

\* This asparagine residue was substituted by histidine in *Paenibacillus* sp. RB01.

Table 3.4 The list of 12 asparagine residues selected for single mutation and the domain location.  $T_{1/2}$  represents the first-order deamidation half-time predicted from the primary amino acid sequence.

Number	Primary Sequence	$T_{1/2}$ (days)	CD Value	Domain <sup>a</sup>
1	SER-ASN336-GLY	24.1	1.004	A2
2	ILE-ASN415-ASN	ND	1.067	A2
3	ASP-ASN326-HIS	10.2	1.347	A2
4	ALA-ASN567-ALA	22.5	1.703	D
5	GLU-ASN188-GLY	25.8	1.901	A-B
6	GLY-ASN370-ASP	28.0	3.854	A-B
7	ASN-ASN620-ALA	ND	10.516	E
8	ILE-ASN247-ASN	ND	19.062	A-B
9	GLY-ASN427-ASN	ND	53.416	C
10	VAL-ASN263-GLU	33.5	68.124	A-B
11	ASN-ASN428-VAL	ND	105.027	C
12	ILE-ASN435-ARG	66.4	158.306	C

\*ND indicates “not determined” since the sequence contains a double amide peptide which calculation of half-life is not straight forward

<sup>a</sup> see domain structure of CGTase in Figure 1.3



- Asn residues which have intermediate CD values (100-200): Asn428 and Asn435 which have CD values of 105.027 and 158.306.
- Asn residues which have high CD values (from 200 up): Asn109, Asn296 and Asn401 which had CD values of 217.335, 478.634 and 1,057.685, respectively.
- Asn residues which are close to the active site: Asn247, Asn263 which have CD values of 19.062 and 68.124, respectively.

A single mutation was performed as described in section 2.7.1. The location of each selected Asn on 3D-structure was shown in Figure 3.7. The colonies of those mutants were confirmed by nucleotide sequencing (data not shown). The result indicated that all mutated positions had G instead of A in the codon AAT which led to the change in amino acid from Asn to Asp residues. All mutants were investigated for their activity and isoform pattern.

Besides 12 single mutations, a double and a triple mutation were also performed. A double mutant (N336D/N415D) and a triple mutant (N336D/N415D/N326D) were also examined for their activity and isoform pattern.

### 3.4 Comparison of dextrinizing activity of CGTase from 3 sources: native, cloned, and mutated CGTase

The dextrinizing activity, protein, and specific activity of all different forms of CGTase; native, cloned and mutated, were compared (Table 3.5). Specific activity of the enzyme from cloned was higher than the native CGTase from *Paenibacillus* sp. RB01. For 13 single, 1 double, and 1 triple mutants, expressed CGTases could be divided into 3 groups, as follows:

1. Those with no change in specific activity as compared to the cloned: N188D, N247D, N336D, N620D
2. Those with lower specific activity as compared to the cloned: N326D, N435D, N567D, N336Q. Extremely low specific activity was observed in N263D, N370D, N427D, N428D, and the triple mutant.
3. Those with higher specific activity as compared to the cloned: N415D, and double mutant N336D/N415D

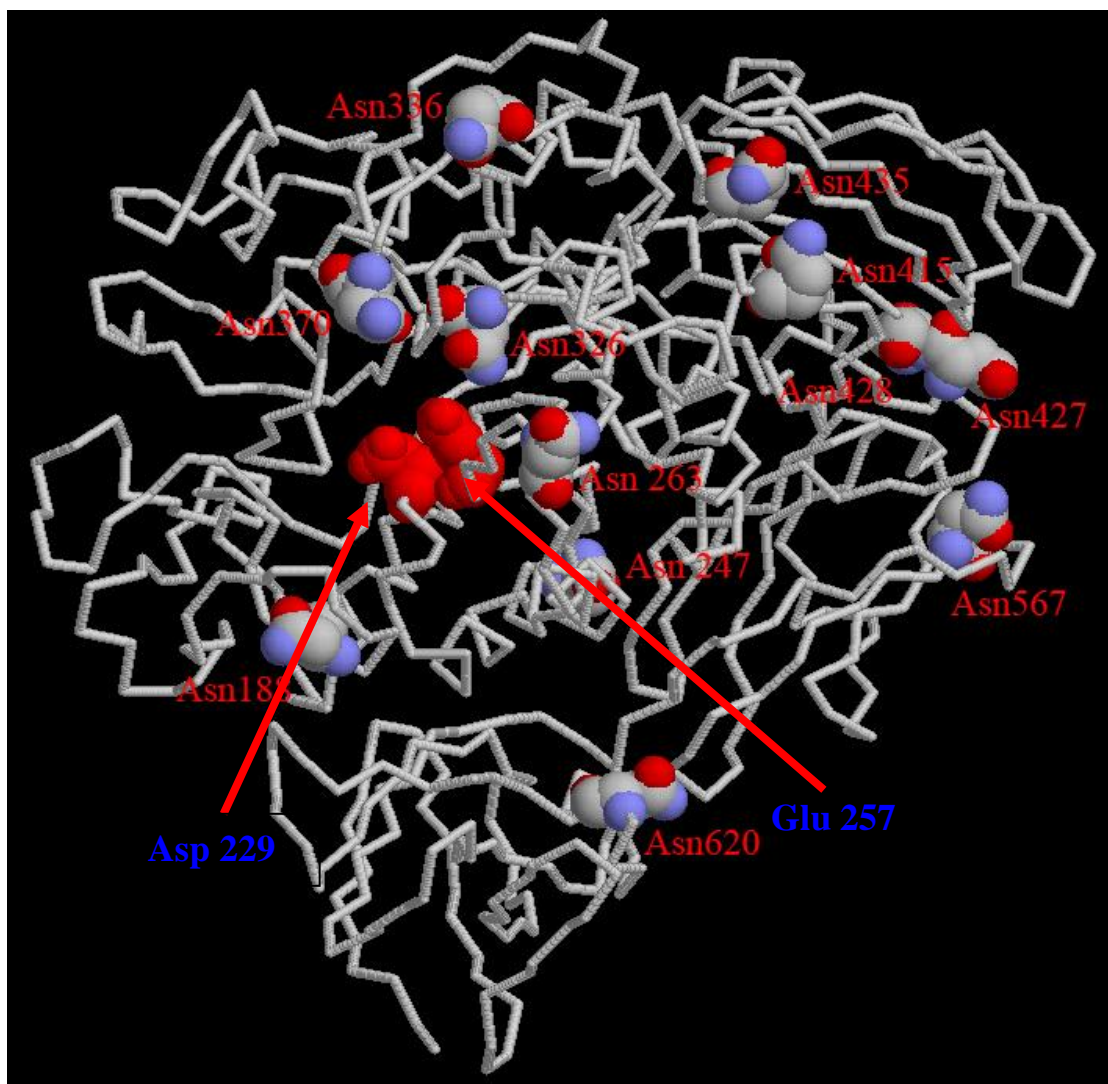


Figure 3.7 Location of selected asparagine residues for site-directed mutagenesis using 3D information of 1PAM. Blue arrow indicates Asp229 and Glu257 which are the active site residues of the CGTase.

Table 3.5 Dextrinizing activities of crude cloned and mutated CGTases expressed by *E.coli* BL21(DE3)

Source of CGTase	Activity (U/ml)	Protein (mg/ml)	Specific activity (U/mg)
Cloned CGTase	15.9	8.1	1.96
N188D	19.8	10.4	1.90
N247D	18.8	9.9	1.88
N263D	2.4	4.7	0.52
N326D	2.1	2.6	0.82
N336D	15.8	8.9	1.77
N370D	1.7	4.2	0.34
N415D	36.3	11.3	3.22
N427D	3.3	9.3	0.36
N428D	2.2	9.7	0.23
N435D	6.2	7.0	0.89
N567D	6.1	6.3	0.98
N620D	6.9	4.2	1.65
N336Q	5.2	4.3	1.20
N336D/N415D	37.6	10.1	3.73
N336D/N415D/N567D	2.2	4.7	0.47

### 3.5 Comparison of the isoform pattern of CGTases from 3 sources: native, cloned and mutated CGTase

#### 3.5.1 Isoform formation of native CGTase from *Paenibacillus* sp. RB01

*Paenibacillus* sp. RB01 was cultivated in Horikoshi medium (pH 9.0) and the enzyme was collected at interval times of 24, 48 and 72 hrs. The isoform pattern of the crude enzyme was immediately investigated on native-PAGE and the gel of dextrinizing activity staining was shown in Figure 3.8. At 24 hrs, the major band on this PAGE was the isoform I (Lane 1). After cultivation for 48 hrs, the isoform II was observed but with less intensity than isoform I (Lane 2). The sample at 72 hrs of cultivation showed isoform II with almost equal intensity as isoform I (Lane 3). In addition to isoform I and II, trace amount of the fast-moving isoform III could be observed at 48 and 72 hrs of cultivation. The net negative charge was increased from isoform I to isoform II to isoform III. However, these isoforms showed the same size on SDS-PAGE.

#### 3.5.2 Isoform formation of cloned CGTase expressed by *E. coli* BL21 (DE3)

The cloned CGTase expressed by *E. coli* BL21 (DE3) was cultivated in LB medium (pH 7.0) and the enzyme after IPTG induction for 24 hrs was collected. The enzyme was further incubated at room temperature for 24 and 48 hrs. The isoform pattern of the crude enzyme was immediately investigated on native-PAGE and the gel of dextrinizing activity staining was shown in Figure 3.9. The cloned enzyme at 24 hrs after IPTG induction (Lane 1) showed only the isoform I. The isoform II at 48 and 72 hrs after IPTG induction was observed in Lane 2 and 3, respectively.

#### 3.5.3 Comparison of Isoform pattern between native CGTase and cloned CGTase

The isoform pattern of native CGTase produced by *Paenibacillus* sp. RB01 and cloned CGTase expressed by *E. coli* BL21 (DE3) were compared on native-PAGE and IEF-PAGE as shown in Figure 3.10A and B. The enzyme showed at least 3 isoforms with difference in the relative mobility (Figure 3.10A Lane 1 and 2). The relative mobilities of those isoforms from both sources on native-PAGE were the same. Also the pI values of the isoforms on IEF-PAGE were the same. It was noticed that the cloned CGTase

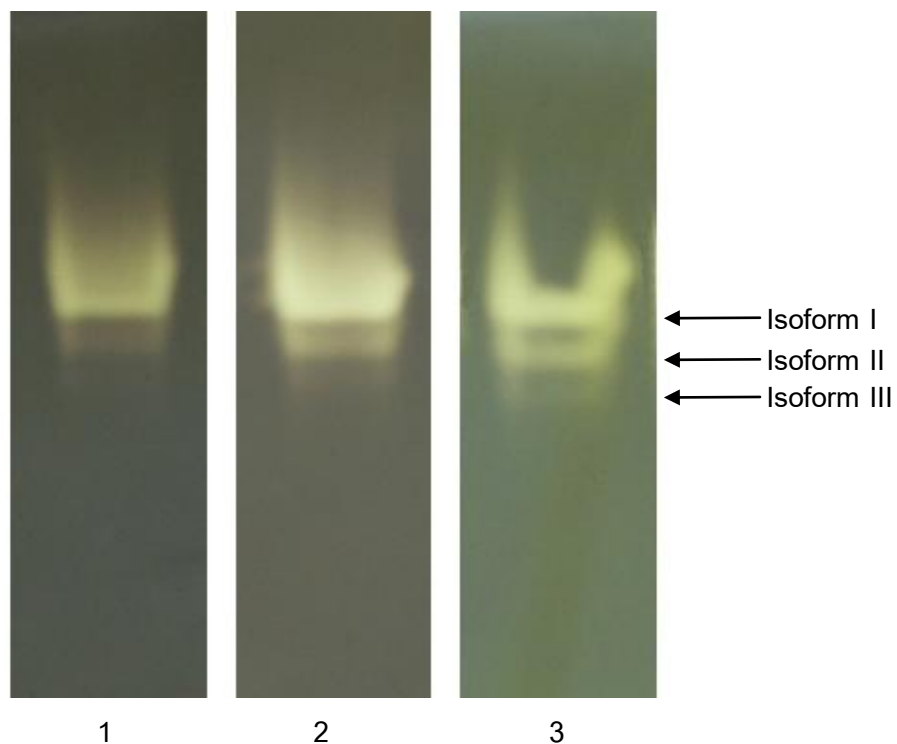


Figure 3.8 Non-denaturing PAGE of crude native CGTase of *Paenibacillus* sp. RB01 at different time of cultivation. Dextrinizing activity staining was performed. The samples were loaded at 0.6 unit/Lane.

Lane 1 = Sample at 24 hrs of cultivation

Lane 2 = Sample at 48 hrs of cultivation

Lane 3 = Sample at 72 hrs of cultivation

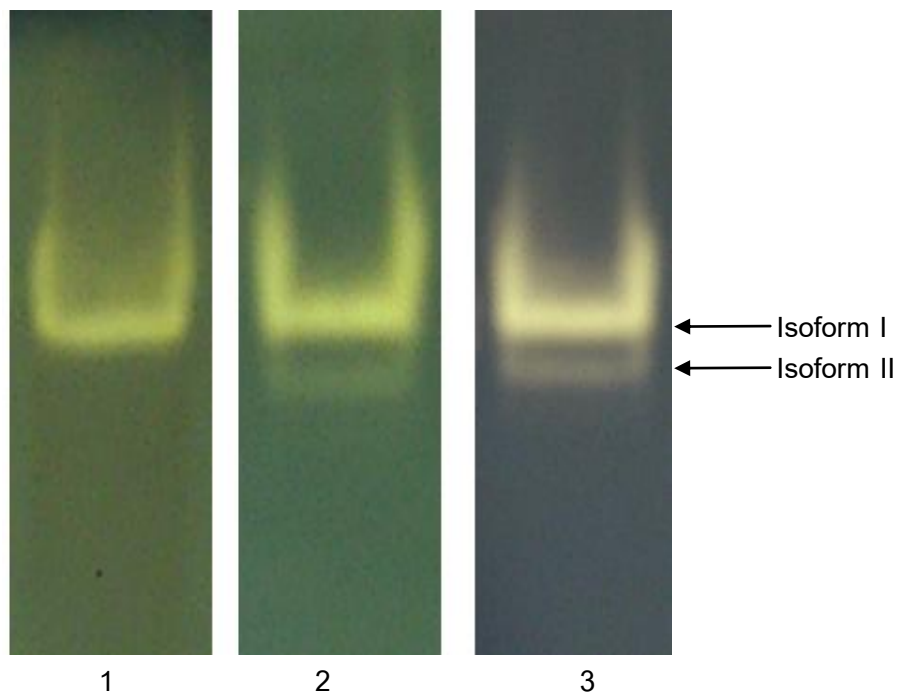


Figure 3.9 Non-denaturing PAGE of crude cloned CGTase expressed by *E. coli* BL21 (DE3) at different time after IPTG induction. Dextrinizing activity staining was performed. The samples were loaded at 0.6 U/Lane.

Lane 1 = Sample at 24 hrs after IPTG induction

Lane 2 = Sample at 48 hrs after IPTG induction

Lane 3 = Sample at 72 hrs after IPTG induction

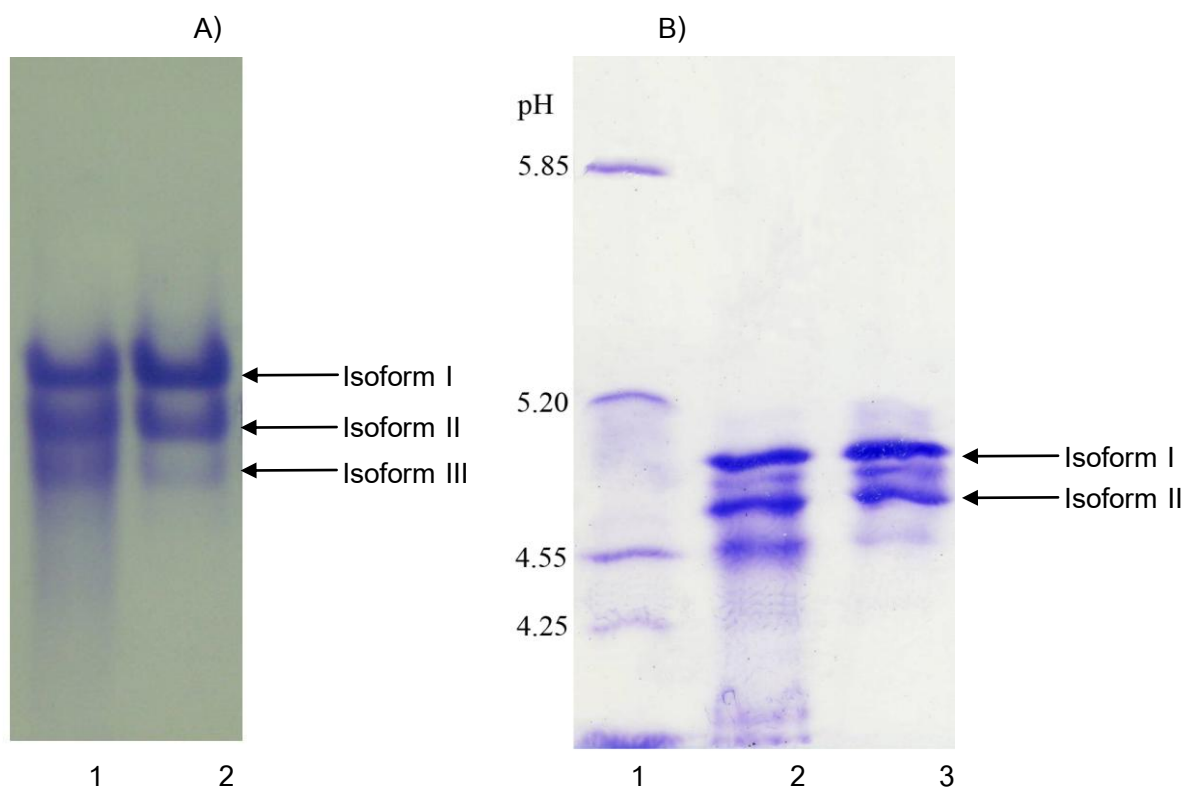


Figure 3.10 Coomassie blue staining of isoform pattern of CGTase from *Paenibacillus* sp. RB01 compared with cloned CGTase expressed by *E. coli* BL21 (DE3) on A) native-PAGE and B) IEF-PAGE. Both CGTases were in the partially purified form by starch adsorption.

A) Isoform pattern on 7% native-PAGE

Lane 1 = native CGTase from  
*Paenibacillus* sp. RB01

Lane 2 = cloned CGTase from *E. coli*  
BL21 (DE3)

B) Isoform pattern on IEF-PAGE.

Lane 1 = pI marker proteins

Lane 2 = native CGTase from  
*Paenibacillus* sp. RB01

Lane 3 = cloned CGTase from *E. coli*  
BL21 (DE3)

showed less isoform III than the native enzyme. And an intermediate band between isoform I and II was observed on IEF-PAGE (Figure 3.10 A and B). The pI values of the isoforms were calculated by comparison with standard curve of pI (Figure 3.11) and the pI values were 4.87, 4.75 and 4.55 for the isoform I, II and III, respectively.

### **3.5.4 Comparison of isoform pattern between cloned and mutated CGTase expressed by *E. coli* BL21 (DE3)**

#### **3.5.4.1 Isoform pattern of cloned vs. single mutated enzymes on native-PAGE**

The mutated CGTases were created by site-directed mutagenesis in which the selected Asn residue was changed into Asp residue. This mutation influenced to the net charge of the mutated enzyme. The isoform pattern of mutated CGTases on native-PAGE was investigated and shown in Figure 3.12 A and B. According to the relative mobility of the major isoform (band) of mutated CGTase compared to the cloned CGTase (Figure 3.12A and B), the mutated enzymes can be divided into 2 groups:

- 1) The mutated enzymes of which the major band showed similar relative mobility as the isoform II of cloned CGTase. They are from the mutants N336D, N415D, N567D, N427D, N428D, N435D and N188D (Figure 3.12A Lane 2-8).
- 2) The mutated enzymes of which the major band showed different relative mobility from the isoform II of cloned CGTase. They are from the mutants N263D, N326D, N370D, N620D and N247 (Figure 3.12B Lane 2-6).

On the other hands, the mutation at position 336 from Asn into Gln (N336Q) in Figure 3.12B Lane 7 showed that the relative mobility of the major band was similar to the isoform I of cloned CGTase. This result supported that the relative mobility of N336D was changed because of the increasing of negative charge from Asp residue.

#### **3.5.4.2 Isoform pattern of cloned vs. double and triple mutated enzymes on native-PAGE**

Double and triple mutation was performed by selected the pair and group of single mutation. Based on the CD values and relative mobilities of mutated CGTases on



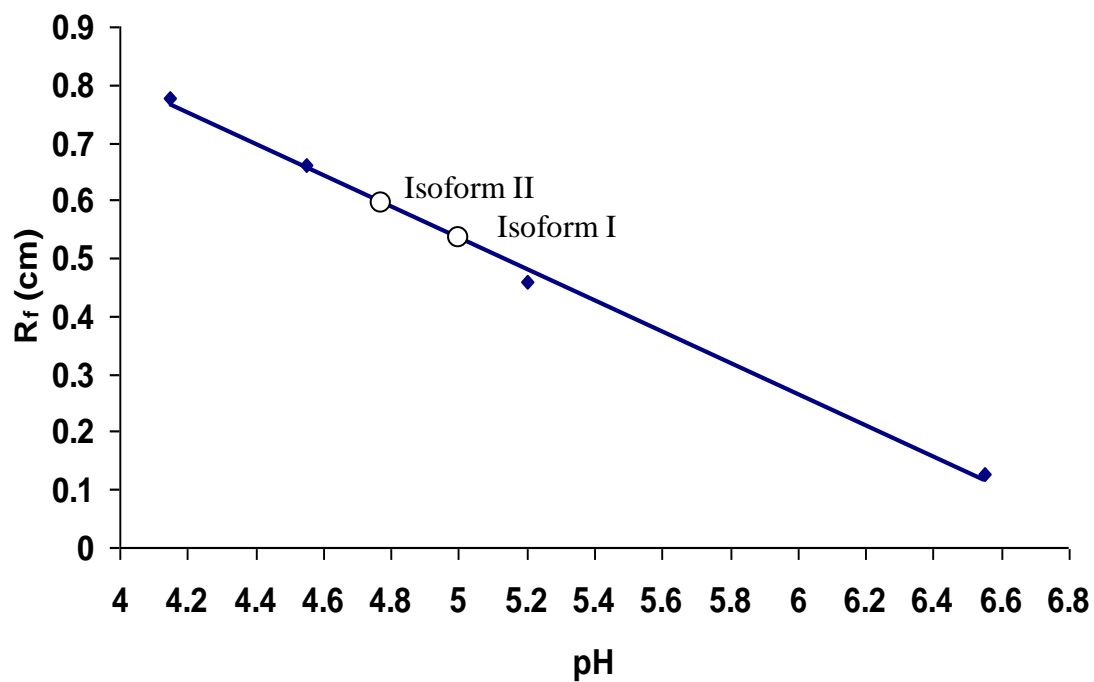


Figure 3.11 Standard curve of pI and relative mobility on IEF-PAGE.

◆ pI marker proteins:

carbonic anhydrase B (bovine) pI 5.85

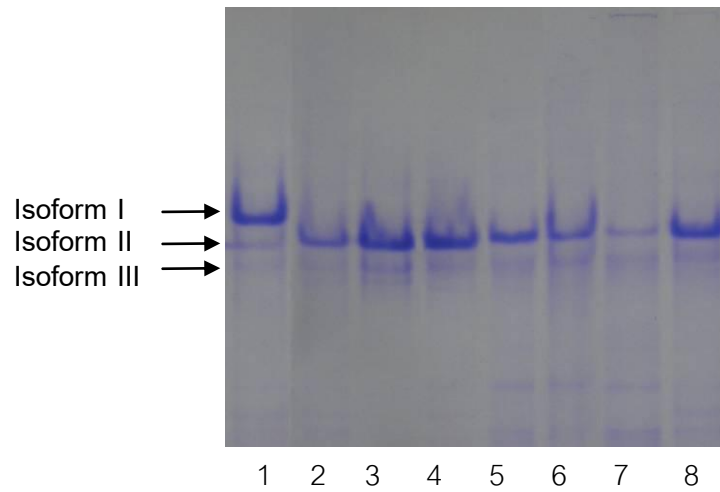
$\beta$ -lactoglobulin A pI 5.20

trypsin inhibitor pI 4.55

glucose oxidase pI 4.20

○ CGTase Isoforms

A)



B)

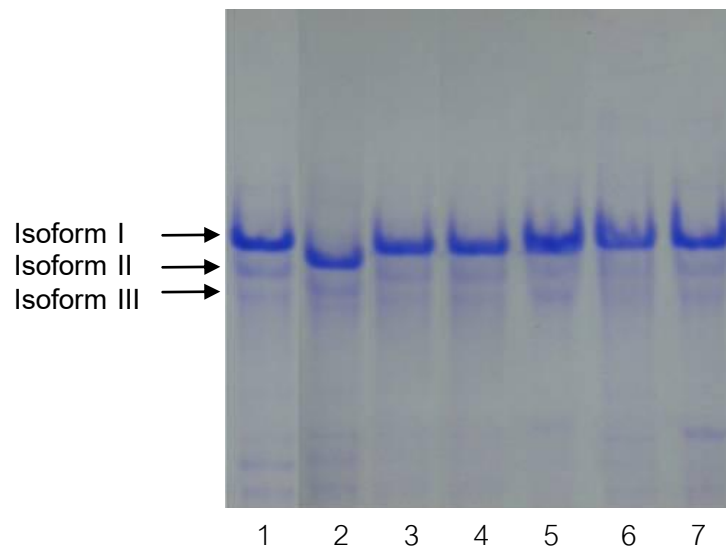


Figure 3.12 Coomassie blue staining of non-denaturing PAGE of crude cloned and mutated CGTase. The samples were loaded at 20  $\mu$ g/Lane.

A)

Lane 1 = Cloned CGTase

Lane 2 = N336D

Lane 3 = N415D

Lane 4 = N567D

Lane 5 = N427D

Lane 6 = N428D

Lane 7 = N435D

Lane 8 = N188D

B)

Lane 1 = Cloned CGTase

Lane 2 = N263D

Lane 3 = N326D

Lane 4 = N370D

Lane 5 = N620D

Lane 6 = N247D

Lane 7 = N336Q

N = Asn, D = Asp, Q = Gln

native-PAGE, pairs of N336 and N415 were selected to create a double mutated CGTase. The relative mobility of cloned CGTase compared with double mutated CGTase was shown in Figure 3.13 Lane 1 and 2 respectively. The result showed that the major band of N336D/N415D had a relative mobility similar to the isoform III of cloned enzyme.

From the result of double mutation and the CD value in Table 3.3, Asn326 was the third labile Asn residue following Asn336 and Asn415, so this position was chosen to create the triple mutation. The relative mobility of this triple mutated CGTase (N336D/N415D/N326D) was also checked on native-PAGE. However, the major band of the triple mutated CGTase had the same relative mobility as the double mutated CGTase (N336D/N415D) (Fig 3.13, Lane 2 and 3). The result was not surprised because the single mutant (N326D) showed the major band which had the same relative mobility as isoform I of cloned CGTase (Figure 3.12B Lane 3).

The double and triple mutated CGTases had the same pI value as shown in Figure 3.14

#### 3.5.4.3 Isoform pattern of cloned vs. mutated CGTase on IEF-PAGE

The crude cloned and mutated CGTases were dialyzed against water to remove salt from the medium (LB medium contained 0.5% NaCl). They were then compared by running on IEF-PAGE with ampholine in the pH range 6.0-4.0. For the cloned CGTase, the isoform I had highest positive charge (highest pI value, approximately 4.91). Isoform II showed more negative charge and had pI around 4.74. The isoform III which run the fastest in native-PAGE (Fig 3.10A and 3.13) seemed to be resolved in two bands on IEF, one below isoform II and another between isoform I and II (this was confirmed in Fig 3.10B and 3.14A).

For the mutated CGTases, the major band of single mutated CGTase compared with cloned CGTase can be separated into 2 groups;

1. The mutants which showed pI values similar to that of isoform II of cloned CGTase are N336D, N415D, N567D and N427D (Figure 3.14 Lane 2, 3, 4, and 6, respectively).
2. The mutants which showed different pI values from that of isoform II of cloned CGTase are N428D, N435D, N188D (Figure 3.14 Lane 7, 8, and 9),

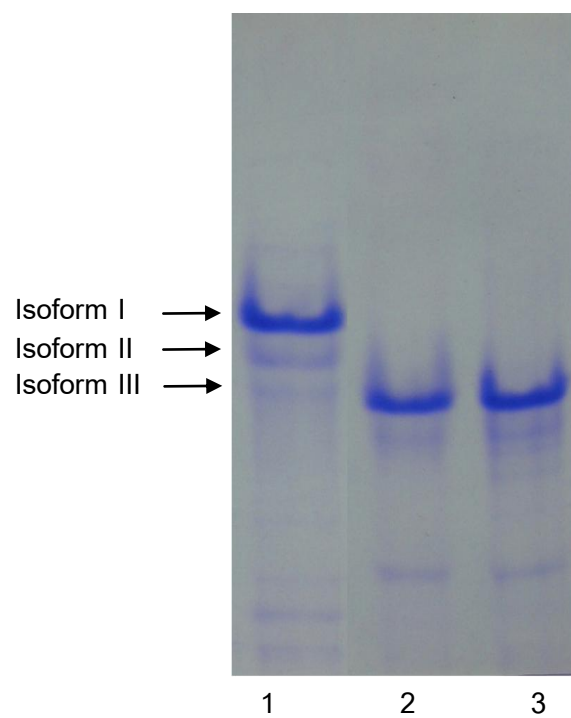


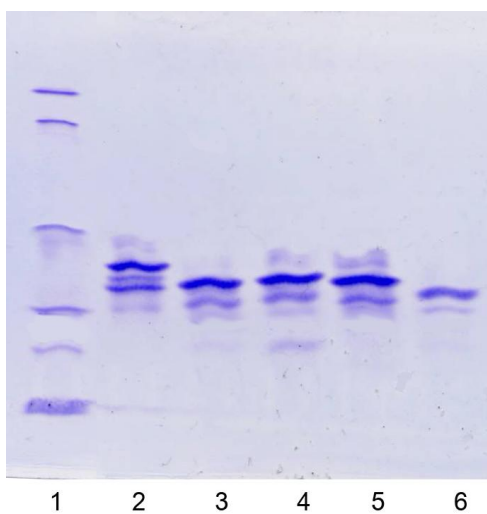
Figure 3.13 Coomassie blue staining of non-denaturing PAGE of cloned CGTase compared with N336D/N415D and N336D/N415D/N326D mutated CGTase expressed by *E. coli* BL21 (DE3).

Lane 1 = Cloned CGTase

Lane 2 = N336D/N415D double mutant CGTase

Lane 3 = N336D/N415D/N326D triple mutant CGTase

A)



B)

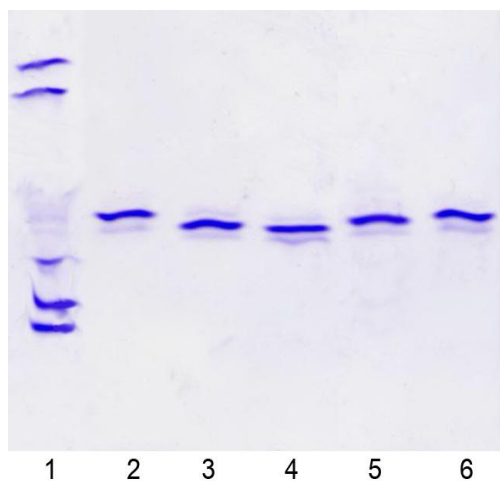


Figure 3.14 IEF-polyacrylamide gel electrophoresis of crude cloned CGTase from *Paenibacillus* sp. RB01 compared with mutated enzyme.

A)

Lane 1 = pI marker

Lane 2 = Cloned CGTase

Lane 3 = N336D

Lane 4 = N415D

Lane 5 = N567D

Lane 6 = N336D/N415D

B)

Lane 1 = pI marker

Lane 2 = Cloned CGTase

Lane 3 = N336D

Lane 4 = N427D

Lane 5 = N428D

Lane 6 = N435D

N263D, N326D, N370D, N620D, N247D and N336Q (Figure 3.14 B Lane 2, 3, 4, 6, and 7 respectively).

The double and triple mutated CGTases showed very similar pI values (Figure 3.15 Lane 9 and 10, respectively) which were lower than that of isoform II of cloned CGTase.

### 3.6 Separation of CGTase isoforms

The partially purified CGTase from starch adsorption was further separated in order to obtain the isolated isoforms. Four methods were performed, as followed :

- Preparative gel electrophoresis under non-denaturing condition
- FPLC with anion exchange column (Mono Q)
- FPLC with chromatofocusing column (Mono P)
- IEF-PAGE with slab gel electrophoresis

#### 3.6.1 CGTase isoform separation by preparative gel electrophoresis

The concentrated partially purified enzyme was loaded onto a discontinuous preparative polyacrylamide gel electrophoresis, performed on a Model 491 Prep cell (Figure 3.16A). After the dye front reached the bottom of the gel, elution was followed by Tris-glycine buffer, pH 8.5. The fractions were checked for activity and isoform pattern on native-PAGE with dextrinizing activity stain. The result (Figure 3.16B.) showed the isoform III was first eluted (lane 1-2) followed by isoform II (lane 3-8), mixture of isoform I and II (lane 9-18) and the isoform I (lane 19-20), respectively.

#### 3.6.2 CGTase isoform separation by FPLC system with anion exchange column (Mono Q)

The sample was applied to Mono Q column FF pre-equilibrated with 10 mM phosphate buffer, pH 6.5. The isoforms were eluted from the column by a gradient of 0-0.5 M NaCl in the same buffer in 30 minutes. The chromatogram (Figure 3.17) showed two major protein peaks which were corresponded to the two dextrinizing activity peaks in the initial phase of the gradient (fraction 7-20). At around fraction 37-42, another major  $A_{280}$  peak was observed, but with no enzyme activity detected. The isoform enzyme activity detected. Figure 3.18 showed the isoform pattern on native-PAGE with

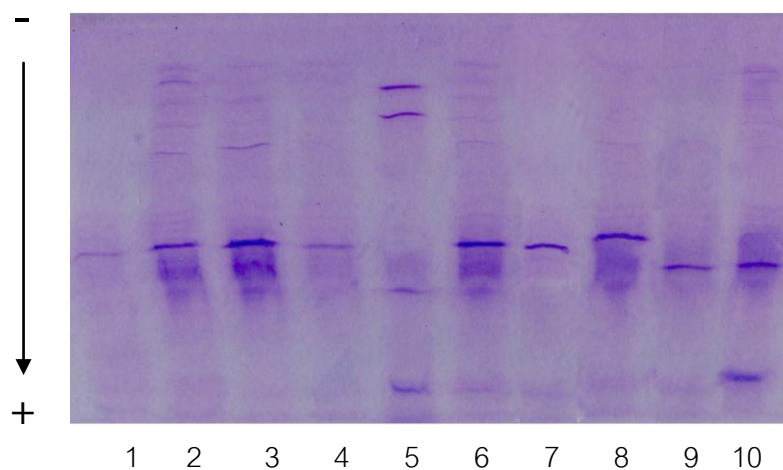


Figure 3.15 IEF-polyacrylamide gel electrophoresis of crude cloned CGTase from *Paenibacillus* sp. RB01 compared with mutated enzyme.

Lane 1 = Cloned CGTase

Lane 2 = N263D

Lane 3 = N326D

Lane 4 = N370D

Lane 5 = pI marker

Lane 6 = N620D

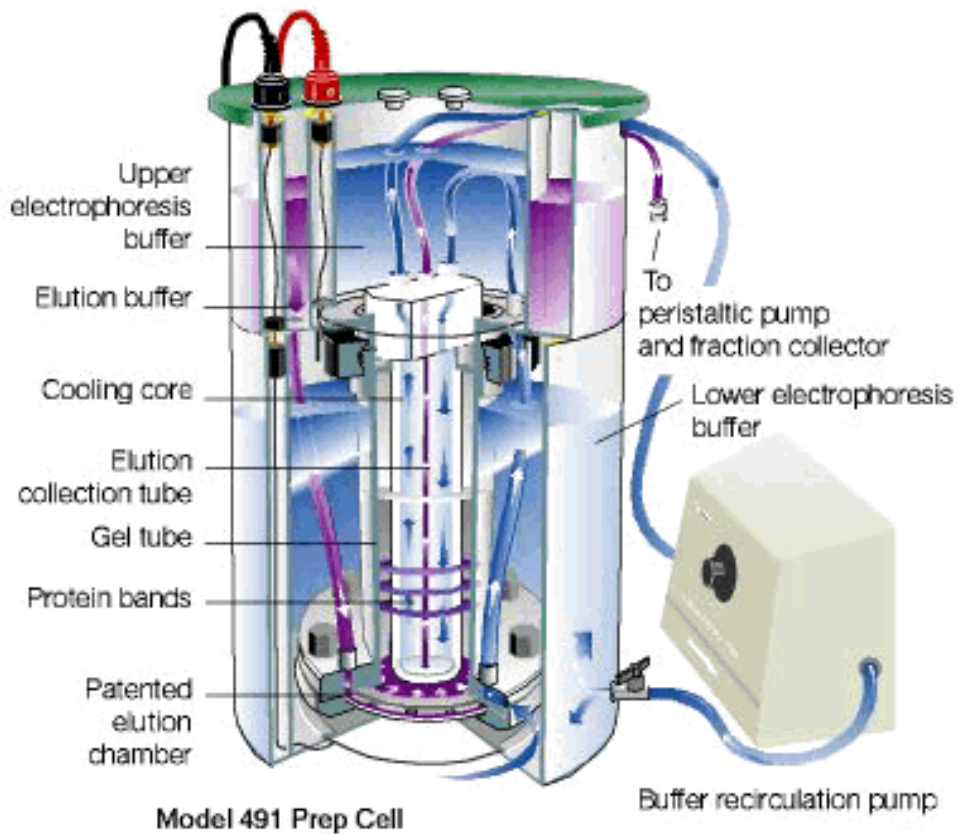
Lane 7 = N247D

Lane 8 = N336Q

Lane 9 = N336D/N415D

Lane 10 = N336D/N415D/N326D

A)



B)

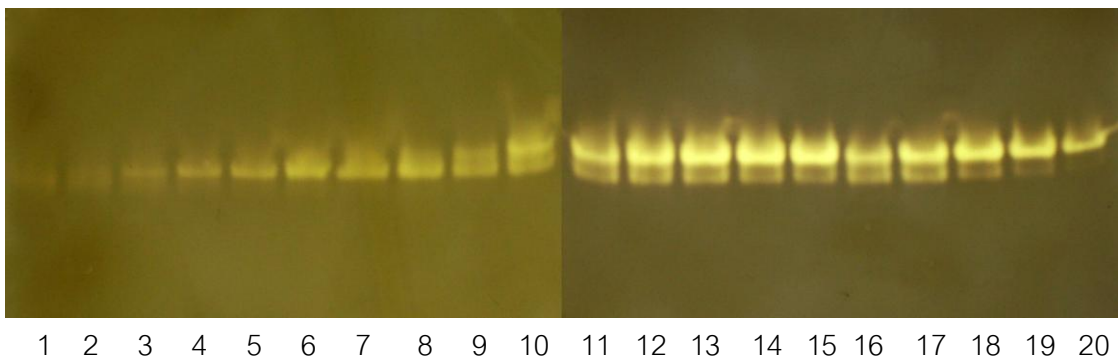


Figure 3.16 A) Preparative gel electrophoresis unit

B) Separation pattern of CGTase isoforms by Preparative gel electrophoresis, as analyzed on non-denaturing PAGE with amylolytic activity staining. Lane number 1-20 was from fraction 25- 44. One ml per fraction was collected from Prep Cell.



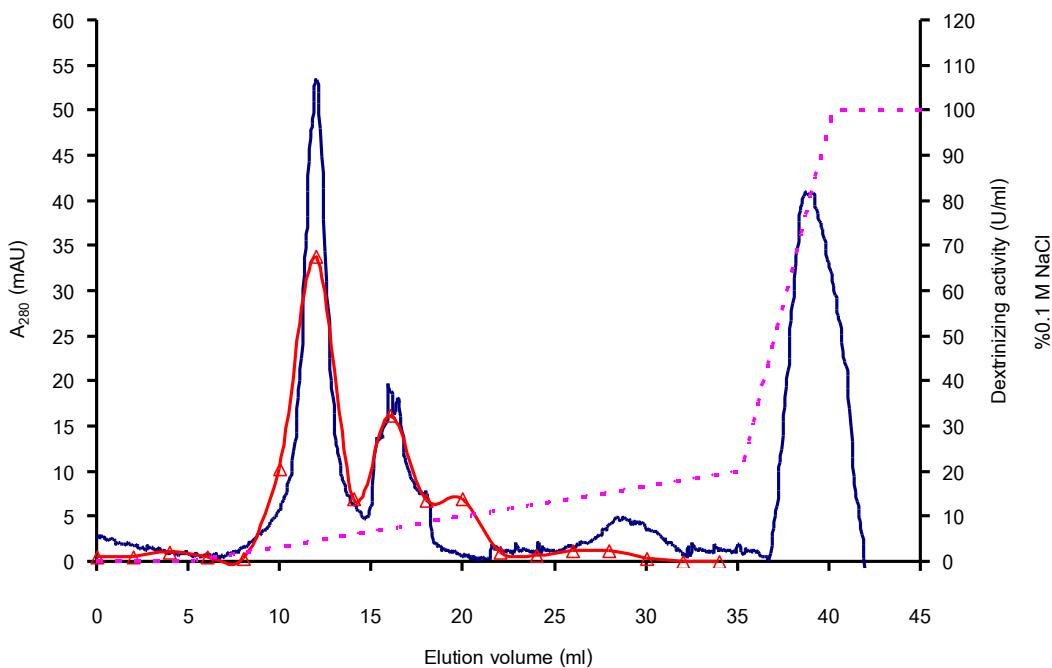


Figure 3.17 Chromatogram of CGTase isoform separation on a Mono Q FF column.

The column was equilibrated with 10 mM phosphate buffer pH 6.0 and eluted with gradient of NaCl 0-0.5 M in buffer in 30 minutes. 0.5 ml per fraction was collected.

— A280,  $\Delta$  Dextrinizing activity, --- %0.1 M NaCl.

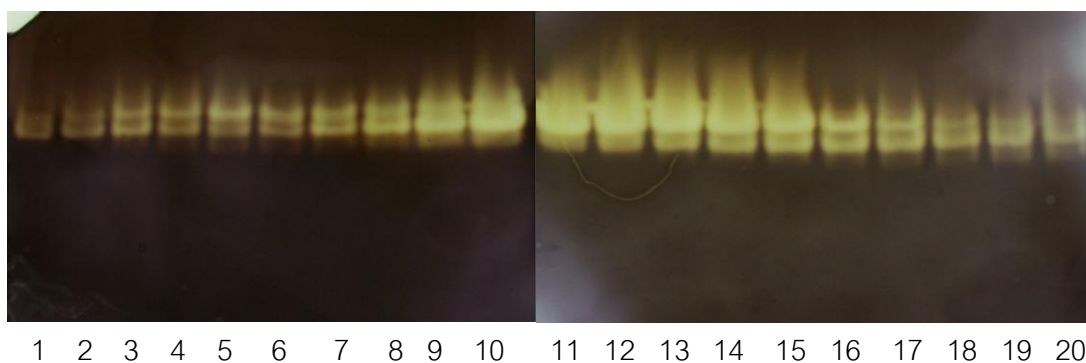


Figure 3.18 Isoform pattern on native-PAGE of CGTase separated by Mono Q FF column. Staining was by amylolytic activity. Fraction 0.25 mL was collected. 5  $\mu$ l of sample from each fraction was loaded on each lane. Lane number 1-20 was from fraction at elution volume 8-26 ml.

dextrinizing activity staining was investigated for fraction 1-20. The gel illustrated that the isoform I was eluted at around 20-25 mM NaCl (Lane 10 and 11) and the isoform II was eluted at NaCl concentration around 50 mM (Lane 19-20). The very low activity peak around fraction number 23-30 might be isoform III, they were not analyzed on native-PAGE due to low activity. Though from the column profile, two main activity peaks were well separated, but from native-PAGE analysis, separation between isoform I and II showed low efficiency. The fractions which showed only isoform I was removed and collected at  $-80^{\circ}\text{C}$  while the rest of the fractions which had isoform I mixed with isoform II was reloaded onto the column and separated with the same condition to collect the high concentration of isoform II.

### **3.6.3 CGTase isoform separation by FPLC system with chromatofocusing column (Mono P)**

The column was equilibrated by 25 mM bis-Tris HCl pH 6.5 until the eluent had the same pH as the buffer. The sample was applied to the column and eluted by the polybuffer pH 4.2. The chromatogram (Figure 3.19) showed two protein peaks, the major peak with pI value about 4.4 and minor peak with pI value about 4.2. The result of isoform pattern determined by native-PAGE was shown (Figure 3.20). The isoform I was found in the major peak (Lane 5-7) while the isoform II was shown in the minor peak (Lane 11-13). The result confirmed that the isoform I and isoform II had different pI values and can be separated by chromatofocusing column. Moreover, the native gel showed that the separation efficiency of this column was higher than the anion exchange column. The isoforms I and II were pooled and kept at  $-80^{\circ}\text{C}$  for the next experiment.

### **3.6.4 CGTase isoform separation by IEF-PAGE**

The isoforms were separated by their pI values on the polyacrylamide gel electrophoresis as shown in Figure 3.10. However, the isoforms separated by this method lost their activity since the gel was immersed in the coomassie blue staining solution which was composed of acetic acid and methanol. So the separated isoforms from this PAGE were further used in only the experiment that did not require the existence of CGTase activity e.g. in the digestion by trypsin.

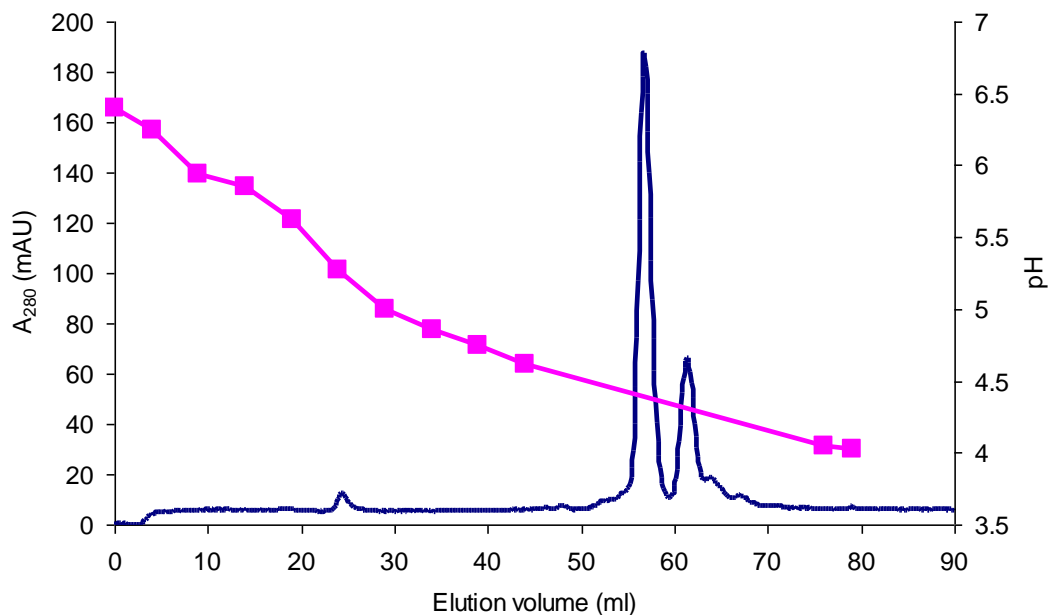
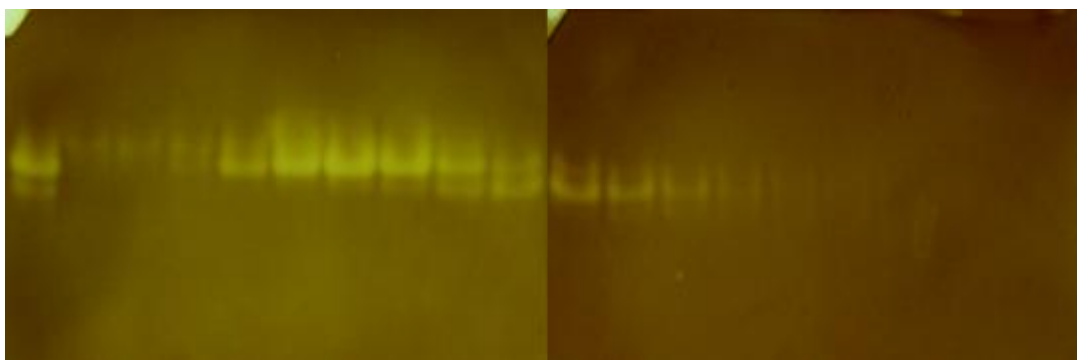


Figure 3.19 Chromatogram of CGTase isoform separation on a Mono P column. The column was equilibrated with 25 mM bis-Tris HCl pH 6.5 and eluted by 20X polybuffer pH 4.2. 0.5 ml per fraction was collected. —  $A_{280}$ , —■— pH



1 2 3 4 5 6 7 8 9 10 11 12 13 14 15 16 17 18 19 20  
 Figure 3.20 Isoform pattern on native-PAGE of cloned CGTase isolated by chromatofocusing column (Mono P). Staining was by amylolytic activity. Each lane was loaded with 5  $\mu$ l of sample. Lane number 1 was CGTase prior to column, while lane 2-20 was from fraction number 52-70.

In summary, Table 3.6 showed advantages and disadvantages of the isoform separation methods. Purified isoforms from Mono Q FF and Mono P FF were used in the experiments on isoaspartate quantitation (section 3.8.2) and enzyme characterization (section 3.10), respectively. While those separated by IEF-PAGE were used for trypsin digestion experiment, followed by separation of tryptic peptides by reverse phase HPLC and MALDI-TOF mass determination (section 3.9).

### **3.7 CGTase isoform pattern on two-dimensional gel electrophoresis**

#### **3.7.1 Isoform pattern of cloned CGTase**

The crude enzyme of cloned CGTase produced by *E. coli* BL21(DE3) was prepared, then dialyzed against distilled water to remove salt present in the LB culture medium (contained 0.5 g% NaCl). The sample was mixed with ampholyte pH 6.0-4.0 and developed onto a dry gel strip, then subjected to the IEF first-dimension electrophoresis whereby separation by pI was obtained. The electricity power was applied to create the pH gradient which the sample was separated by their pI value under non-denaturing condition. The sample was then denatured by immerse the strip into the SDS-equilibrate buffer containing urea, dithiothreitol (DTT) and iodoacetamide (IAA). And the second dimension on 7% SDS-PAGE was used to separate the isoforms by size (see details in Methods section 2.12.2). The result of the isoform pattern of cloned CGTase on 2D gel electrophoresis was shown in Figure 3.21. As expected, the cloned CGTase showed the major band (isoform I) which had the least negative charge and run the slowest on the first-dimension gel. The two minor bands (isoform II and III) had more negative charge than isoform I. However, all isoforms showed the same size on SDS-PAGE, about 70 kDa.

#### **3.7.2 Comparison of isoform II of cloned CGTase and the mixture of isoform II with mutated CGTase**

The isoform I and II were separated from crude cloned CGTase by FPLC using Mono Q column, then the purity was checked on non-denaturing PAGE as shown in Figure 3.22A. The pattern indicated that the separated isoform I and II were of major band, though trace amount of contaminated isoform still exist as faint smear band below.

Table 3.6 Comparison of separation methods of CGTase isoforms

Method	Equipment	Principle	Result	Advantage	Disadvantage
Preparative gel electrophoresis	Prep cell Model 491	Net charge and shape of the isoform in non-denaturing condition	Isoform III was the first eluted followed by isoform II and isoform I	Simple Relatively not expensive	Time consuming Sample was diluted by elution buffer
Anion exchange chromatography	Mono Q <sup>TM</sup> HR 5/5	Net charge of the isoform in native condition	Isoform I was first eluted followed by isoform II	Fast	Efficiency of isoform I and II separation was low
Isofocusing chromatography	Mono P <sup>TM</sup> HR 5/5	Isoelectric point of the isoform	Isoform I was first eluted followed by isoform II	Fast High efficiency to separate the isoform I and II	Need the specific elution buffer, high cost
Isofocusing-PAGE	IEF-Gel Apparatus	Isoelectric point of the isoform	All isoforms were separated according to pI values on PAGE and visualized by coomassie blue	All isoforms were separated	The isoforms lost their activity

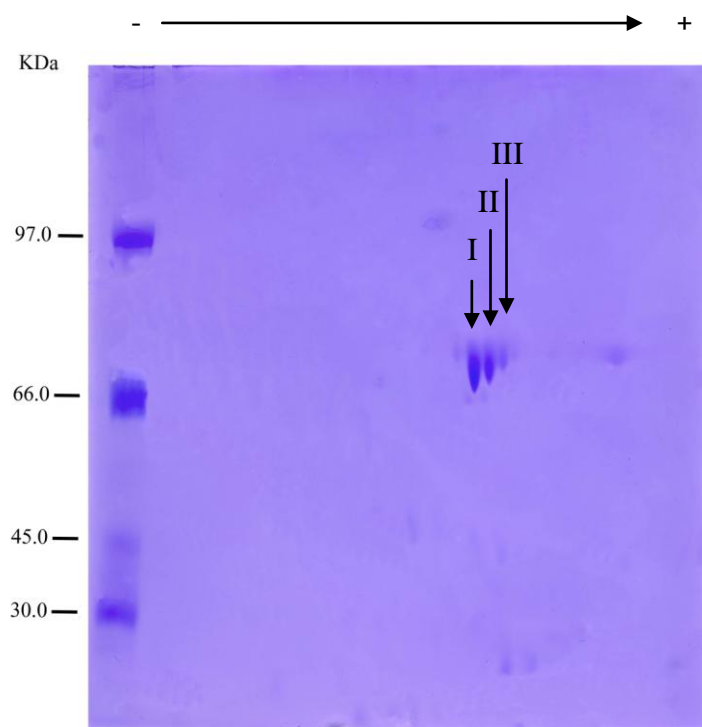


Figure 3.21 Separation on two-dimension gel electrophoresis of the crude cloned CGTase isoforms. The first dimension was separated by IEF on ampholyte of pH range 6.0-4.0 and the second dimension was on 7% SDS-PAGE. The dialyzed crude enzyme of 42.5 mg was loaded.

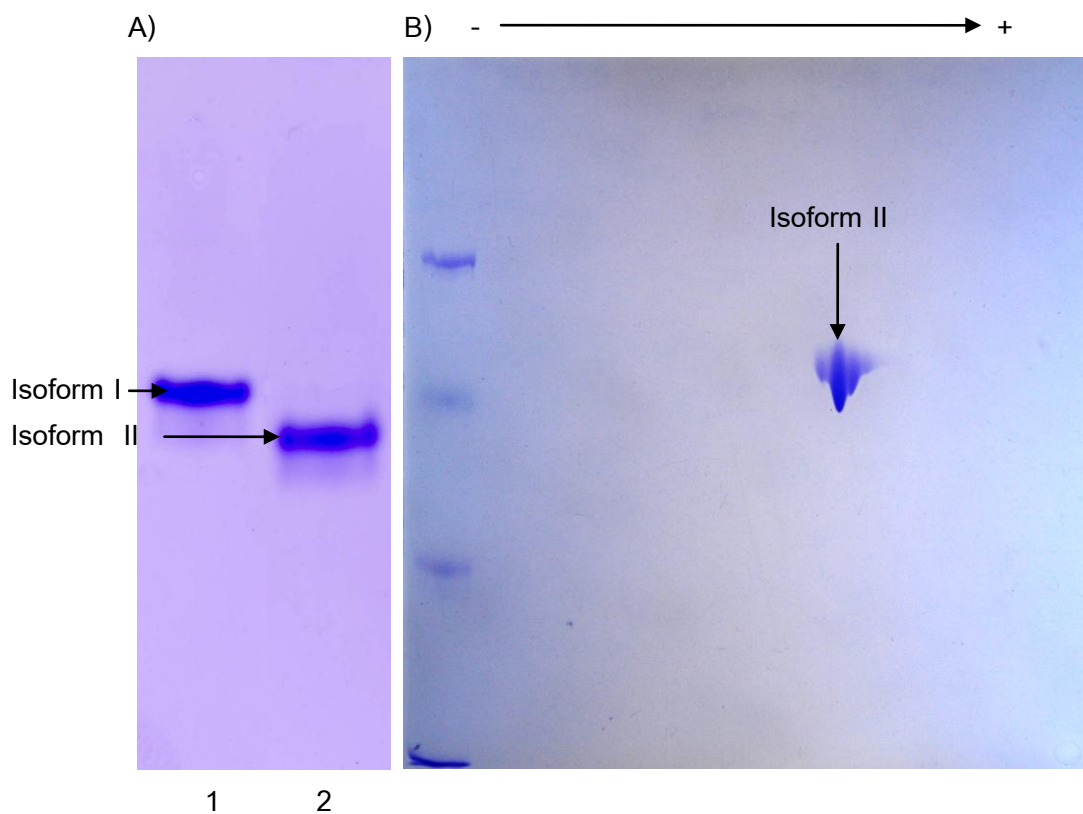


Figure 3.22 Coomassie blue staining of CGTase isoforms isolated by FPLC Mono Q column on A) non-denaturing PAGE and B) isolated isoform II on two-dimension gel electrophoresis.

A) Non-denaturing PAGE

Lane 1 = Isoform I (15  $\mu$ g)

Lane 2 = Isoform II (15  $\mu$ g)

B) Two dimension gel electrophoresis

The first dimension was run on IEF with pI 4-6 and the second dimension was on 7% of SDS-PAGE. The amount of isoform II loaded was 15  $\mu$ g.

The separated isoform II (Lane 2) was dialyzed against distilled water and was subjected to the 2D gel electrophoresis in the same procedure as the cloned CGTase in section 3.1. The result showed that majority of the proteins was isoform II, however trace of isoform I and III which had pI very close to isoform II were still present in this purified preparation of isoform II (Figure 3.22B).

2D gel electrophoresis was further used in the attempt to differentiate between isoform II and mutated CGTases. The pattern of isoform II (at 15  $\mu$ g) and the mixture of isoform II and the mutated CGTase: N336D, N427D, N567D, N415D and N620D (at 15  $\mu$ g each) were shown in Figure 3.23A-F. From the result, the electrophoretic pattern of isoform II mixed with mutated CGTase from N336D, N427D, N567D (Figure 3.23B-D) did not show the change in the mobility, intensity and the band shape of isoform II (for the better comparison of the intensity and band shape, see also the example of zoom in picture in Figure 3.24A and B). On the other hand, the mixture of isoform II and mutated CGTase from N415D and N620D showed the change in the band shape of the isoform II (Figure 3.24C, D compared to A). The mutated CGTase N415D showed wider major band while the mutated CGTase N620D forced the major band to move slower or show less negative charge than isoform II in IEF dimension. The mobility of isoform III in Figure 3.23F in the IEF dimension toward anode was 2.9 cm from origin line while that in frame A was 3.1 cm. These results suggested that the deamidation at Asn position 336, 427 or 567 might be the cause of isoform formation in native CGTase because these mutated enzymes showed the same pI and size as isoform II of the cloned CGTase.

### 3.8 The effect of deamidation on isoform formation of cloned CGTase

To support the hypothesis that non-enzymatic deamidation of Asn is the cause of isoform formation in CGTase of *Paenibacillus* sp. RB01, two experimental approaches were carried out.

#### 3.8.1 The effect of pH and incubation time on isoform formation

In the first approach, we followed the change in isoform pattern when pH of incubation buffer was increased and incubation time was proceeded. Since deamidation



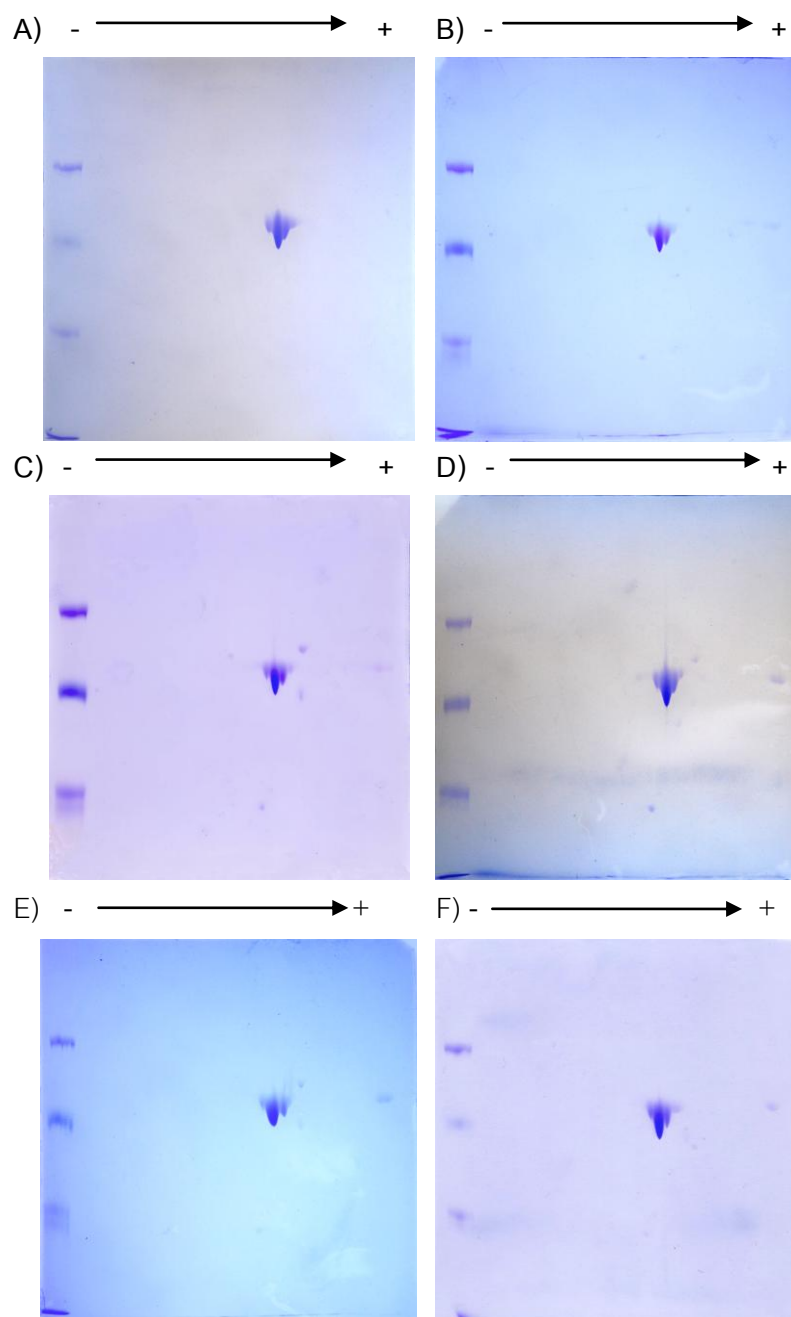


Figure 3.23 Two-dimension gel electrophoresis of isoform II and isoform II mixed with mutated CGTases. First dimension was run on isoelectric focusing with pI 4-6 and the second dimension was on 7% of SDS-PAGE. The sample of 15  $\mu$ g each was mixed before loading.

- |                                |                                |
|--------------------------------|--------------------------------|
| A) Isoform II                  | B) Isoform II mixed with N336D |
| C) Isoform II mixed with N427D | D) Isoform II mixed with N567D |
| E) Isoform II mixed with N415D | F) Isoform II mixed with N620D |

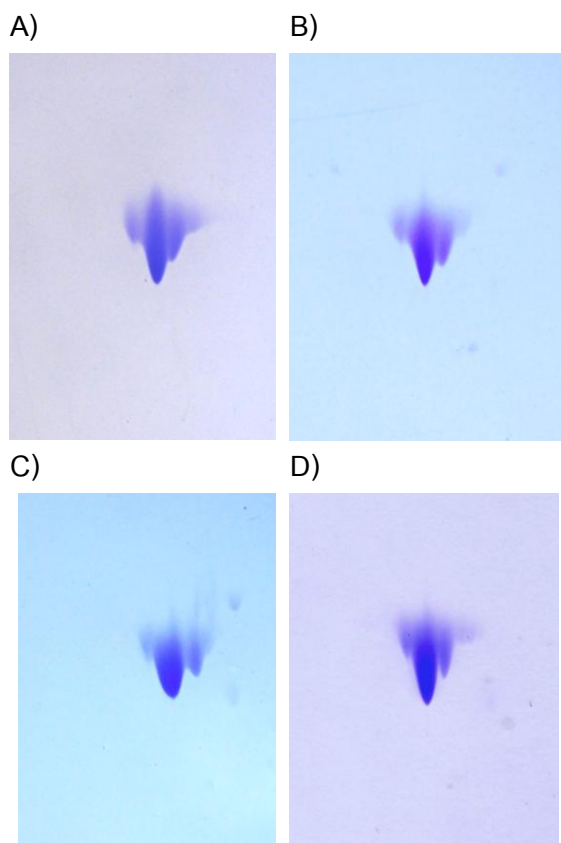


Figure 3.24 Zoom-in of the two-dimension gel electrophoresis of isoform II and isoform II mixed with mutated CGTases.

A) Isoform II

B) Isoform II mixed with N336D

C) Isoform II mixed with N415D

D) Isoform II mixed with N620D

reaction has been known to proceed better at the more alkaline pH, deamidation buffer at pH 9.0 and 6.0 was used to compare the effect on isoform formation.

The isoform I of cloned CGTase (2.5 mg/ml) isolated by mono Q FF was used in this experiment. The sample was dialyzed against distilled water, then incubated in deamidation buffer (25 mM acetic acid, 25 mM Tris and 25 mM ethanolamine) either at pH 6.0 or 9.0. The samples were collected at time intervals 0, 3, 7 and 15 days and the isoform pattern on non-denaturing-PAGE, IEF-PAGE and SDS-PAGE was followed as shown in Figure 3.25, 3.26, and 3.27, respectively.

On non-denaturing PAGE in which the gel was stained with amylolytic activity or coomassie blue, the number of isoform was increased when incubation time was increased, especially at pH 9.0 which showed the isoform II band from the third days of incubation. While at pH 6.0, the isoform II band was significantly appeared at 15 days of incubation (Figure 3.25A, B and C, D). The isoform III was significantly detected in reaction at pH 9.0 after incubation for 15 days. From the isoform formation on native PAGE, it can be concluded that the reaction in the high pH buffer was driven to forward faster than the low pH buffer and the isoform formation was sequentially changed from isoform I to isoform II and isoform II to isoform III, respectively.

The result analyzed by IEF-PAGE was similar to what observed in the native PAGE in a sense that isoform II and III were increased as incubation time and pH were increased, and the effect at pH 9.0 was more intensified (Fig 3.26). In this gel system, traces of isoform II and III were earlier observed when compared to the native PAGE. The result that was a surprise was that the isoform III, the most negatively charge isoform, migrated in between isoform I and II.

As expected, as our preliminary data and previous reports showed that all CGTase isoforms of *Paenibacillus* sp. RB01 and also the cloned enzyme had the same size, the result analyzed on SDS-PAGE at any time of incubation and at both pHs showed no change in the electrophoretic pattern (Fig 3.27).

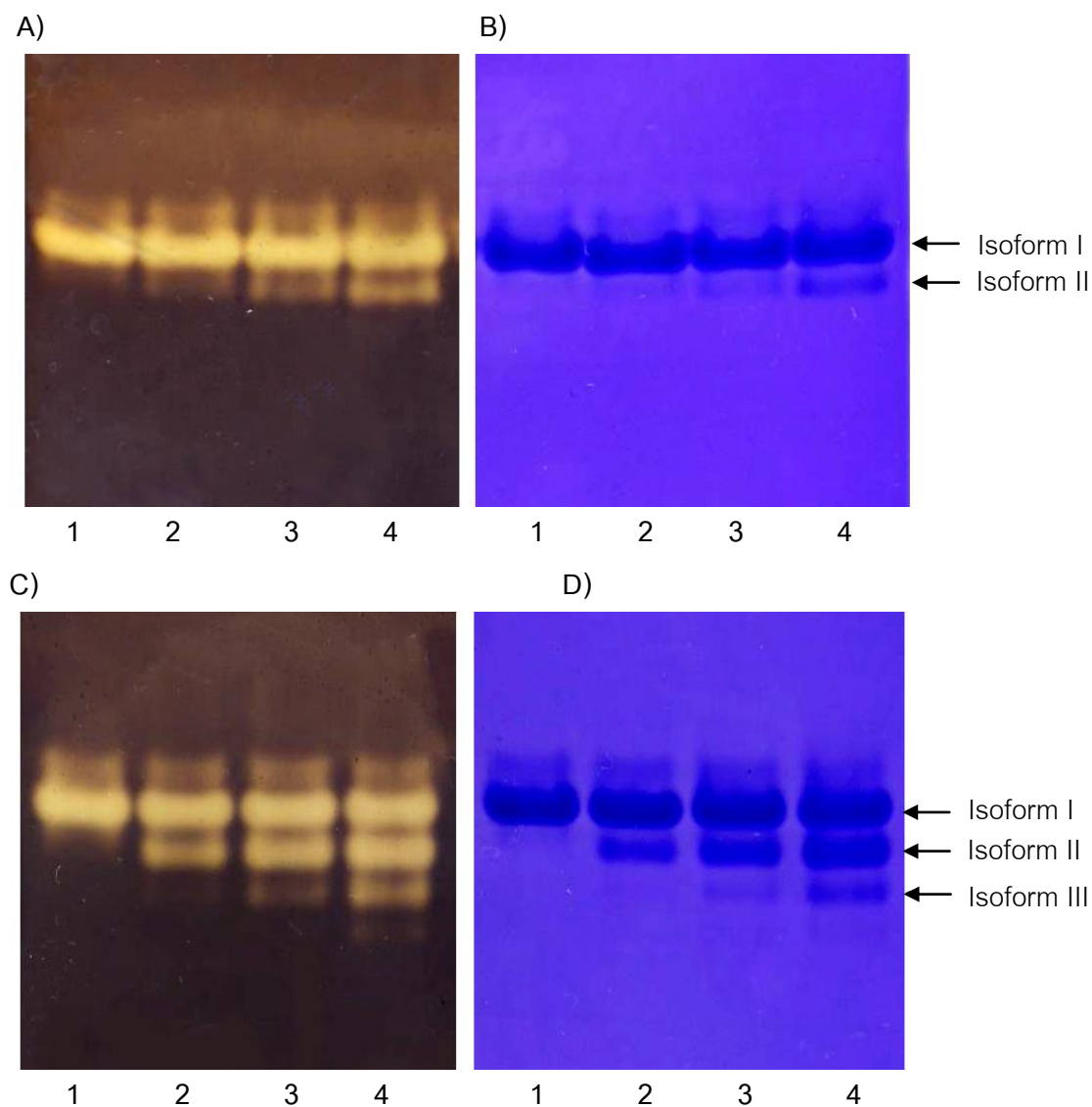


Figure 3.25 Dextrinizing activity and coomassie blue staining on non-denaturing PAGE of CGTase isoform I incubated in deamidation buffer pH 6.0 (A, B) and 9.0 (C,D) at 37°C. A, C = dextrinizing activity staining, B, D = coomassie blue staining

Deamidation buffer = 25 mM acetic acid, 25 mM Tris and 25 mM ethanolamine

Lane 1 = 0 day of incubation

Lane 2 = 3 days of incubation

Lane 3 = 7 days of incubation

Lane 4 = 15 days of incubation

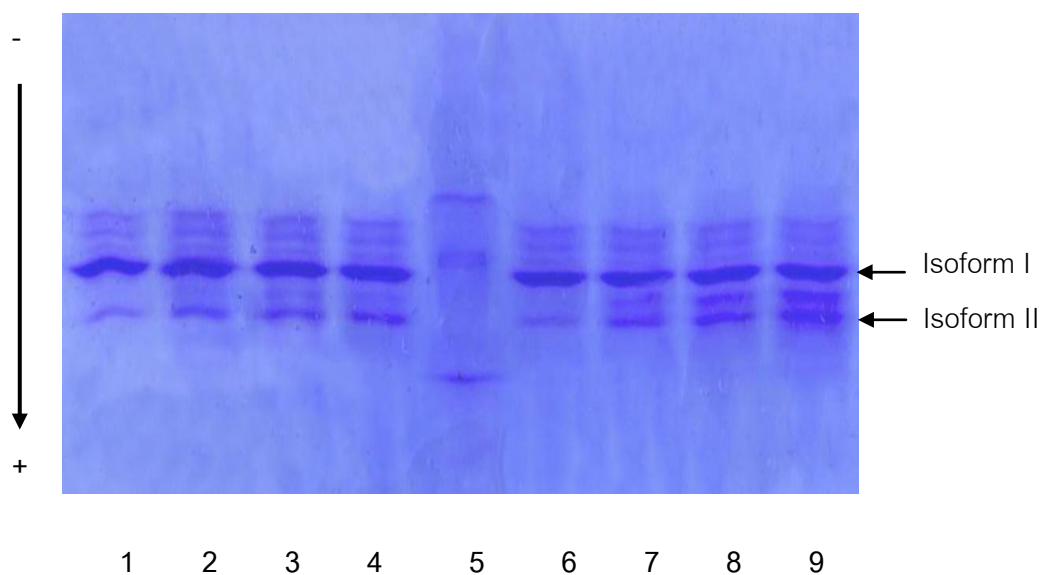


Figure 3.26 IEF-PAGE of CGTase isoform I incubated in deamidation buffer.

deamidation = 25 mM acetic acid, 25 mM Tris and 25 mM ethanolamine

Lane 1 = 0 day of incubation in buffer pH 6.0

Lane 2 = 3 days of incubation in buffer pH 6.0

Lane 3 = 7 days of incubation in buffer pH 6.0

Lane 4 = 15 days of incubation in buffer pH 6.0

Lane 5 = pI marker

Lane 6 = 0 day of incubation in buffer pH 9.0

Lane 7 = 3 days of incubation in buffer pH 9.0

Lane 8 = 7 days of incubation in buffer pH 9.0

Lane 9 = 15 days of incubation in buffer pH 9.0

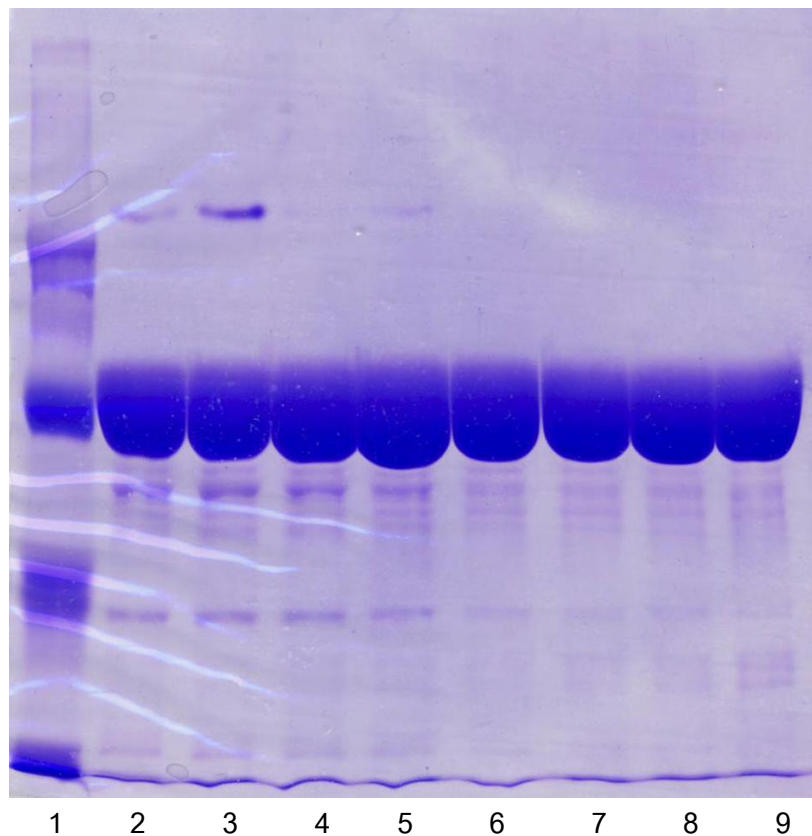


Figure 3.27 Coomassie blue stain of SDS-PAGE of CGTase isoform I incubated in deamidation buffer at 37°C.

deamidation buffer = 25 mM acetic acid, 25 mM Tris and 25 mM

Lane 1 = Protein molecular weight markers [myosin (200 kDa),  
 $\beta$ -galactosidase (116.2 kDa), phosphorylase b (97.1 kDa), BSA  
 (66.2 kDa) and ovalbumin (45 kDa)]

Lane 2 = 0 day of incubation in buffer pH 6.0  
 Lane 3 = 3 days of incubation in buffer pH 6.0  
 Lane 4 = 7 days of incubation in buffer pH 6.0  
 Lane 5 = 15 days of incubation in buffer pH 6.0  
 Lane 6 = 0 day of incubation in buffer pH 9.0  
 Lane 7 = 3 days of incubation in buffer pH 9.0  
 Lane 8 = 7 days of incubation in buffer pH 9.0  
 Lane 9 = 15 days of incubation in buffer pH 9.0

### 3.8.2 Determination of isoaspartate content in CGTase isoforms

During deamidation reaction, the rearrangement reaction of asparagine residue into aspartic acid residue is characterized by the formation of isoaspartate intermediate (Figure 2.1). The ISOQUANT isoaspartate detection kit (Promega) was used to analyze the isoaspartate content in CGTase isoforms (see Method Section 2.14.5). The kit contained the enzyme Protein Isoaspartyl Methyltransferase (PIMT) to catalyze the transfer of a methyl group from S-adenosyl-L-methionine (SAM) to isoaspartic acid at the  $\alpha$ -carboxyl position, generating S-adenosyl homocysteine (SAH) in the process which can be quantitated by HPLC. The amount of isoaspartate content in the CGTase sample was calculated by comparing with standard SAH (see Appendix 6).

The CGTase sample used was the same as in 3.5.1. Cloned CGTase isoform I was incubated at pH 6.0 and 9.0 for 0-15 days. For each sample, the isoaspartate content was then determined. In the buffer pH 6.0, the amount of isoaspartate at 0, 3, 7 and 15 days were 0.015, 0.017, 0.019 and 0.020 pmoles/pmole of CGTase, respectively (Figure 3.28). While those corresponding values for the buffer pH 9.0 were 0.020, 0.023, 0.028 and 0.035, pmoles/pmole of CGTase, respectively. The result showed that after incubation for 15 days (where isoform II and III were increased, as observed in Fig 3.25 and 3.26) the amount of the isoaspartate was increased by 33% and 75% at pH 6.0 and 9.0, respectively.

In summary, the increasing of the number of CGTase isoform corresponded to the increasing in isoaspartate content. These results support that non-enzymatic deamidation might be the cause of CGTase isoform formation and the process occurred via the formation of isoaspartate intermediate.

## 3.9 Tryptic digestion of isoforms of cloned and mutated CGTase

### 3.9.1 Separation of tryptic peptides by HPLC

To identify the labile Asn(s) in CGTase which was (were) deamidated giving rise to the change in isoform I to isoform II (as seen in Figure 3.25) the purified isoforms from cloned and mutants were digested by trypsin and the peptides were compared by separation in a HPLC system.

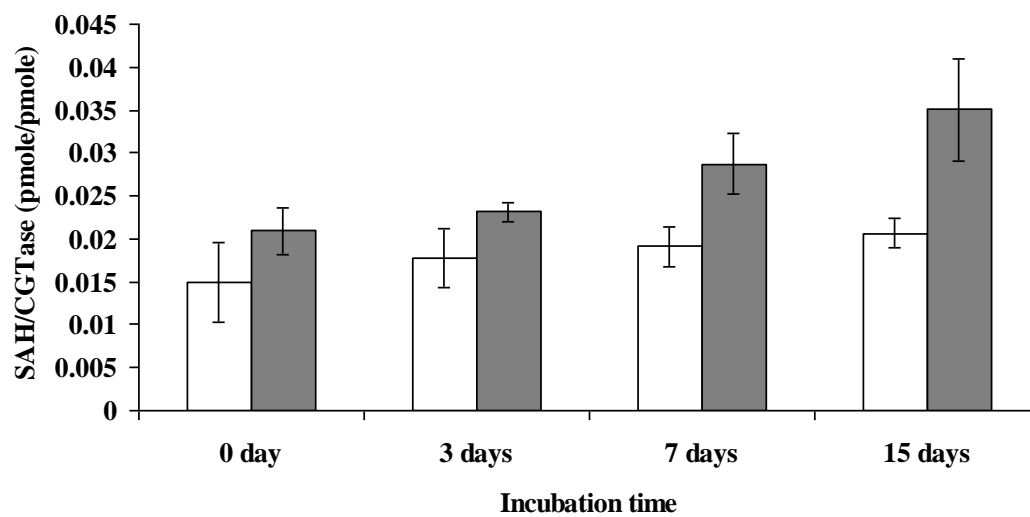


Figure 3.28 Isoaspartate content in CGTase after the isoform I was incubated in deamidation buffer at pH 6.0 and 9.0 for various incubation time.

□ pH 6.0

■ pH 9.0



For the cloned enzyme, the concentrated partially purified CGTase by starch adsorption was applied to the IEF-PAGE to separate the isoforms. The gel was stained with coomassie blue to visualize the bands of the isoforms as shown in Figure 3.10B. Each protein band which represents the major isoforms, isoform I and II, of CGTase was cut. The samples were subjected to in gel tryptic digestion as described in section 2.14.2. The peptides were extracted from the gel and the reverse phase HPLC system using C<sub>18</sub> column was performed. The tryptic peptides were eluted from the column by gradient of acetonitrile. Figure 3.29A and B showed the chromatogram of tryptic digested peptides separation from isoform I and II, respectively. Approximately 35-40 peptide peaks in the Rt range of 10-30 minutes were observed in both profiles. Some peaks were clearly resolved e.g. Rt 19.8, 20.9, 21.8, 22.1, 23.6, 24.9, and 26.0, respectively. However, several peaks e.g. Rt 16.9-17.2, 20.4-20.5, and 21.2-21.5 minutes, could not be well separated in this elution system. When compared both profiles, similar pattern was observed. The lower peak height in peptides from isoform II should result from less amount of the enzyme subjected to in gel tryptic digestion. The single mutated (N415D), double mutated (N336D/N415D) and triple mutated CGTase (N336D/N415D/N326D) CGTase were also digested by trypsin, using the same protocol as the cloned enzyme. The chromatograms of peptide separation on reverse phase HPLC were shown in Figure 3.30A, B and C, respectively. No significant difference in the peptide pattern was observed among the three mutated CGTases. And when compared peptides of mutated CGTases with those of the cloned which looked overall similar, it was hard to identify any different peptide(s). The result indicated that this system of reverse phase HPLC could not identify the difference between the cloned and the mutated CGTase which suggested that the target peptide(s) could not be separated by polar/nonpolar property.

### 3.9.2 Mass of tryptic peptides determined by matrix-assisted laser desorption/ionization time of flight-mass spectrometry (MALDI-TOF)

Since the mass of Asp is higher than Asn by 1 Da (NH<sub>3</sub> versus OH,  $\Delta = 1$  Da), differences in size of tryptic peptide containing mutated Asn residue in each mutant comparing to the corresponding peptide of native CGTase were investigated by MALDI-

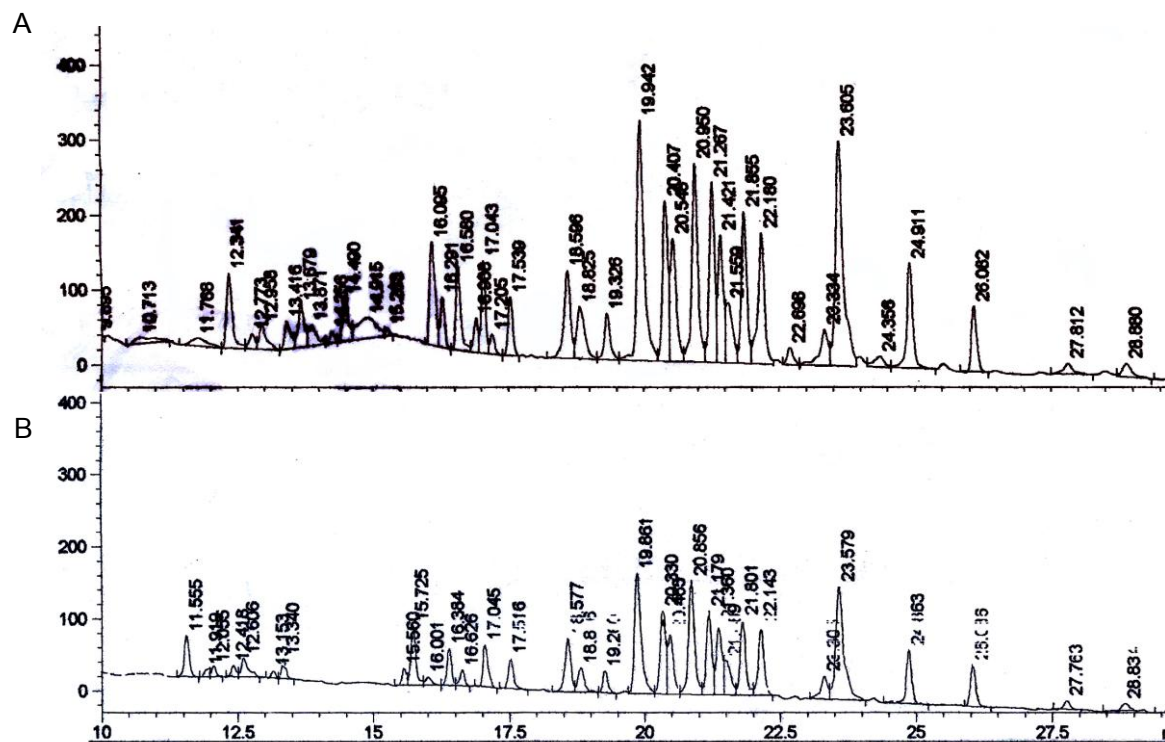


Figure 3.29 HPLC profile of the in gel tryptic peptides of isoform I (A) and II (B) of cloned CGTase separated by  $C_{18}$  column. The column was equilibrated with 0.12% TFA in water then the peptides were separated by a gradient of 0-100 in 60 min of 0.07%TFA in acetonitrile.

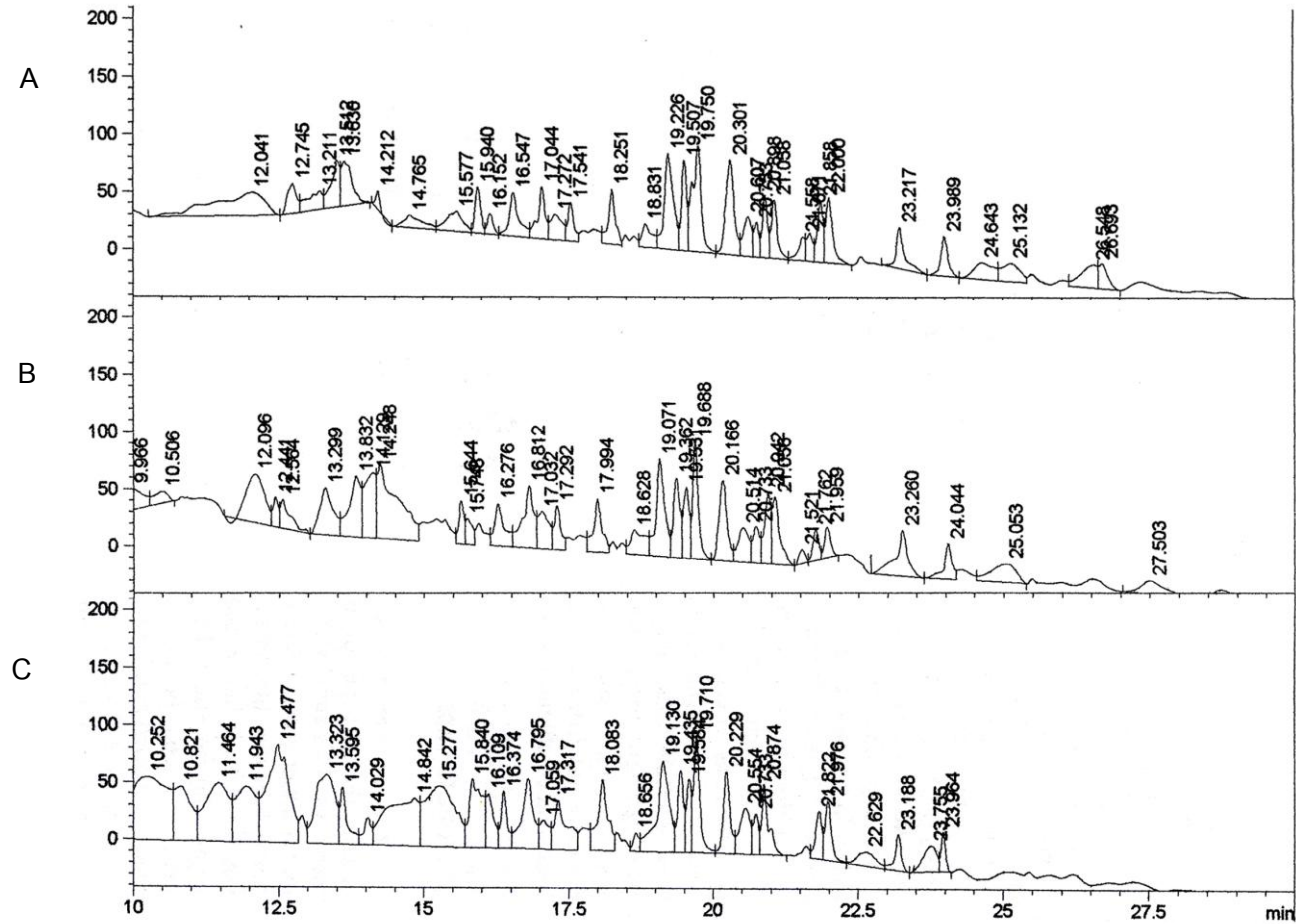


Figure 3.30 HPLC Profile of the in the gel tryptic peptides of mutated CGTase from N415D (A), N336D/N415D (B) and N336D/N415D/N326D separated by HPLC using  $C_{18}$  column (C). The column was equilibrated with 0.12% TFA in water then the peptides were separated by a gradient of 0-100 in 60 min of 0.07% TFA in acetonitrile.

TOF. Among the CGTases of mutants created by site-directed mutagenesis, the enzyme from the single mutation (N415D, N427D and N567D) and from the double mutation (N336D/N415D) were chosen for this experiment and used as positive control since these single and double mutations of CGTase yielded the enzymes with the same electrophoretic patterns as isoform II and III, respectively (see Figure 3.12 and 3.13). The major band of CGTase of those mutants were separated by IEF-PAGE and subjected to in gel tryptic digestion. The digested samples were then analyzed by MALDI-TOF. The theoretical and experimental monoisotopic mass ( $[M + H^+]$ ) of the tryptic digested peptide fragments at the mutated Asn residues were shown in Table 3.7 (Tryptic peptide fragments and their theoretical mass were estimated using the software program from [www.matrixscience.com](http://www.matrixscience.com)). The fragments with monoisotopic mass of 1435.87, 1274.67 and 2696.25 represented the size of tryptic fragments containing the residues Asn415, Asn427 and Asn567, respectively, were detected in the MS profiles (Figure 3.31). They showed increasing mass of 1 Da from the theoretical mass. Moreover, two peptide fragments of the double mutated CGTase with the mass of 934.41 and 1435.74, which represented the tryptic fragments containing the residues Asn336 and Asn415 also showed increasing monoisotopic mass by 1 Da. The result confirmed that mutation made by changing Asn to Asp was subsequently followed by the increase of monoisotopic mass of peptide fragment by 1 Da.

Based on the hypothesis of deamidation, labile Asn residue (at least one) at some position(s) in isoform I is deamidated, giving rise to isoform II. Then, there must be at least one tryptic peptide fragment containing the deamidated residue in isoform I and II which show 1 Da size difference. To identify this different peptide, the isoform I and II of the cloned CGTase separated by IEF-PAGE were subjected to in gel tryptic digestion using the same protocol as the mutated CGTase. The samples were then analyzed by MALDI-TOF and the results were shown in Figure 3.32 and 3.33. The comparison of monoisotopic mass between isoform I and II of cloned CGTase were indeed analyzed by focusing on the peptides containing interested Asn residues shown in Table 3.8. The result showed that the monoisotopic mass of tryptic digested fragments containing Asn326, Asn336, Asn370, Asn415, Asn428, Asn435 and Asn567 from isoform I and II did not show any detectable difference.

Table 3.7 Theoretical and experimental monoisotopic mass ( $[M + H^+]$ ) of the tryptic digested peptide fragment at the mutated Asn residues determined by MALDI-TOF.

Mutant	Monoisotopic mass ( $[M + H^+]$ )		Amino acid sequence of tryptic peptide
	Theoretical	Experimental	
N415D	1434.74	1435.87	W <u>N</u> NDV <u>I</u> IYER
N427D	1273.70	1274.67	FG <u>N</u> NVAVVAINR
N567D	2695.33	2696.25	V <u>A</u> N <u>A</u> AAGAASNIYDNFEVLTGDQQT <u>V</u> R
N336D/ N415D	933.96, 1434.74	934.41 1435.879	HTS <u>N</u> NGDR W <u>N</u> NDV <u>I</u> IYER

\* underline letters are asparagine residues which were mutated

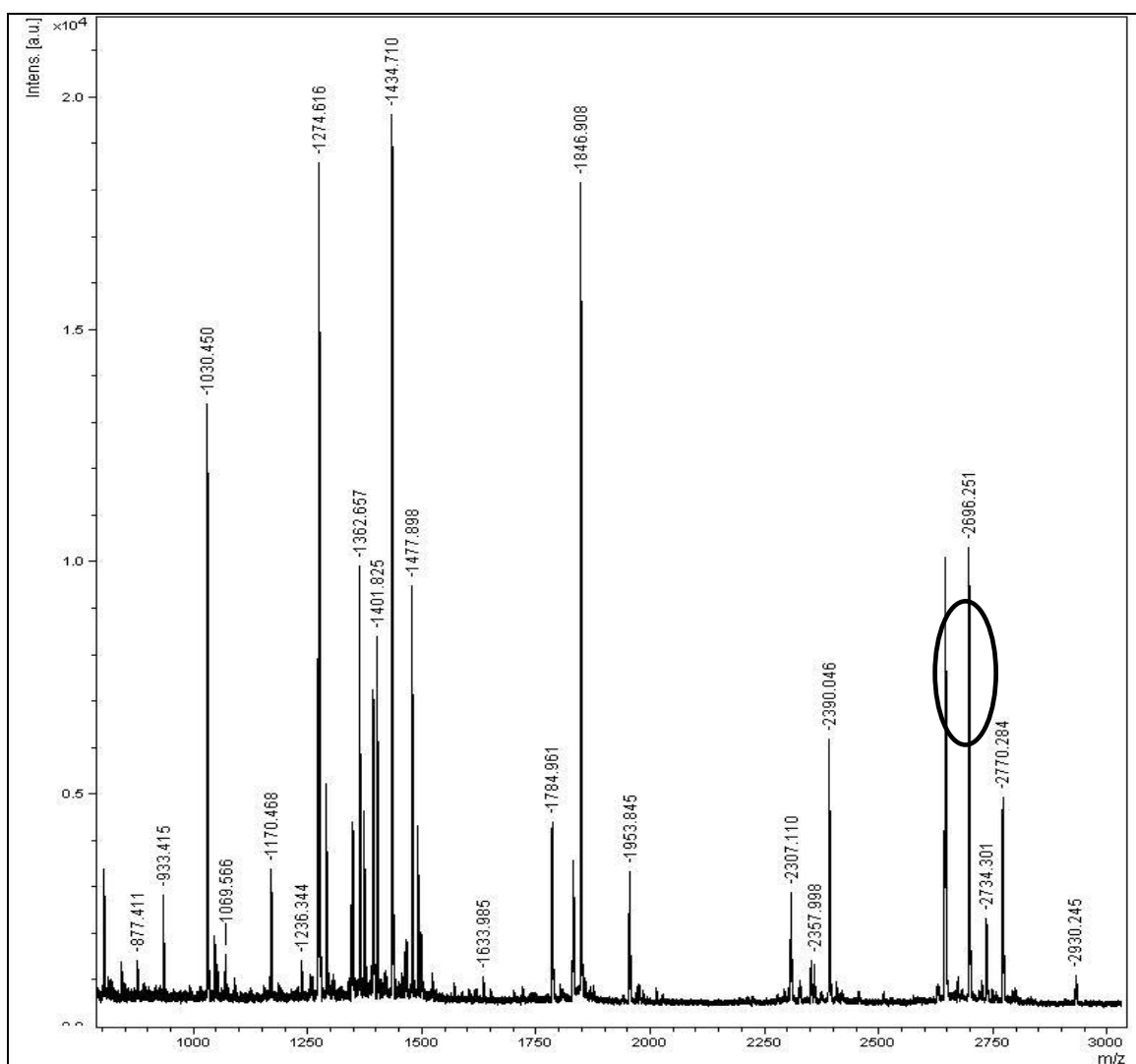


Figure 3.31 Mass spectra of tryptic digested peptide of N567D

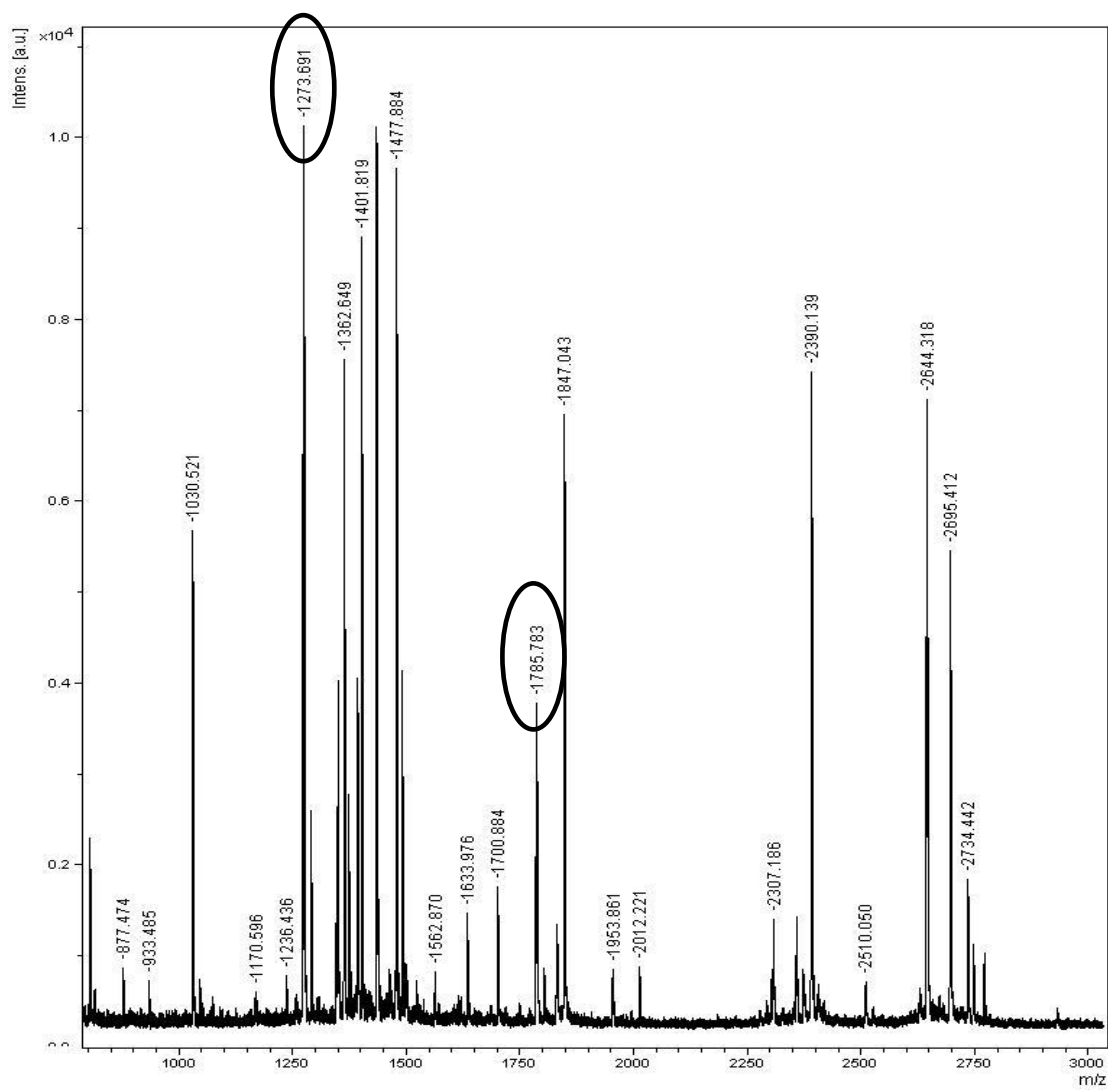


Figure 3.32 Mass spectra of tryptic digested peptide of isoform I

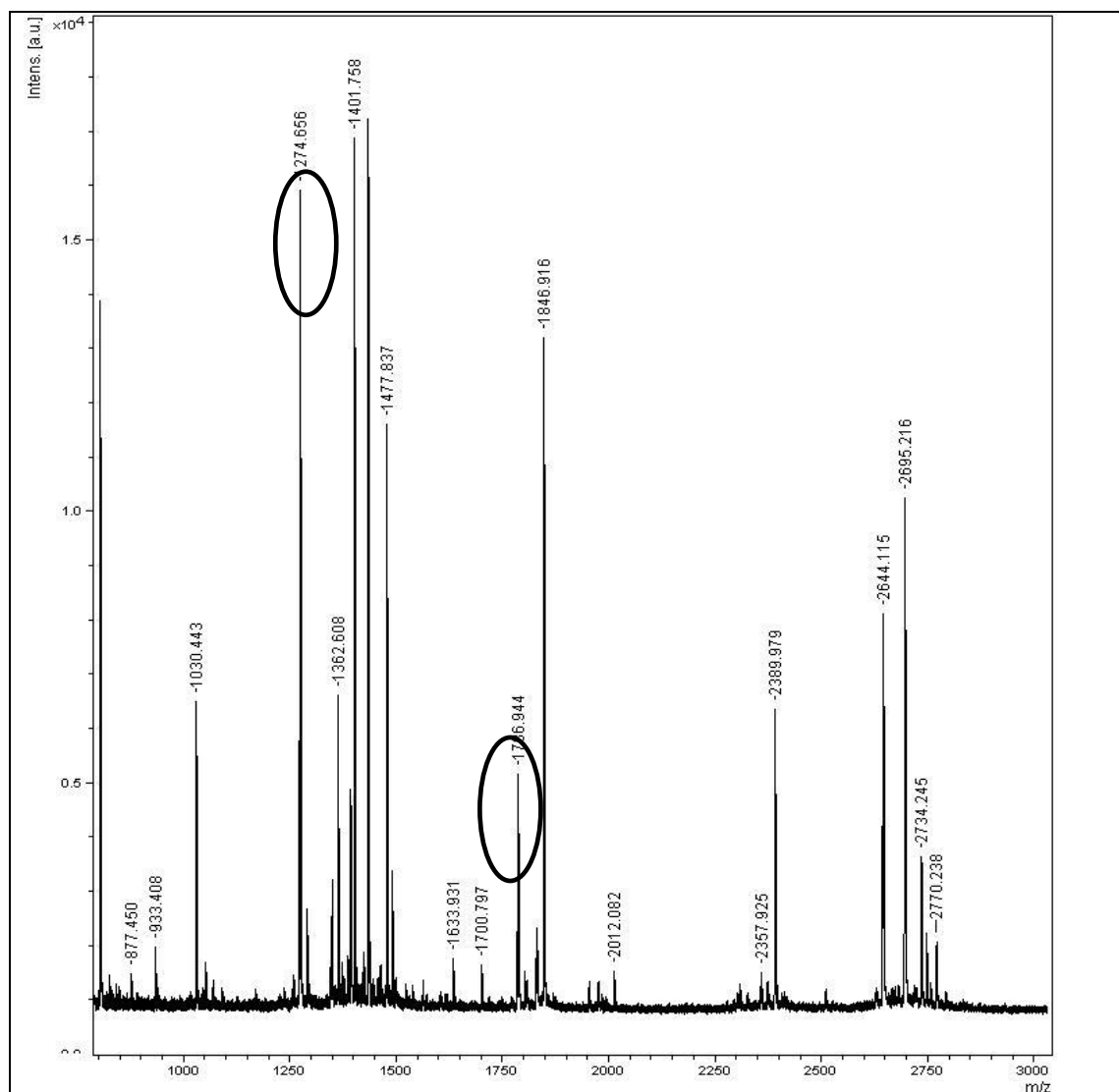


Figure 3.33 Mass spectra of tryptic digested peptide of isoform II



Only the peak at  $m/z$  of 1273.69 of isoform I changed to 1274.65 of isoform II (Figure 3.32 and 3.33), this mass was equal to fragments containing Asn 427 (however, this peak difference was not observed in all reported run). For the other mass at 1785.78 and 1786.94 Da, they did not contain any Asn. The fragments larger than 4000 Da which contained Asn188, Asn247, Asn263, Asn620 could not be detected because of the limitation of the matrix used in the MALDI-TOF. And when compared experimental mass of fragments involving those mutated residues in Table 3.7 with those corresponding fragments from isoform I and II in Table 3.8, the result confirms that mutation was accomplished and difference in 1 Da could be detected in this system. These MS results suggests that Asn427 might relate to isoform pattern of CGTase

However, there are some reports about deamidation reaction in the *B. anthracis* protective antigen (Zomber, *et al.*, 2005) and human phenylalanine hydroxylase (Solstad, *et al.*, 2003) indicated that the increasing of the intensity of successive isotope was found by comparing the quantitation of the isotopic distribution. Therefore, the percentage of isotopic distribution of the interested fragments of isoform I and isoform II were compared. The result revealed that only fragment which contained Asn336 ( $m/z = 933.6 : 934.6 : 935.6$ ) and Asn415 ( $m/z = 1434.7 : 1435.9 : 1436.9$ ) showed a significant difference in the percentage of isotopic distribution between isoform I and isoform II (Figure 3.34A and B). The percentages of second isotope (mass = 934.6 and 1435.9) in isoform II were increased comparing to the isoform I. The fragment containing Asn567 ( $m/z = 2695.7 : 2696.7 : 2697.7$ ) showed only a slight difference in the second isotope of isoform II due to relatively high deviation obtained in isoform I (Figure 3.34C). The involvement of Asn 427 in isoform formation was supported by another experiment in which isoform I of cloned CGTase was incubated at pH 9.0 for 0, 3, and 7 days. Isoform II and III were appeared on day 3 and 7, respectively (Figure 3.35). The sample from each day was digested by trypsin and subjected to isoaspartate and MALDI-TOF analysis. Isoaspartate content was increased from 0.023 to 0.054 to 0.068 pmole/pmole CGTase, respectively. And only the fragment which contained Asn427 ( $m/z = 1273.73 : 1274.72 : 1275.72$ ) showed a difference in the percentage of second isotope.

Table 3.8 Comparison of monoisotopic mass of tryptic digested fragments of cloned CGTase isoform I and isoform II from *Paenibacillus* sp. RB01.

Asn position	Monoisotopic mass ( $[M + H^+]$ )		Amino Acid Sequence of Tryptic Peptide	
	Theoretical	Experimental		
		Isoform I		Isoform II
188	4053.33	-	-	LYDNGNLLGGYTNDTQNLFHHYGGTDFSTI <u>N</u> GIYK
247	5151.76	-	-	SFMSTI <u>N</u> NYKPVFTFGWFLGVNEISPEYHQFANESGMSLLDFR
263	5151.76	-	-	SFMSTINNYKPVFTFGWFLGV <u>N</u> EISPEYHQFANESGMSLLDFR
326	3126.36	3126.12	3126.11	AMLEGSEVDYAQVNDQVTFID <u>N</u> HDMER
336	933.96	933.60	933.37	FHTS <u>N</u> GDR
370	2390.03	2390.04	2390.05	GVPAIYYGSEQYMSGG <u>N</u> DPDNR
415	1434.74	1434.75	1434.75	WI <u>N</u> NDVIIYER
427	1273.70	1273.69	1274.65 1273.71•	FG <u>N</u> NVAVAINR
428	1273.70	1273.72	1273.72	FG <u>N</u> NVAVAINR
435	1273.70	1273.72	1273.72	FG <u>N</u> NVAVAI <u>N</u> R
567	2695.33	2695.34	2695.35	VA <u>N</u> AAGAASNIYDNFEVLTGDQQVTR
620	6831.59	-	-	FVIN <u>N</u> ATTALGQNVFLTGNVSELGNWDPNNAIGPMYNQVVYQYPTWYYDVSPAGQTIEFK

\* underline letters are asparagine residues which were mutated

• values obtained from different run

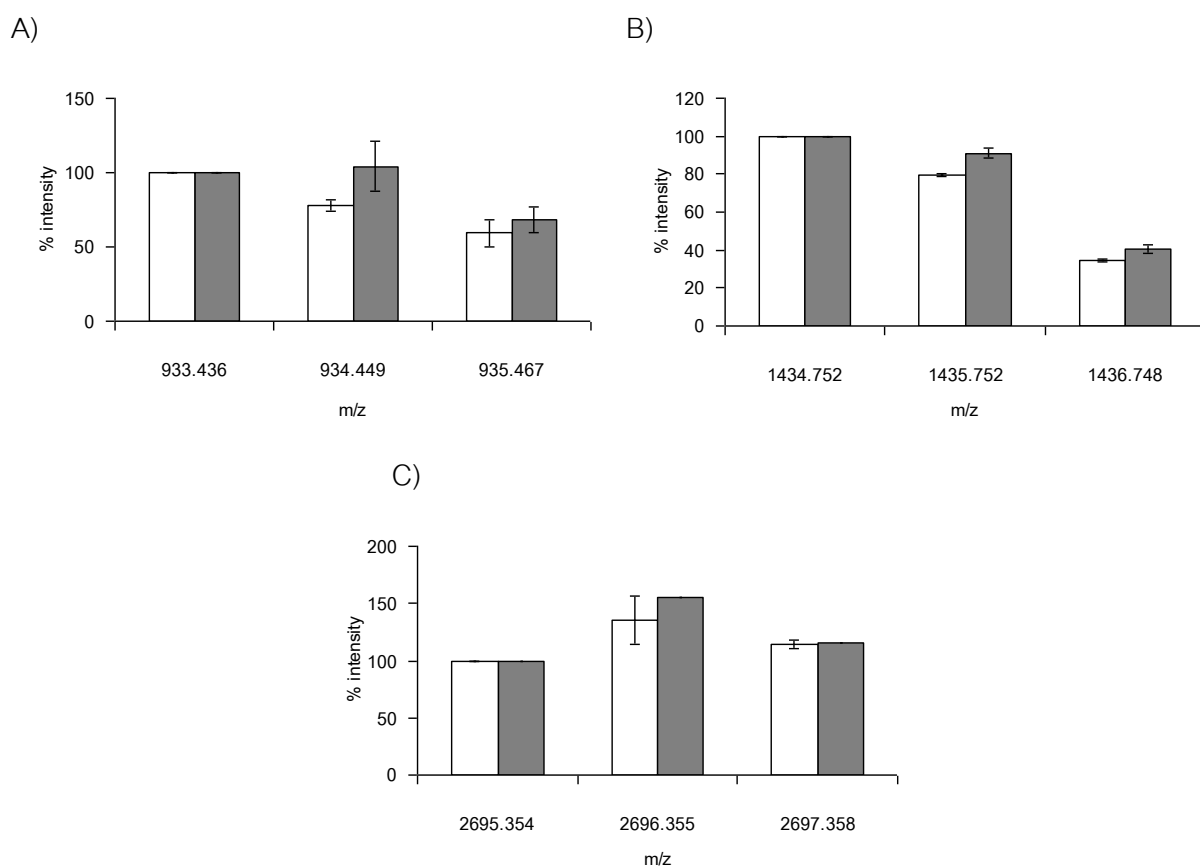


Figure 3.34 The percentage of isotopic distribution of tryptic digested peptides containing interested asparagine residues in CGTase. Isoform I (□) and II (■).

A) Fragment containing Asn336

B) Fragment containing Asn415

C) Fragment containing Asn567

The intensity of the first isotope of isoform I was referred as 100%. The result was averaged from two experimental data set.

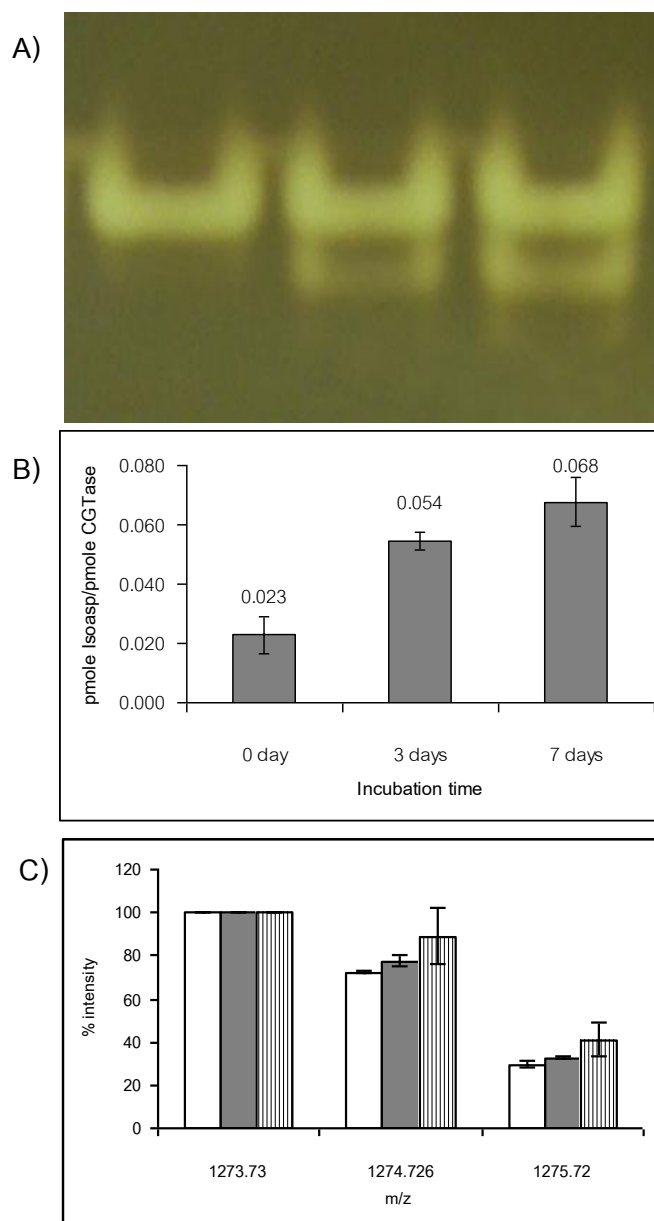


Figure 3.35 Analysis of the charge in isoform pattern and tryptic peptides upon incubation of isoform I. A) isoform pattern on native-PAGE, B) isoAsp content of tryptic peptides from each day sample, C) The percentage of isotopic distribution of tryptic peptides containing Asn427 (□) 0 day (■) 3 days (▨) 7days.

The isoform I was incubated at pH 9.0, 37°C for time intervals, then the samples at various days were digested (in solution) by trypsin and analyzed for isoAsp and mass by MALDI-TOF. From the results of MALDI-TOF, the hypothesis that isoform formation of *Paenibacillus* sp.RB01 CGTase is caused by deamidation of Asn was supported. Asn427 shows significant involvement, however, Asn336 and Asn567 were also likely to take part in isoform formation of CGTase (see Appendix 7 for other mutants profile).

### 3.10 Comparison of properties of CGTase isoforms from the cloned and mutants:

#### 3.10.1 Optimum temperature

The isoform I and II of cloned CGTase separated by FPLC using Mono Q column were used. The cyclizing activity and dextrinizing activity of both isoforms were determined, and the relative activities at different temperature and pH were compared.

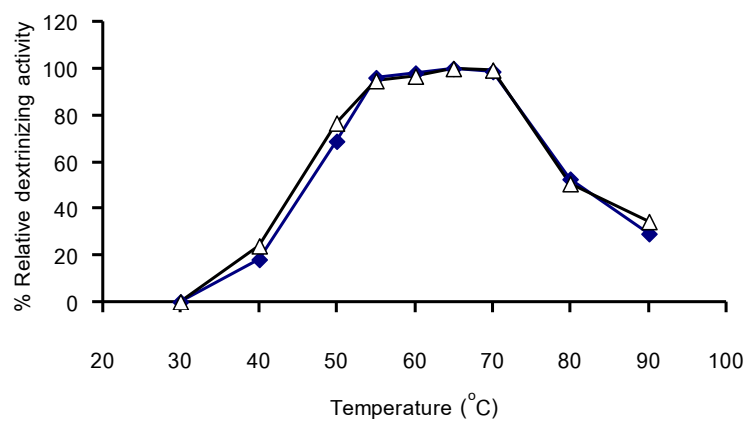
Figure 3.36A and B showed the optimum temperature of the isoform I and II of cloned CGTase. By incubating the enzyme in Tris-HCl pH 7.0 at various temperatures, both isoforms showed highest dextrinizing and cyclizing activities at temperatures of 65-70°C. However, broad optimum temperatures were observed in the range of 55-70°C. Both isoforms significantly lost their activity when temperature was higher than 70°C. At 90°C the enzyme showed only 25% relative activity compared with the maximum activity.

#### 3.10.2 Optimum pH

In the first protocol, the universal buffer which composed of the mixture of citric acid,  $\text{KH}_2\text{PO}_4$ ,  $\text{H}_3\text{BO}_3$ , and diethylbarbituric acid was used. The result showed the difference in dextrinizing vs. cyclization activity profile. For dextrinizing, both isoforms showed highest activity at pH 5.0 while at pH 6.0-8.0 the activity was decreased to 80% (Fig 3.37). On the cyclizing activity, both isoforms showed optimum pH at 6.0-7.0, while 80% of relative activity was obtained at pH 5.0 and 8.0. The activity of both isoforms was completely lost at pH 3.0 and 10.0.

When different buffer systems were used: citrate buffer (pH 3.0-5.0), acetate buffer (pH4.0-6.0), phosphate buffer (pH 6.0-8.0), and Tris-glycine buffer (pH 8.0-10.0), the broad pH optimum was observed. Figure 3.38 showed that optimum pH for isoform I

A)



B)

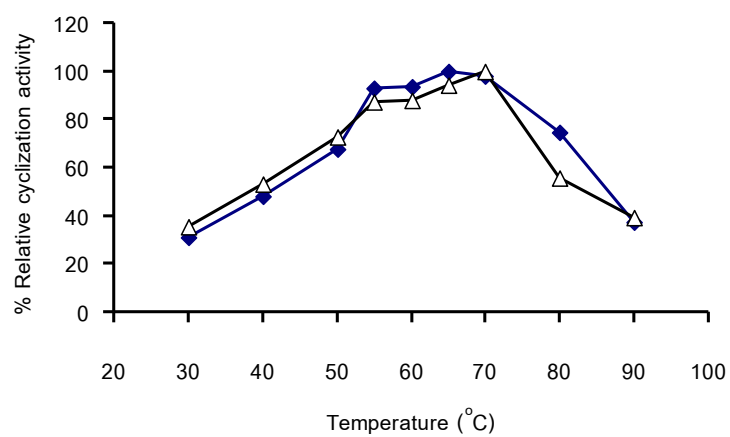
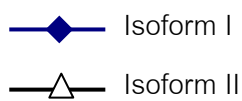


Figure 3.36 Optimum temperature for dextrinizing activity (A) and cyclizing activity (B) of the isoform I and II of cloned CGTase from *Paenibacillus* sp. RB01.



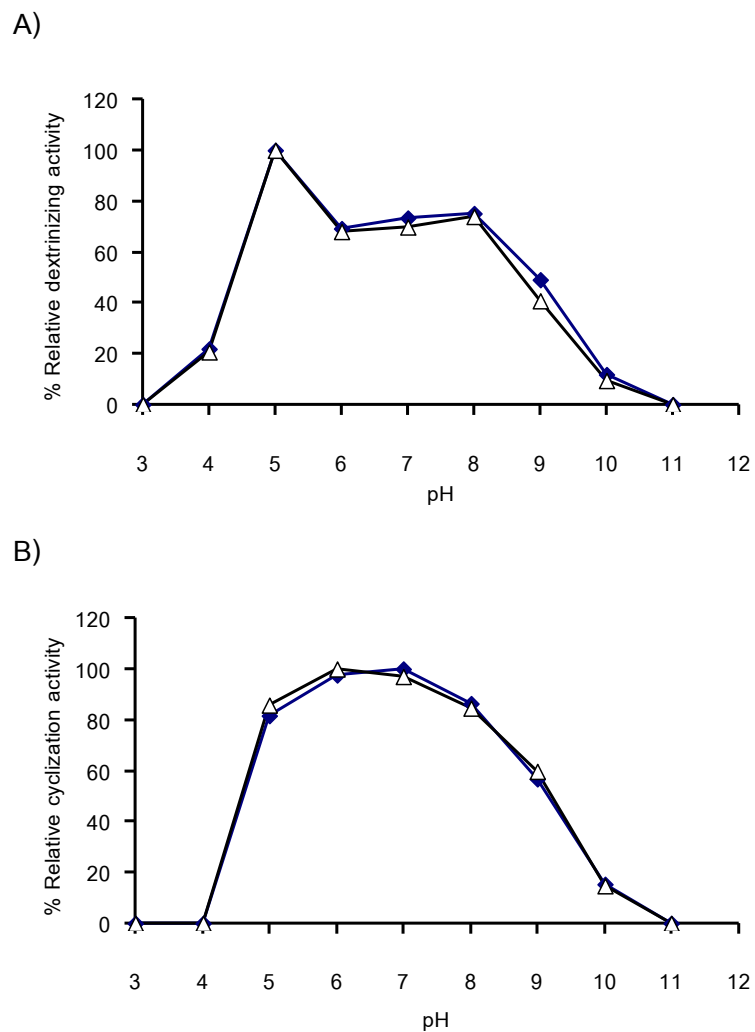
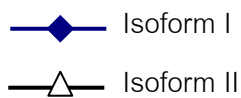


Figure 3.37 Optimum pH for dextrinizing activity (A) and cyclizing activity (B) of the isoform I and II of cloned CGTase from *Paenibacillus* sp. RB01 in the universal buffer. The 0.1 M universal buffer (citric acid,  $\text{KH}_2\text{PO}_4$ ,  $\text{H}_3\text{BO}_3$ , diethylbarbituric acid) was used.



was at pH 5.0 for dextrinizing and at pH 6.0 for cyclizing activity. The enzyme showed more than 80% relative activity in all buffer at pH 5.0-10.0. The isoform II also showed the same optimum pH as the isoform I (Figure 3.39).

### 3.10.3 Kinetic parameters of isoforms of cloned and mutated CGTase

Kinetics of CGTase was studied by coupling reaction with  $\beta$ -CD as donor substrate and 10 mM cellobiose as acceptor. This pair of substrate was chosen because this CGTase was a  $\beta$ -CGTase (Yenpetch, 2002) and cellobiose was previously determined to be an efficient acceptor (Wongsangwattana 2000). The coupling reaction was performed at 55°C for 5 minutes. The amount of released reducing sugar (glucose) was determined by dinitrosalicylic acid method as described in Methods. Lineweaver-Burk plot using nonlinear least square regression analysis of varying concentrations of  $\beta$ -CD was shown in Figure 3.40 and the summarized result was shown in Table 3.9. The isoform I and II showed the  $K_m$  values of 1.67 and 1.43 mM, respectively. The mutated CGTases N336D, N427D and N567D had the  $K_m$  values lower than those isoforms, especially the N336D which showed the lowest  $K_m$ . When  $k_{cat}$  was concerned, isoform I gave the highest value while isoform II and N567D CGTase had similar values. The two mutants, N336D and N427D expressed CGTases which catalyzed the coupling reaction between  $\beta$ -CD and cellobiose with significantly lower  $k_{cat}$  than isoform I and II. However, when catalytic efficiency was concerned, CGTases from N336D and N567D mutants were as efficient as the isoform I of cloned CGTase in the coupling reaction. Whereas isoform II had lower  $k_{cat}/K_m$  value and N427D CGTase showed the lowest catalytic efficiency.

### 3.10.4 Comparison of CD production by HPAEC-PAD

The crude CGTases from cloned and mutants were used in this CD production experiment. The reaction was performed at 60°C in Tris-HCl buffer pH 7.0 using a 4% soluble starch as substrate and 3 Units (Dextrinizing) of CGTase. After the cyclization reaction stopped, the linear oligosaccharides were digested with glucoamylase, then the CD products were detected by HPAEC-PAD. In this system, the CD products were separated with anion exchange column by differences in degree polymerization (DP) of



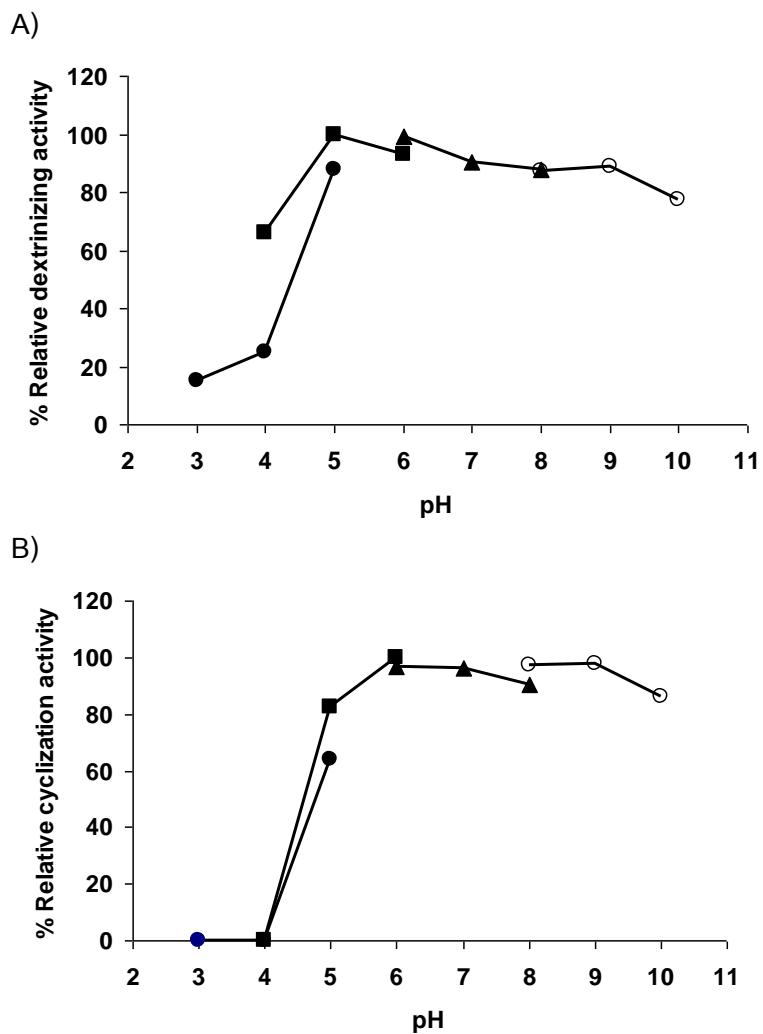


Figure 3.38 Optimum pH for dextrinizing activity (A) and cyclizing activity (B) of the isoform I of cloned CGTase from *Paenibacillus* sp. RB01 in various buffers.

- Citrate buffer (pH 3-5)
- ▲— Acetate buffer (pH 4-6)
- Phosphate buffer (pH 6-8)
- Tris-Glycine buffer (pH 8-10)

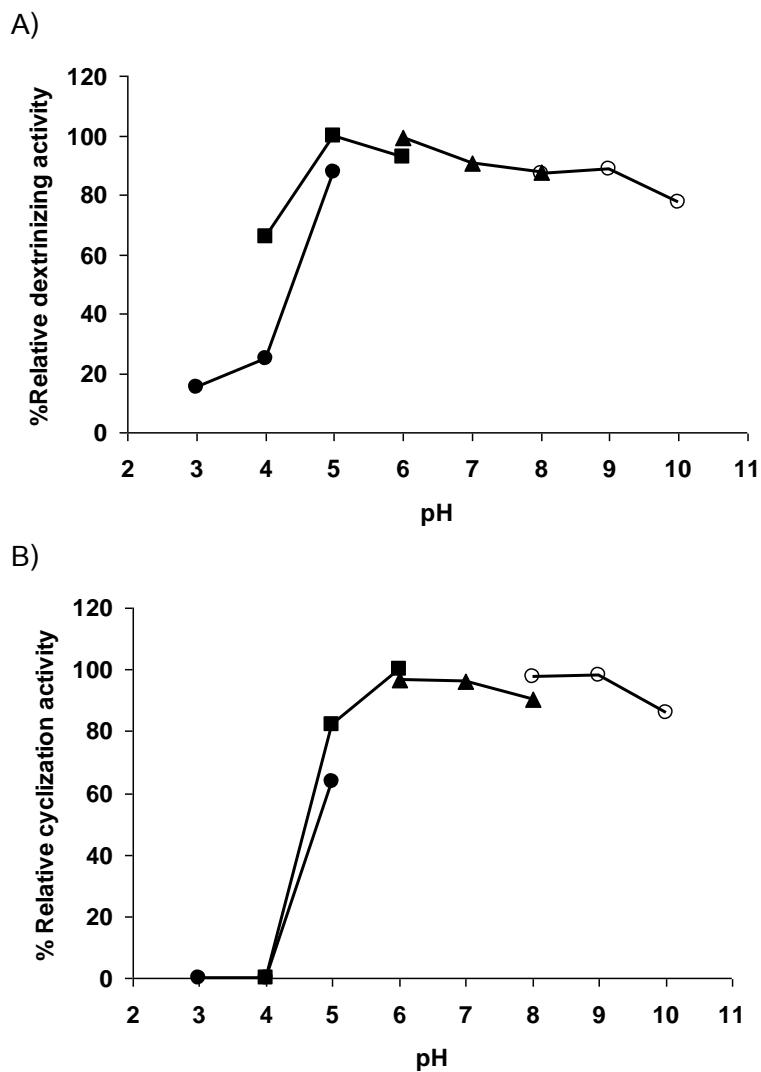


Figure 3.39 Optimum pH for dextrinizing activity (A) and cyclizing activity (B) of the isoform II of cloned CGTase from *Paenibacillus* sp. RB01 in various buffers.

- Citrate buffer (pH 3-5)
- ▲ Acetate buffer (pH 4-6)
- Phosphate buffer (pH 6-8)
- Tris-Glycine buffer (pH 8-10)

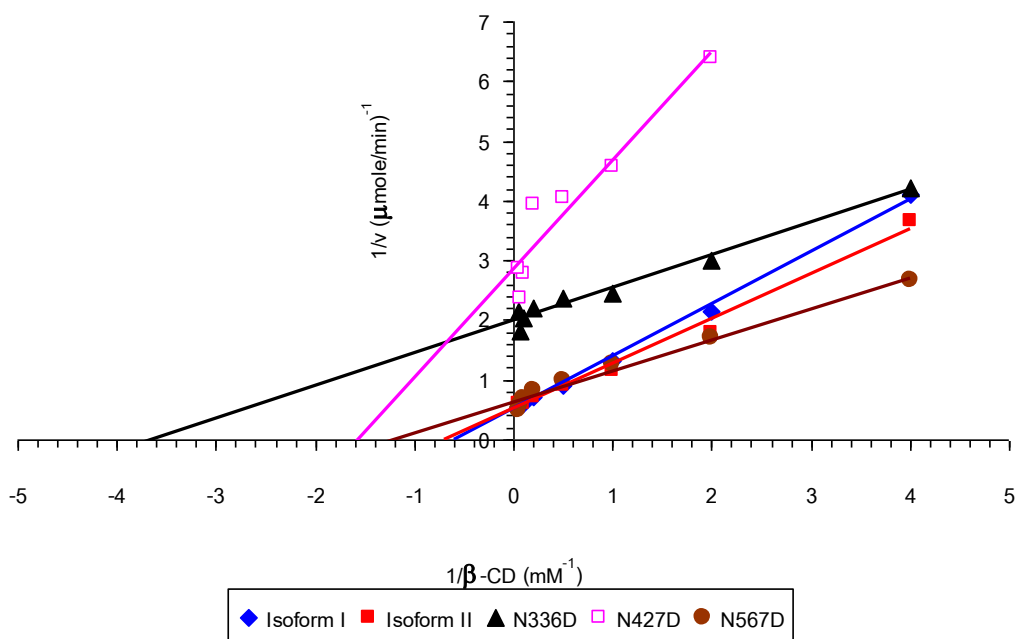


Figure 3.40 Lineweaver-Burk plot of CGTase on coupling reaction with  $\beta$ -cyclodextrin as donor and cellobiose as acceptor. CGTase was incubated with 10 mM cellobiose and various concentrations of  $\beta$ -cyclodextrin in 50 mM acetate buffer, pH 6.0 at 55°C for 5 minutes. 4 units of *Aspergillus niger* glucoamylase was added to convert linearized oligosaccharides to glucose incubated at 55°C for 1 hour. Release of reducing sugar was determined by dinitrosalicylic acid method.

Table 3.9 Kinetic parameters of CGTases from coupling reaction with various concentrations of  $\beta$ -CD donor and fixed concentration of cellobiose acceptor.

CGTase	$K_m$ (mM)	$k_{cat}$ ( $\text{min}^{-1}$ )	$k_{cat}/K_m$ ( $\text{mM}^{-1}\text{min}^{-1}$ )
Isoform I	1.67	5.91	3.55
Isoform II	1.43	3.94	2.76
N336D	0.28	0.98	3.55
N427D	0.63	0.66	1.04
N567D	0.87	3.28	3.78

glucose units. An example of separation profile of CD products was shown in Figure 3.41. The products were identified by comparing the retention time with that of standard CDs. The result showed that the small ring (CD6) was first eluted followed by CD7, CD8, then the large ring CDs. It should be noticed that CD9 was not eluted in order of DP. From the peak area, the main product was CD7 which confirmed this CGTase was the  $\beta$ -CGTase. And the products were composed of CD6 to approximately CD25.

The isoform I and II of cloned CGTase separated by Mono P isofocusing column were used to study on the CD production. The CD products at 6, 12 and 24 hrs were determined and shown in Figure 3.42(A-F). At 6 hrs of production, in addition to CD6 to CD8, both isoforms also produced a high amount of the large ring CDs (>CD9) but the amount of these large ring CDs were decreased at 12 and 24 hrs of production. It was observed that CD6 to CD8 were increased at 24 hrs. The chromatogram of CD products of the isoform I compared with the isoform II of cloned CGTase were not different, CD7 ( $\beta$ -CD) was the main CD product at all time of production. The ratio of CD6 : CD7 : CD8 at 24 hrs for the isoform I and isoform II were 0.25 : 1.00 : 0.60 and 0.22 : 1.00 : 0.62, respectively.

The ratio of CD products of cloned CGTase (mixtures of isoforms) and mutated CGTases was also determined and compared (Table 3.10 and Figure 3.43). Isolated isoform I and II produced higher  $\gamma$ -CD (CD8) than the mixture of all isoforms (cloned). For all CGTases, CD7 was the major product and CD8 was higher than CD6. When comparing the CD6 : CD7 : CD8, no significant difference from the isoform I and II was found in mutated CGTases from N188D, N415D, N427D, N567D, N336Q, and the double mutant N336D/N415D. Mutated CGTases from N247D, N370D produced higher CD6 while those from N326D, N428D, N620D, and the triple mutant N336D/N415D/N567D produced significantly lower CD6 than isoform I and II. And lower CD8 production was clearly observed in N336D, N428D, and N435D. These results suggested that mutation at some Asn residues had an effect on product formation, while mutation at Asn 415, 427, and 567 had no effect.

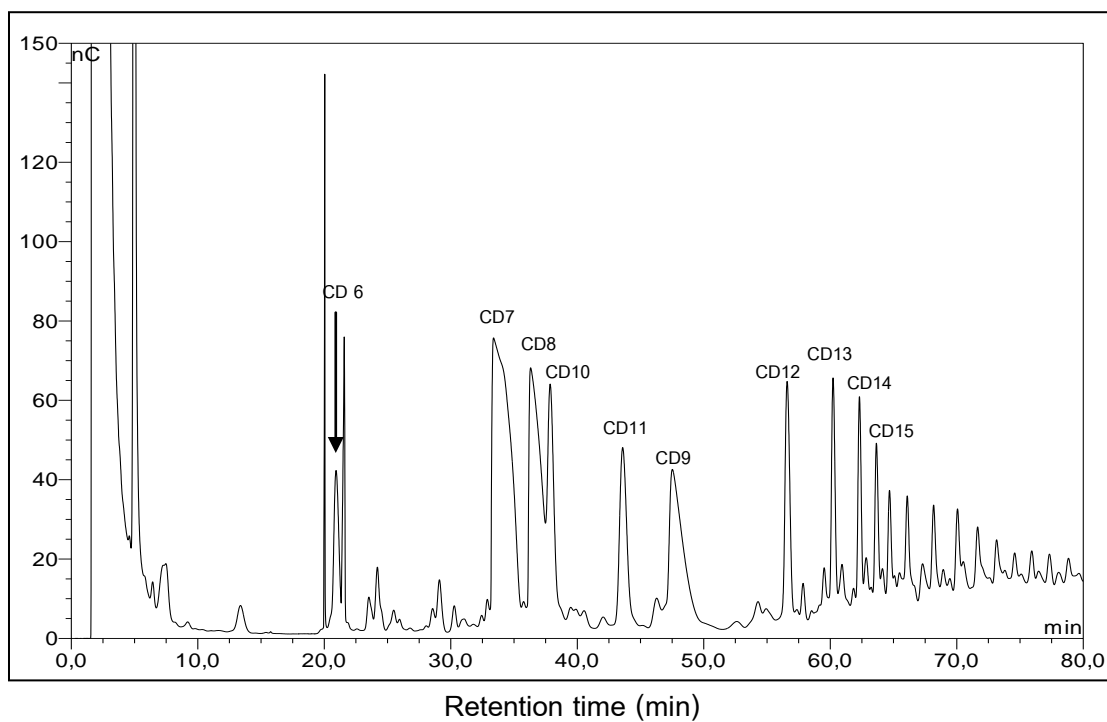


Figure 3.41 Example of HPAEC elution profile the CDs produced by CGTase from *Paenibacillus* sp. RB01. Degree polymerization was shown above each peak. Carbopac PA-100 analytical column was used. The main eluent was 150 mM NaOH and the gradient of 200 mM NaNO<sub>3</sub> in 150 mM NaOH was performed in 85 minutes.

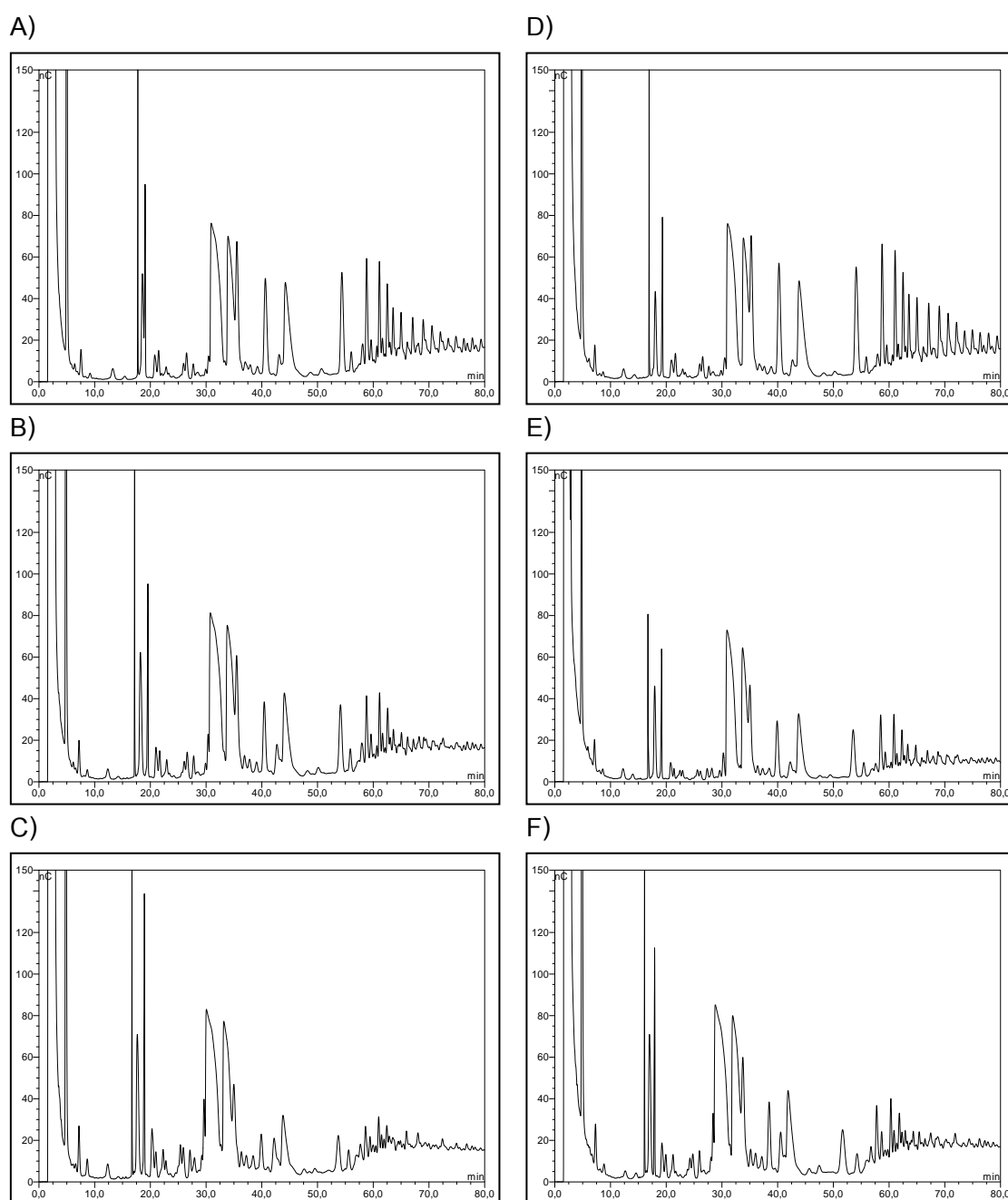


Figure 3.42 HPAEC chromatogram of CD products of isoform I and II of cloned CGTase, The enzyme 3 unit was mixed with 4% soluble starch at 60°C. The reaction was collected at various times.

A) Isoform I at 6 hrs

D) Isoform II at 6 hrs

B) Isoform I at 12 hrs

E) Isoform II at 12 hrs

C) Isoform I at 24 hrs

F) Isoform II at 24 hrs

Table 3.10 Cyclodextrin products from crude CGTases with 3 Units activity per reaction.

Source of CGTase	Product (g)			Ratio ( $\alpha$ : $\beta$ : $\gamma$ -CD)
	$\alpha$ -CD	$\beta$ -CD	$\gamma$ -CD	
Cloned CGTase	0.072	0.411	0.147	0.18 : 1.00 : 0.36
Isoform I**	0.116	0.531	0.230	0.25 : 1.00 : 0.60
Isoform II**	0.129	0.518	0.223	0.22 : 1.00 : 0.62
N188D	0.072	0.327	0.178	0.22 : 1.00 : 0.54
N247D	0.140	0.386	0.229	0.36 : 1.00 : 0.59
N263D	0.080	0.442	0.193	0.18 : 1.00 : 0.44
N326D	0.020	0.173	0.083	0.12 : 1.00 : 0.48
N336D	0.066	0.375	0.144	0.18 : 1.00 : 0.38
N370D	0.068	0.217	0.126	0.31 : 1.00 : 0.58
N415D	0.050	0.309	0.152	0.16 : 1.00 : 0.50
N427D	0.054	0.224	0.133	0.24 : 1.00 : 0.59
N428D	0.065	0.487	0.186	0.13 : 1.00 : 0.38
N435D	0.058	0.346	0.114	0.17 : 1.00 : 0.33
N567D	0.082	0.476	0.248	0.17 : 1.00 : 0.52
N620D	0.032	0.302	0.180	0.10 : 1.00 : 0.60
N336Q	0.060	0.369	0.209	0.16 : 1.00 : 0.56
N336D/N415D	0.031	0.203	0.109	0.15 : 1.00 : 0.53
N336D/N415D/N567D	0.035	0.281	0.158	0.12 : 1.00 : 0.56

\*\* purified sample



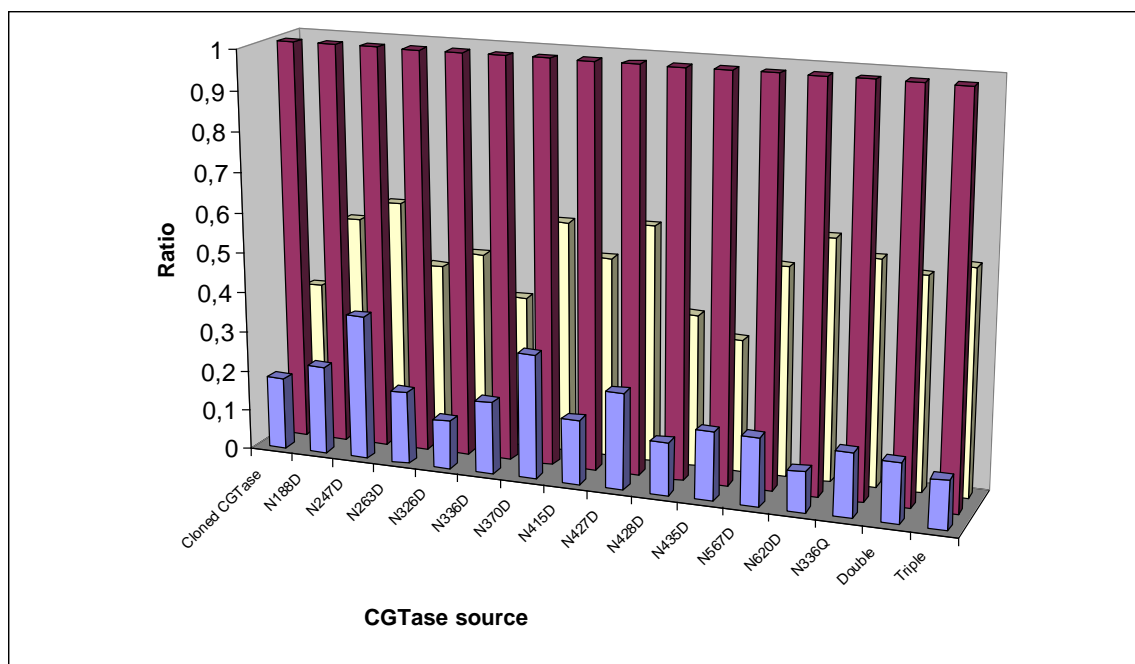


Figure 3.43 Ratio of  $\alpha$ -CD (■),  $\beta$ -CD (■) and  $\gamma$ -CD (■) by crude CGTase 3 Units per reaction.

### 3.10.5 Amino acid sequence

The amino acid sequence was predicted by comparison of the monoisotopic mass of tryptic digested peptides from isoform I and isoform II of cloned CGTase with the available database ([www.matrixscience.com](http://www.matrixscience.com)). Table 3.11 and 3.12 showed the detail of expected mass and the calculated mass including the sequence of deduced amino acid sequence when the observed monoisotopic mass  $[M+H]^+$  were subjected into the web site.

Table 3.11 Monoisotopic mass of tryptic digested peptides of isoform I from cloned CGTase analyzed and matching amino acid sequence predicted by the available program at [www.matrixscience.com](http://www.matrixscience.com)

Start - End	Observed	Mr (expt)	Mr (calc)	Delta	Miss	Sequence
1 - 24	2746.4000	2745.3927	2745.3246	0.0681	1	--APDTSVSNKQNFSTDVIIYQIFTD.R.F
10 - 24	1847.0430	1846.0357	1845.8897	0.1460	0	K.QNFSTDVIIYQIFTD.R.F
108 - 119	1372.6130	1371.6057	1371.6129	-0.0072	0	K.TNPAYGTMQDFK.N
120 - 131	1345.6390	1344.6317	1345.7102	-1.0785	0	K.NLIDTAHAHNIK.V
132 - 156	2644.3180	2643.3107	2643.2201	0.0906	0	K.VIIDFAPNHTSPASSDDPSFAENGR.L
193 - 212	2307.1860	2306.1787	2306.1179	0.0609	0	K.NLYDLADLNHNNSVDVYLK.D
193 - 216	2734.4420	2733.4347	2733.3609	0.0738	1	K.NLYDLADLNHNNSVDVYLKDAIK.M
217 - 227	1275.7010	1274.6937	1273.6489	1.0448	0	K.MWLDLGV DGIR.V
233 - 240	1030.5210	1029.5137	1029.4855	0.0283	0	K.HMPFGWQK.S
291 - 304	1700.8840	1699.8767	1699.7988	0.0779	1	R.QVFRDNTDNMYGLK.A
295 - 304	1170.5960	1169.5887	1169.5023	0.0864	0	R.DNTDNMYGLK.A
332 - 339	933.4850	932.4777	932.4100	0.0677	0	R.FHTSNGDR.R
341 - 353	1477.8840	1476.8767	1476.8300	0.0467	1	R.KLEQALAF TLT SR.G
342 - 353	1349.7430	1348.7357	1348.7350	0.0007	0	K.LEQALAF TLT SR.G
354 - 375	2390.1390	2389.1317	2389.0281	0.1036	0	R.GVPAIYYGSEQYMSGGNDPDNR.A
376 - 393	2012.2210	2011.2137	2011.0738	0.1399	1	R.ARLPSFSTTTTAYQVIQK.L
378 - 393	1785.7830	1784.7757	1783.9356	0.8401	0	R.LPSFSTTTTAYQVIQK.L
413 - 423	1434.8220	1433.8147	1433.7303	0.0844	0	R.WINNDVIIYER.K
413 - 424	1562.8700	1561.8627	1561.8252	0.0375	1	R.WINNDVIIYERK.F
424 - 436	1401.8190	1400.8117	1400.7888	0.0229	1	R.KFGNNVAVVAINR.N
425 - 436	1273.6910	1272.6837	1272.6939	-0.0101	0	K.FGNNVAVVAINR.N
527 - 552	2770.4390	2769.4317	2769.3862	0.0456	0	K.GTVYFGTTAVTGADIVAWEDTQIQVK.I
553 - 564	1270.7190	1269.7117	1269.7081	0.0036	0	K.IPAVPGGIYDIR.V
565 - 590	2695.4120	2694.4047	2694.3249	0.0798	0	R.VANAAGAASNIYDNFEVLTGQVTVR.F
655 - 668	1490.7850	1489.7777	1489.7274	0.0504	1	K.KQGSTVTWEGGANR.T
656 - 668	1362.6490	1361.6417	1361.6324	0.0093	0	K.KQGSTVTWEGGANR.T

Match to: 1PAMA Score: 186 Expect: 8.1e-13, Nominal mass (M<sub>r</sub>): 75125; Calculated pI value: 5.21,

Number of mass values matched: 26, Sequence Coverage: 42%

Matched peptides shown in underline letters

1 APDTSVSNKQ NFSTDVIIYQI FTDRFSDGNP ANNPTGAAFD GSCTNLRLYC  
51 GGDWQGIINK INDGYLTGMG ITAIWISQPV ENIYSVINYS GVNNTAYHGY  
101 WARDFKKTNP AYGTMQDFKN LIDTAHAHNI KVIIDFAPNH TSPASSDDPS  
151 FAENGRLVDN GNLLGGYTND TQNLFHYYGG TDFSTIENGI YKNLYDLADL  
201 NHNNSVDVY LKDAIKMWLD LGVDGIRVDA VKHMPFGWQK SFMATINNYK  
251 PVFTFGEWFL GVNESPEYH QFANESGMSL LDFRFAQKAR QVFRDNTDNM  
301 YGLKAMLEGS EVDYAQVNDQ VTFIDNHME RFHTSNGDRR KLEQALFTL  
351 TSRGVPAIYY GSEQYMSGGN DPDNRARLPS FSTTTTAYQV IQKLAPLRKS  
401 NPAIAYGSTH ERWINNDVII YERKFGNNVA VVAINRNMNT PASITGLVTS  
451 LPRGSYNDVL GGILNGNTLT VGAGGAASNF TLAPGGTAVW QYTTDATTPI  
501 GNVGPMMAK PGVTITIDGR GFGSGKGTVY FGTTAVTGAD IVAWEDTQIQ  
551 VKIPAVPGGI YDIRVANAAG AASNIYDNFE VLTDGQVTVR FVINNATTAL  
601 QQNVFLTGNV SELGNWDPNN AIGPMYNQVV YQYPTWYYDV SVPAGQTIEF  
651 KFLKKQGSTV TWEGGANRTF TTPTSGTATV NVNWQP

Table 3.12 Monoisotopic mass of tryptic digested peptides of isoform II from cloned CGTase analyzed analyze and matching amino acid sequence predicted by mascot program at [www.matrixscience.com](http://www.matrixscience.com)

Start - End	Observed	Mr (expt)	Mr (calc)	Delta	Miss	Sequence
1 - 24	2746.1890	2745.1817	2745.3246	-0.1429	1	-.APDTSVSNKQNFSTDVIYQIFTD.R.F
10 - 24	1846.9160	1845.9087	1845.8897	0.0190	0	K.QNFSTDVIYQIFTD.R.F
120 - 131	1345.5830	1344.5757	1345.7102	-1.1345	0	K.NLIDTAHAHNIK.V
132 - 156	2644.1150	2643.1077	2643.2201	-0.1124	0	K.VIIDFAPNHTSPASSDDPSFAENGR.L
193 - 216	2734.2450	2733.2377	2733.3609	-0.1232	1	K.NLYDLADLNHNSSVDVYLKDAIK.M
217 - 227	1274.6560	1273.6487	1273.6489	-0.0002	0	K.MWLDLGVGDGIR.V
217 - 232	1786.9440	1785.9367	1785.9447	-0.0080	1	K.MWLDLGVGDGIRVDAVK.H
233 - 240	1030.4430	1029.4357	1029.4855	-0.0497	0	K.HMPFGWQK.S
291 - 304	1700.7970	1699.7897	1699.7988	-0.0091	1	R.QVFRDNTDNMYGLK.A
332 - 339	933.4080	932.4007	932.4100	-0.0093	0	R.FHTSNGDR.R
341 - 353	1477.8370	1476.8297	1476.8300	-0.0003	1	R.KLEQALAFLLTSR.G
342 - 353	1349.7070	1348.6997	1348.7350	-0.0353	0	K.LEQALAFLLTSR.G
354 - 375	2389.9790	2388.9717	2389.0281	-0.0564	0	R.GVPAIYYGSEQYMSGGNDPDNR.A
376 - 393	2012.0820	2011.0747	2011.0738	0.0009	1	R.ARLPSFSTTTTAYQVIQK.L
378 - 393	1784.9180	1783.9107	1783.9356	-0.0249	0	R.LPSFSTTTTAYQVIQK.L
413 - 423	1434.7280	1433.7207	1433.7303	-0.0096	0	R.WINNDVIIYER.K
424 - 436	1401.7580	1400.7507	1400.7888	-0.0381	1	R.KFGNNVAVVAINR.N
425 - 436	1273.6280	1272.6207	1272.6939	-0.0731	0	K.FGNNVAVVAINR.N
527 - 552	2770.2380	2769.2307	2769.3862	-0.1554	0	K.GTVYFGTTAVTGADIVAWEDTQIQVK.I
553 - 564	1270.6640	1269.6567	1269.7081	-0.0514	0	K.IPAVPGGIYDIR.V
565 - 590	2695.2160	2694.2087	2694.3249	-0.1162	0	R.VANAAGAASNIYDNFEVLTGDQVTVR.F
655 - 668	1490.7250	1489.7177	1489.7274	-0.0096	1	K.KQGSTVTWEGGANR.T
656 - 668	1362.6080	1361.6007	1361.6324	-0.0317	0	K.QGSTVTWEGGANR.T

Match to: 1PAMA Score: 189 Expect: 4.1e-13, Nominal mass (M<sub>r</sub>): 75125, Calculated pI value: 5.21

Number of mass values searched: 34, Number of mass values matched: 23

Sequence Coverage: 41%

Matched peptides shown in underline letters

1 APDTSVSNKQ NFSTDVIYQI FTDRFSDGNP ANNPTGAAFD GSCTNLRLYC  
51 GGDWQGIINK INDGYLTGMG ITAIWISQPV ENIYSVINYS GVNNTAYHGY  
101 WARDFKKTNP AYGTMQDFKN LIDTAHAHNI KVIIDFAPNH TSPASSDDPS  
151 FAENGRLYDN GNLLGGYTND TQNLFHYYGG TDFSTIENGI YKNLYDLADL  
201 NHNSSVDVY LKDAIKMWLD LGVDGIRVDA VKHMPFGWQK SFMATINNYK  
251 PVFTFGWFL GVNEISPEYH QFANESGMSL LDFRFAQKAR QVFRDNTDNM  
301 YGLKAMLEGS EVDYAQVNDQ VTFIDNHME RFHTSNGDRR KLEQALFTL  
351 TSRGVPAIYY GSEQYMSGGN DPDNRARLPS FSTTTTAYQV IQKLAPLRKS  
401 NPAIAYGSTH ERWINNDVII YERKFGNNVA VVAINRNMNT PASITGLVTS  
451 LPRGSYNDVL GGILNGNTLT VGAGGAASNF TLAPGGTAWW QYTTDATTPI  
501 IGNVGPMMAK PGVTITIDGR GFGSGKGTVY FGTTAVTGAD IVAWEDTQIQ  
551 VKIPAVPGGI YDIRVANAAG AASNIYDNFE VLTGDQVTVR FVINNATTAL  
601 GQNVFLTGNV SELGNWDPNN AIGPMYNQV YQYPTWYYDV SVPAGQTIEF  
651 KFLKQGSTV TWEGGANRTF TTPTSGTATV NVNWQP

## CHAPTER IV

### DISCUSSION

#### 4.1 Cloning of *cgt* from *Paenibacillus* sp. RB01

The CGTase gene (*cgt*) from *Paenibacillus* sp. RB01 was cloned and expressed in *E. coli* JM109 with vector pGEM-T by Chareonsakdi (2005). The nucleotide sequence was reported. However, the system of pGEM-T vector is not suitable to be used as an expression vector. From the nucleotide and amino acid sequence alignment, the *cgt* was successfully cloned into the vector pET 19b and expressed by *E. coli* BL21 (DE3). The CGTase gene had an ORF of 2,142 bp and deduced into a protein with 713 amino acid residues including 27 amino acids as signal sequence. In *Thermoanaerobacter*, the *cgtA* gene encodes a total of 710 amino acid residues. It is significant that the first segment of 27 amino acids of the predicted amino acid sequence has the typical features of a prokaryotic signal peptide. From automated Edman degradation of most CGTase sequences, N-terminal sequence of A P D T S V S N V V was corresponded to the predicted amino acid sequence indicated that this enzyme was in fact removed the proposed signal peptide to yield a mature protein (Jorgensen, 1997).

From the alignment of deduced amino acid sequence with *cgt* sequence in NCBI database, our CGTases show 100% similarity with the enzyme of *Paenibacillus* sp. A11, cloned by Rimpanichayakit, 2005 And when compared with CGTase of *Bacillus* sp. 1011, of which 3D-structure has been known, 98% similarity was observed.

#### 4.2 Isoforms of CGTase

A few CGTase has been reported to have multiple forms (Table 1.4). Two to more than seven isoforms were found in different bacteria, mostly *Bacillus*. All isoforms reported had the same size but different pI values, usually within 0.1-0.2 pH units, except those from *Bacillus* INMIA which had different size and charge (Abelyan *et al.*, 1994). No studies on the detail comparison of reaction of each isoform, and the cause of isoform formation have been reported. However, a study in *B. circulans* E192 suggested that the amino acid composition of isoforms were different (Bovetto *et al.*, 1992).

Our research group previously demonstrated the existence of CGTase isoforms in *Paenibacillus* sp. A11. In 1994, the isoforms of this CGTase was isolated by chromatofocusing column in the pH range of 6.2-4.0 (Rojtinnakorn, 2001). It was found that the enzyme had 4 isoforms with different in pI values; 4.73, 4.49, 4.40 and 4.31 (Kaskangam, 1998). Further study suggested that the cause of isoform formation was by post-translational modification of a single protein; not by having multiple genes for CGTase (Prasong, 2002). And modification of carboxyl residues in the enzyme resulted in the change in electrophoretic mobility similar to the occurrence of isoform. Since the thermotolerant *Paenibacillus* sp. RB01 which was screened by Tesana (2001) showed 100% similarity in amino acid sequence as the A11 strain, it may be assumed that isoform formation in both strains had the same cause.

Several reports on formation of multiple forms of various proteins/enzymes have been found to involve with Asn deamidation. Isoforms of rat kidney cytochrome c with different pI values were studied (Flatmark and Sletten, 1968). Deamidation was demonstrated to occur at two Asn positions in the fragment AlaThrAsn(103)GluCOOH and AsnLysAsn(54)LysGly, which resulted in the change from isoform I to isoform II with the 0.23 pH unit decreased in the pI value (Flatmark and Vesterberg, 1966).

In another study, 4-5 isoforms of human phenylalanine hydroxylase were observed. Deamidation of labile Asn32 in the peptide fragment AsnGlnAsn(32)GlyAla resulted in the change of the isoform pattern which increased the catalytic efficiency of the enzyme (Solstad, 2003).

#### 4.3 Evidences support Asn deamidation as the cause of formation of CGTase isoforms

##### 4.3.1 Effect of pH, incubation time, and isoAsp content

The experiment that isoform I of cloned CGTase changed to isoform II in deamidation buffer at pH 9.0 (Figure 3.25 and 3.26) pointed the possible involvement of deamidation reaction. And when the enzyme samples from different incubation time were measured for isoAsp content, the amount of this intermediate was found to be significantly increased. This result supports that Asn deamidation really occurred and led to the formation of different isoform pattern of CGTase.

IsoAsp content was determined by using ISOQUANT kit, making use of catalysis by PIMT resulted in S-adenosyl homocysteine product which can be quantified by HPLC (Aswad, 2000). Examples of proteins which the amount isoAsp was determined by this method are:

- a. Different isoaspartate content was found in each isoform of purified monoclonal IgG1 antibody, MMA383 and the two site of deamidation were identified (Perkins, 2000).
- b. The high content of isoAsp in ribosomal protein S11 was estimated to be  $\sim 0.5$  mol/mol during a rapid growth. The possibility that isoAsp may play a unique role in ribosome protein S11 function was raised (David, 1999).
- c. The isoAsp content in fibronectin (freshly isolated from human plasma) and FN-30kDa fragment was 0.048 and 0.026 pmol/pmol of protein. They suggested that time-dependent generation of isoAspGlyArg may represent a sort of molecular clock for activating latent integrin binding sites in fibronectin proteins (Curnis, 2006).

#### 4.3.2 Prediction of labile Asn residues

CD values which reflect deamidation rate of each Asn are used to predict residues which are labile. Computer algorithm stated in [www.deamidation.org](http://www.deamidation.org) developed by Robinson and Robinson, 2001 is an important tool for calculation of CD values. Although it was investigated that protein deamidation rates depend on primary, secondary, tertiary, and quaternary protein structure, and numerous examples have been found, it was not possible to devise a useful deamidation prediction procedure until a complete library of deamidation rates as a function of primary sequence was available. These rates can now be combined with 3D data to provide a useful deamidation prediction procedure. Each amide residue has an intrinsic sequence-determined deamidation rate, which depend on charge distribution, steric factors, and other aspects of peptide chemistry.

Those proteins for which experimental deamidation half-times and the corresponding values of  $(100)/CD$  for those Asn have been reported (Table 4.1). For most examples, the overall differences are well within the range expected from variations in buffer type and other solvent conditions.

From the amino acid sequence of CGTase from *Paenibacillus* sp. RB01, 63 total Asn residues out of 713 amino acids are found. However, the 3D-structure of CGTase from alkalophilic *Bacillus* sp. 1011 (1PAM) with the same size of 713 amino acids and 98% similarity in amino acid sequence, but with 64 Asn residues was used to calculate the deamidation rate (CD value) of each Asn. Asn 93 in 1 PAM was replaced by His93 in RB01, *Bacillus* sp. N-227, *Bacillus* sp. 38-2, and *Bacillus* sp. 1-5 (Figure 3.4).

Thus, these differences in the structure between 1PAM and RB01, though relatively not much, must be taken into account whether or not they had the effect on the CD values. Those Asn with relatively low CD values (value 1-100) was selected for site-directed mutagenesis experiment. However, one intermediate value was also selected (Asn435 with a CD value of 158.3). Fifteen mutants were constructed, when compared with cloned CGTase, 9 of the mutants showed lower CGTase activity, 2 showed higher activity, and 4 showed no change in activity (Table 3.4). And from the analysis of isoform pattern on several gel systems: native-PAGE, IEF-PAGE, 2D-gel electrophoresis, those single mutants N336D, N427D, and N567D were shown to have similar migration as the isoform II of cloned CGTase. Thus, these mutants (including N415D which showed suspected results) were taken for further analysis. Three of the four mutants (N336D, N415D, and N567D) chosen had very low CD values of 1.0-1.7 with theoretical half-time of 22-24 days (Table 3.4), only N427D had higher CD of 53.4. However, the half-time of Asn415 and Asn 427 could not be determined due to a double amide sequence presence. Asn336 and 415 were in domain A2 (catalytic domain), Asn427 in domain C (starch-binding domain), and Asn567 in domain D of CGTase (no clear function) (von der Veen, 2000). And from the nearest neighbor hypothesis (Robinson and Robinson, 2001), comparing between these 4 mutants, Asn366 should be hot spot since Gly is at the  $n+1$  position and also Ser is at its  $n-1$  position (Table 3.4).



Table 4.1 Deamidation half-times in days at 37°C, pH 7.4 vs. estimates by (100)(CD)  
(Robinson and Robinson, 2001)

	Experimental*	Calc (100)(CD)
Hpr-phosphocarrier protein (Asn38)	10	57
Angiogenin (Asn61 and Asn109)	23 <sup>†</sup>	17 <sup>†</sup>
Hemoglobin ( $\alpha$ -Asn50)	25	18
Growth hormone (Asn149 and Asn152)	29 <sup>†</sup>	48
Hpr-phosphocarrier protein (Asn12)	31	21
Triose phosphate isomerase (Asn71)	38	78
Hemoglobin ( $\beta$ -Asn82)	42	19
Fibroblast growth factor (Asn7)	60	64
Hemoglobin ( $\beta$ -Asn80)	71	173
Ribonuclease A (Asn67)	64	85 <sup>‡</sup>
Insulin ( $\beta$ -Asn3)	135	117

\* Buffer conditions vary. pHs at or close to 7.4

<sup>†</sup>Reported rate for sum of both Asn residues.

<sup>‡</sup>Buffer (Tris) identical to that of model peptides used to calculate CD

#### 4.3.3 Isolation of CGTase isoforms

In this work, cloned CGTase isoforms were purified by four methods: preparative gel electrophoresis, FPLC on a Mono Q column, FPLC on a Mono P column, and IEF-PAGE. Preparative gel electrophoresis was developed for isoform separation of CGTase from *Paenibacillus* sp. A11 (Kaskangam, 1998). Chromatofocusing column was used to separate isoforms of the same enzyme, with the advantage of obtaining the pI values (Rojtinnakorn, 2001). For other research paper, most CGTase isoforms were studied in the non-isolated form. Among the four methods used in the present work, Mono P FF isofocusing chromatography demonstrated highest separation efficiency with fast separation but relatively with high cost.

#### 4.3.4 Analysis of tryptic digested peptides

Trypsin hydrolyzes at the C-side of Arg and Lys in proteins (Nelson and Cox, 2000). Forty-seven estimated peptide fragments were predicted when CGTase was subjected to trypsin hydrolysis according to [www.matrixscience.com](http://www.matrixscience.com) (Table 3.11). However, in practical, digestion might not be complete. After in gel tryptic digestion of isoform I, isoform II, and the four mutated enzymes, peptides were analyzed by reverse phase HPLC. The HPLC system used could not identify the difference of those enzyme forms (Figure 3.29 and 3.30). This may be due to the fact that the peptide fragment which contained mutated residue could not be well separated or showed no difference in hydrophobicity when compared with the corresponding fragment in the cloned. For other proteins, e.g. tryptic peptides of calmodulin, native and aged, were separated into HPLC peaks and peptides identified by amino acid composition after hydrolysis (Potter *et al.*, 1993).

MALDI-TOF was then employed for tryptic peptide analysis. The theoretical and experimental monoisotopic mass of the peptide fragments at the mutated Asn residues of the four single mutants N336D, N415D, N427D and N567D and a double mutant (N336D/N415D) were compared (Table 3.7). As shown in Figure 3.31 as an sample, mass spectra of the peptides of N567D CGTase showed an expected m/z of 2696.2, the size of fragment containing Asn 567, with an increase in 1 Da due to change of Asn to Asp. Then, the spectrum of peptides from isoform I and II were compared (Figure 3.22

and 3.23), the isoform II showed the peak at 1274.6 which suggested that Asn427 (Table 3.8) was deamidated. However, in some other studies, to identify the difference in peptide mass, the intensity of successive isotope had to be investigated. For example, the analysis of tryptic peptide of protective antigen from *B. anthracis* (Zomber *et al.*, 2005) and of human phenylalanine hydroxylase (Solstad *et al.*, 2003). Thus, the isotopic distribution of the target fragments which contained mutated Asn at the very labile positions e.g. those at 336, 415, and 567 were analyzed. The result (Figure 3.34) which showed the increase in the second isotope especially for the Asn336 containing fragment suggested that in addition to Asn427 (Figure 3.35), the involvement of other labile residues like Asn336 was also observed.

In our MS system, the matrix used allows size measurement in the range of 800-4000 Da. Thus, some peptides of our CGTase could not be detected since the sizes were out of this range. Also for some fragments with more than one Asn e.g. F G N N V A V V A I N R which contains N427, N428, and N435, only the result from mass analysis could not identify Asn427 as the deamidated position. But other results e.g. migration on native-PAGE, etc. could support.

Reports on other proteins which identification of deamidated Asn was accomplished by mass analysis are:

- 1) The microheterogeneity of recombinant wt-hPAH expressed in *E. coli* observed on isoelectric focusing and two-dimensional electrophoresis has been shown to be the result of multiple nonenzymatic deamidation of Asn residues. It was found that the 20-residue peptide (Phe131–Lys150) containing Asn133, with a single monoisotopic peak at  $m/z$  2193.06 in the 2-h expressed enzyme revealed on 24-h expression an additional peak at  $m/z$  2194.07; the apparent intensity ratio of the two mass peaks 2193.06 was 14.1:1 (Carvalho *et al.*, 2003)

- 2) Using the tetanus toxin C fragment (TTCF) antigen as a test case, it was demonstrated that spontaneous Asn deamidation readily occurred and that this could influence antigen processing and presentation. We identified two tryptic peptides with an isotopic distribution consistent with a proportion of the peptide having gained 1 mass

unit were identified. The most abundant isotope for peptide 1214–1223 (DGNAFNLDLDR) was the monoisotopic mass 1135.51 Da for TTCF4, but for TTCF37, the second isotopic mass of 1136.51 Da was the most abundant. Similarly, the isotopic distribution for peptide 1179–1191 (YTPPNNEIDSFVK) shifted upwards by one unit to 1427.68 Da (Moss, 2005)

3) The *Bacillus anthracis* Protective Antigen (PA): Under mild room temperature storage conditions, cytotoxicity decreased ( $t_{1/2} \approx 7$  days) concomitant with the generation of new acidic isoforms. They suggested that PA inactivation during storage is associated with susceptible deamidation sites, which are intimately involved in both mechanisms of PA cleavage by furin and PA-receptor binding. The Asp149–Arg167 peptide of 2269.3 Da clearly demonstrated a gradual increase in mass of 1 Da, as evident from the decreased intensity of the monoisotopic mass of 2269.3 Da, concomitant with an increased intensity of the successive isotopes, indicating progress in deamidation. The quantitation results indicated 28 and 70% deamidation following 14 and 30 days of PA storage (Zomber, 2005).

#### 4.4 Enzyme characterization

##### 4.4.1 CD production

It was known that different ratio of CDs production may be performed by varying incubation time. Terada *et al.* (2001) once compared the cyclization reaction of three bacterial cyclomalto-dextrin glucanotransferases. The results suggested that the larger cycloamyloses initially produced were converted into smaller cycloamyloses and finally into mainly  $\alpha$ - :  $\beta$ - :  $\gamma$ -CD. Purified enzyme (wild type CGTase) of *Paenibacillus* sp. RB01 produced  $\alpha$ - :  $\beta$ - :  $\gamma$ -CD of 0.56 : 1.00 : 0.22 (Yenpetch, 2002). There was previous report by Volkova *et al.* (2000), that crude CGTase from *Bacillus* sp. 1070 produced the three CDs in the ratio of 0.6 : 5.7 : 0.6 while purified enzyme gave 0.6 : 9.0 : 0.0. These three enzymes also differed in their hydrolytic activities, which seemed to accelerate the conversion of larger cycloamyloses into smaller cycloamyloses. Furthermore, Bovetto *et*

*al.* (1992) reported the production ratio of  $\alpha$ - :  $\beta$ - :  $\gamma$ -CD by CGTase from *Bacillus macerans* E192, at initial was 1 : 7 : 2 while at the equilibrium condition the ratio was 3 : 3 : 1. Another report showed that the ratio of CDs produced by CGTase from *B. macerans* IFO 3490 was almost constant regardless of the pH range (4.0-8.5) of the reaction system (Kitahata and Okada, 1974).

When compared product ratio of cloned, isolated isoforms, and mutated CGTase, isoform I and II gave very similar ratio (Table 3.10). The mutated CGTase of interest, N427D and N567D showed no change in product ratio comparing to the isoform. However, N336D CGTase gave lower  $\gamma$ -CD than the isoform I and II, but showed very similar product ratio to the cloned CGTase (which is the isoforms mixture). These results suggest that deamidation at these Asn residues did not give rise to the change in product formation.

#### 4.4.2 Kinetic study

To determine the kinetic parameters by coupling reaction, a ring of CD molecule is opened and combined with a linear oligosaccharide chain to produce a longer linear oligosaccharide (Nakamura *et al.*, 1993).  $\beta$ -CD acts as donor and cellobiose as acceptor (Wongsangwattana, 2000), a linear oligosaccharide generated then acts as a substrate, which is susceptible to hydrolytic cleavage by glucoamylase. The liberation of the reducing sugar measured by conventional method gives the procedure the ease and convenience of routine sugar analysis, dinitrosalicylic acid method (Miller, 1959). The activities were calculated from the consumed amounts of cyclodextrin calibrated from the amount of glucose in glucoamylase-treated reaction mixture. . When kinetic parameters of purified CGTase isoform I and II from cloned CGTase separated by Mono Q column and the crude enzyme of those interested mutants (N336D, N427D, and N567D) were compared, the catalytic efficiency of isoform I and the two mutated CGTase (N336D and N567D) was similar, however, the  $K_m$  and  $k_{cat}$  values of both

mutated enzymes were lower than those of isoform I. Isoform II showed somewhat lower catalytic efficiency than isoform I. Interestingly, N427D CGTase demonstrated a significant decrease in catalytic efficiency compared with the cloned enzyme. The conformation of CGTase isoform may be slightly different in the Asn → Asp/isoAsp deamidated form (isoform II in our case) and the Asn → Asp mutant form (N336D/N427D/N567D in our case) which may account for the quantitative difference observed between the kinetic properties of the two enzyme forms. Similar observation was also reported with the study of deamidation of labile Asn residues in human phenylalanine hydroxylase (Solstad *et al.*, 2003).

In conclusion, the increase in isoAsp intermediate upon incubation of CGTase isoform I in deamidation buffer, pH 9.0 and the conversion to isoform II support that deamidation really occurs. From the mass analysis of tryptic peptides, Asn336, Asn427, and Asn 567 are the most labile Asn residues responsible for the formation of CGTase isoform.

## CHAPTER V

### CONCLUSIONS

- 1) The *cgt* from *Paenibacillus* sp. RB01 was successfully cloned into the vector pET 19b and expressed by *E. coli* BL21 (DE3). The CGTase gene had an ORF of 2,142 bp and deduced into a protein with 713 amino acid residues including 27 amino acids as signal sequence. The cloned CGTase showed similar isoforms patterns on native-PAGE to the native enzyme.
- 2) The isoforms could be purified by preparative gel electrophoresis, FPLC on a Mono Q column, FPLC on a Mono P column, or IEF-PAGE.
- 3) The intermediate isoAsp significantly increased along with the formation of isoform II from isoform I when incubated in deamidation buffer at longer time. The change at pH 9.0 was higher than pH 6.0.
- 4) Labile Asn residues were selected to perform site-directed mutagenesis. The single mutants N336D, N427D, and N567D showed similar migration as isoform II of cloned CGTase on native-PAGE.
- 5) The labile Asn residues were selected to perform site-directed mutagenesis. By native-PAGE, IEF-PAGE and 2D gel, mutants N336D, N427D, and N567D showed similar migration as the isoform II of cloned CGTase.
- 6) The reverse phase HPLC system used could not identify the different tryptic peptides isoform of I and II.
- 7) From MALDI-TOF result, isoform I and II showed difference in Asn336 and Asn427 containing fragment.
- 8) Catalytic efficiency of N336D, N567D was similar to that of isoform I and isoform II while the value of N427D was significantly increased. The Isoform I, II, N427D and N567 gave similar CD product ratio, while N336D showed slightly different.
- 9) The overall results supports that Asn deamidation is the cause of formation of multiple forms of CGTase, and Asn336, Asn427, and Asn567 are among the susceptible residues responsible for the formation of CGTase isoforms.

## REFERENCES

- Abelian, V. A. Adamian, M. O., Abelian, L. A., Balayan, A. M., and Afrikan, E. K. 1995. A new cyclodmaltodextrin glucanotransferase from halophilic *Bacillus*. *Biokhimiya*. **60**: 891-897. (in Russian).
- Abelyan, V. A., Yamamoto, T., and Afrikyan, E.G. 1994. Isolation and characterization of cyclodextrin glucanotransferase using cyclodextrin polymers and their derivatives. *Biochemistry (Moscow)* **59**: 573-579.
- Aswad, D. W. 1994. *Deamidation and isoaspartate formation in peptides and proteins*. Boca Raton, FL., CRC Press.
- Aswad, D. W., Paranandi, M. V., and Schurter, B. T. 2000. Isoaspartate in peptides and proteins: formation, significance, and analysis. *J. Pharmaceutical and Biomedical Analysis* **21**: 1129-1136.
- Bender, H. 1986. Production, characterization and application of cyclodextrins. *Adv. Biotech, Proc.* **6**: 31-71.
- Bischoff, R., and Kolbe, H. 1994. Deamidation of asparagine and glutamine residues in proteins and peptides: structural determinants and analytical methodology. *J. Chrom. B.* **662**: 261-278.
- Bovetto, L. J., Backe, D. P., Villette, J. R., Sicard, P. J., and Bouquelet, S. J-L. 1992. Cyclomaltodextrin glucanotransferase from *Bacillus circulans* E192 I : Purification and characterization of the enzyme. *Biotechnol. Appl. Biochem.* **15** (1) : 48-58.
- Bradford, M. M. 1976. A rapid and sensitive method for the quantitation of microgram quantities of protein utilizing the principle of protein-dye binding. *Anal Biochem.* **72**: 248-54.
- Buchholz, K., Kasche, V. Bornscheuer, U.T. 2005. *Biocatalysts and Enzyme Technology*. Weinheim: Wiley-VCH Verlag.
- Capasso, S., Mazzarella, L., Sica, F., and Zagari, A. 1989. Solid-state conformations of aminosuccinyl peptides: crystal structure of tert-butyloxycarbonyl-L-leucyl- L-aminosuccinyl-L-phenylalaninamide. *Biopolymers* **28**, 139-147.



- Carvalho, R. N., Solstad, T., Bjorgo, E., Barrosot, J. F., and Flatmark, T. 2003. Deamidations in recombinant human phenylalanine hydroxylase. *J. Biological Chemistry* **278**, 15142-15152.
- Charoensakdi, R., Iizuka, M., Ito, K., Rimpanitchayakit, V., and Limpaseni, T. 2007. A recombinant cyclodextrins glycosyltransferase cloned from *Paenibacillus* sp. strain RB01 showed improved catalytic activity in coupling reaction between cyclodextrins and disaccharides. *J. Incl. Phenom. Macrocycl Chem.* **57**: 53-59.
- Chazin W. J. and Kossiakov A. A. (1995) The role of secondary and tertiary structures in intramolecular deamidation of proteins. In: *Deamidation and Isoaspartate Formation in Peptides and Proteins*, pp. 193–206, Aswad D. W. (ed.), Boca Raton, FL. CRC Press.
- Cox, G. A., Johnson, R. B., Cook, J. A., Wakulchik, M., Johnson, M. G., Villarreal, E. V., and Wang, Q. M. 1999. Identification and characterization of human rhinovirus-14 3C protease deamidation isoform. *J. Biological Chemistry* **274**: 13211-13216.
- Curnis, F., Longhi, R., Crippa, L., Cattaneo, A., Dondossola, E., Bachi, A., and Corti, A. 2006. Spontaneous Formation of L-Isoaspartate and Gain of Function in Fibronectin. *J. Biol. Chem.* **281** (47): 36466–36476.
- David C. L., Keener J. and Aswad D. W. 1999. Isoaspartate in ribosomal protein S11 of *Escherichia coli*. *J. Bacteriol.* **181**: 2872–2877
- DeLuna, A., Quezada, H., Gomez-Puyou, A., and Gonzalez, A. 2005. Asparaginyl deamidation in two glutamate dehydrogenase isoenzymes from *Saccharomyces cerevisiae*. *Biochem. Biophys. Res. Com.* **328**: 1083–1090.
- DePinto, J. A., and Campbell, L. L. 1968. Purification and properties of the amylase of *Bacillus macerans*. *Biochemistry* **7**: 114-120.
- Deverman, B.E., Cook, B.L., Manson, S.R., Niederhoff, R.A., Langer, E.M., Rosová, I., Kulans, L.A., Fu, X., Weinberg, J.S., Heinecke, J.W., Roth, K.A., Weintraub, S.J., 2002. Bcl-XL deamidation is a critical switch in the regulation of the response to DNA damage. *Cell.* **111**: 51–62.

- Fiedler, G. Pajatsch, M., and Bock, A., 1996. Genetics of novel starch utilization pathway in *Klebsiella oxytoca*. *J. Mol. Biol.* **256**: 279-291.
- Flatmark, T. 1967. On the heterogeneity of beef heart cytochrome c II. Some physico-chemical properties of the main subforms (Cy I - Cy III). *Acta Chemica Scandinavica* **20**, 1476-1486.
- Flatmark, T. and Sletten, K. 1968. Multiple forms of cytochrome c in the rat precursor-product relationship between the main component Cy I and the minor components Cy II and Cy III in vivo. *J. Biological Chemistry* **243**, 1623-1629.
- Flatmark, T. and Vesterberg, O. 1966. On the heterogeneity of beef heart cytochrome c IV. Isoelectric fractionation by electrolysis in a natural pH gradient. *Acta Chemica Scandinavica* **20**, 1497-1503.
- Fujita, Y., Stubouchi, H., Inagi, Y., Tomita, K., Ozaki, A., and Nakanishi, K. 1990. Purification and properties of cyclodextrin glycosyltransferase from *Bacillus* sp. AL-6. *J. Ferment. Bioeng.* **70**: 150-154.
- Goel, A., and Nene. N. S. 1995. Modifications in the phenolphthalein method for spectrophotometric estimation of beta cyclodextrin. *Starch/starke.* **47** (10): 399-400.
- Jamuna, R., Saswathi, N., Sheela, R., and Ramakrishna, S. V. 1993. Synthesis of cyclodextrin glucosyl transferase by *Bacillus cereus* for the production of cyclodextrins. *App. Biochem. Biotechnol.* **43**: 163-176.
- Jespersen, H. M., Macgregor, E. A., Sierks, M. R., and Svensson, B. 1991. Comparison of the domain-level organisation of starch hydrolases and related enzymes. *J. Biochem.* **280**: 51-55.
- Jorgensen, S.T., Tangney, M., Starnes, R.L., Amemiya, K. and Jorgensen, P.L. 1997. Cloning and nucleotide sequence of a thermostable cyclodextrin glycosyltransferase gene from *Thermoanaerobacter* sp. ATCC 53627 and its expression in *Escherichia coli*. *Biotechnol. Letters.* **19** (10) 1027-1031.
- Kaskangam, K. 1998. Isolation and characterization of cyclodextrin glycosyltransferase isozymes from *Bacillus* sp. A11. Master's Thesis, Faculty of Science, Chulalongkorn University.

- Kato, T., Horikoshi, K. Immobilized cyclomalto-dextrin glucanotransferase of an alkalophilic *Bacillus* sp. No. 38-2. 1984. *Biotechnol. Bioeng.* **26** (6): 595 – 598.
- Kaulpiboon, J., and Pongsawasdi, P. 2005. Purification and characterization of cyclodextrinase from *Paenibacillus* sp. A11. *Enzyme Microb. Technol.* **36** : 168-175.
- Kitahata, S., and Okada, S. 1974. Action of cyclodextrin glycosyltransferase from *Bacillus metaterium* strain No. 5 on starch. *Agric. Biol. Chem.* **38**: 2413-2417.
- Kitahata, S., and Okada, S. 1982. Purification and some properties of cyclodextrin glucanotransferase from *Bacillus stearthermophilus* TC-90. *J. Jpn. Starch. Sci.* **29**: 7-12.
- Klein, C., Hollender, J., Bender, H., Schulz, G.E. 1992. Catalytic center of cyclodextrin glycosyltransferase derived from X-ray structure analysis combined with site-directed mutagenesis. *Biochemistry* **31**, 8740-8746.
- Kobayashi, S., Kainuma, K. and Suzuki, S. 1978. Purification and some properties of *Bacillus macerans* cycloamylose (cyclodextrin) glucanotransferase. *Carbohydr Res.* **61**: 229-38.
- Koida, M., Lai, C. Y., and Horecker, B. L. 1969. Subunit structure of rabbit muscle aldolase extent of homology of the  $\alpha$  and  $\beta$  subunits and age-dependent changes in their ratio. *Archives of Biochemistry and Biophysics.* **134**, 623-631.
- Kuttiarcheewa, W. 1994. Immobilization of cyclodextrin glycosyltransferase on inorganic carriers. Master's Thesis, Faculty of Science, Chulalongkorn University.
- Lawson, C. L., van Montfort, R., Strokopytov, B., Rozeboom, H. J., Kalk, K. H., de Vries, G. E., Penninga, D., Dijkhuizen, L., and Dijkstra, B.W. 1994. Nucleotide sequence and X-ray structure of cyclodextrin glycosyltransferase from *Bacillus circulans* strain 251 in a maltose-dependent crystal form. *J. Mol. Biol.* **236**: 590-600.
- Li, X., Cournoyer, J., Lin, C., O'Connor, P. B. 2008. Use of <sup>18</sup>O labels to monitor deamidation during protein and peptide sample processing. *Am Soc Mass Spectrom.* **19**(6):855-64.
- Matsuura, Y., Kusunoki, M., and Harada, W. 1984. Structure and possible catalytic residues of Taka-amylase A. *J. Biochem.* **95**: 697-702.

- Mattsson, P., Meklin, S., and Korpela, T. 1990. Analysis of cyclodextrin glucanotransferase isozymes by isoelectric focusing in immobilized pH gradients. *J. Biochem. Biophys. Methods*. **20** (3): 237-276.
- Miller G L., 1959, Use of dinitrosalicylic acid reagent for determination of reducing sugar. *Analytical Chemistry*, **31**, 420–428.
- Moss, C., P. Matthews, S., Lamont, D., and Watts, C. 2005. Asparagine deamidation perturbs antigen presentation on class II major histocompatibility complex molecules. *J. Biol. Chem.* **280** (18): 18498–18503.
- N. E. Robinson and A. B. Robinson, 2004. *Protein Deamidation*, Cave junction, Oregon, Althouse Press.
- Nakamura, A., Haga, K., and Yamane, K. 1993. Three histidine residues in the active center of cyclodextrin glucanotransferase from alkalophilic *Bacillus* sp. 1011: Effects of the replacement on pH dependence and transition-state stabilization. *Biochemistry* **32**: 6624–6631.
- Nakamura, N., and Horikoshi, K. 1976. Purification and properties of cyclodextrin glycosyltransferase of an alkalophilic *Bacillus* sp. *Agric. Biol. Chem.* **40**: 935-941.
- Penninga, D., van der Veen, B. A., Knegtel, R. M. A., van Hijum, S. A. F. T., Rozeboom, H. J., Kalk, K. H., Dijkstra, B. W., and Dijkhuizen, L. 1996. The raw starch binding domain of cyclodextrin glycosyltransferase from *Bacillus circulans* strain 251. *J. Biol. Chem.* **271**: 32777-32784.
- Perkins, M., Theiler, R., Lunte, S., and Jeschke, M. 2000. Determination of the Origin of Charge Heterogeneity in a Murine Monoclonal Antibody. *Pharmaceutical Research* **17** (9): 1110-1117.
- Pongsawasdi, P., Yagisawa, M., 1988. Purification and some properties of cyclomalto-dextrin glucanotransferase from *Bacillus circulans*. *Agric. Biol. Chem.* **52**: 109–1103.
- Pongsawasdi, P. 2008. *Carbohydrate-modifying enzyme in industry*. Bangkok. Chula Press.
- Prasong, W. 2002. Structural analysis of cyclodextrin glycosyltransferase isoforms from *Paenibacillus* sp. A11. Master's Thesis, Faculty of Science, Chulalongkorn University.

- Pully, O. A., and French, D. 1961. Studies on the Schardinger dextrin XI: The isolation of new Schardinger dextrin. *Biochem. Biophys. Res. Com.* **5**: 11-15.
- Rimphanitchayakit V, Tonozuka T, Sakano Y. 2005. Construction of chimeric cyclodextrin glucanotransferases from *Bacillus circulans* A11 and *Paenibacillus macerans* IAM1243 and analysis of their product specificity. *Carbohydr Res.* **340** (14): 2279-89.
- Robinson, A. B. and Rudd, C. J. 1974 Deamidation of glutaminy and asparaginy residues in peptides and proteins. *Current Topics in Cellular Regulation* **8**, 247-295.
- Robinson, A. B., Mckerrow, J. H. and Cary, P. 1970. Controlled deamidation of peptides and proteins: an experimental hazard and a possible biological timer. *Proc Nat Acad Sci U S A.* **66**(3): 753-7.
- Robinson, N. E. and Robinson, A. B. 2001. Molecular clocks. *Proc. Natl. Acad. Sci. USA* **98**, 944-949.
- Rojtinnakorn, J., Kim. P., Laloknam, S., Tongsim, A., Kamolsiripichai, S., Limpaseni, T., and Pongsawasdi, P. 2001. Immunoaffinity purification and characterization of cyclodextrin glycosyltransferase from *Bacillus cereus* A11. *Science Asia.* **27**: 105-112.
- Saenger, W. 1982. Structure aspect of cyclodextrin inclusion compounds. In J. Szejtli (ed.), *Proceedings of the 1<sup>st</sup> International Symposium on Cyclodextrins*, Budapest, Akademiai Kiado: 141-145.
- Sambrook, J. and Russell, W. D. 2001. *Molecular cloning: a laboratory manual*. 3rd. Cold spring harbor, Cold spring harbor laboratory press.
- Schmid, G. 1989. Cyclodextrin glycosyltransferase production: Yield enhancement by overexpression of clone genes. *Trends Biotechnol.* **7**: 244-248.
- Sin, K.A., Nakamura, A., Kobayashi, K., Masaki, H., and Uozumi, T. 1991. Cloning and sequencing of a cyclodextrin glucanotransferase gene from *Bacillus ohbensis* and its expression in *Escherichia coli*. *Appl. Microbiol. Biotechnol.* **35**: 600-605.

- Solstad, T., Carvalho, R. N., Andersen, O. A., Waidelich, D. and Flatmark, T. 2003. Identification of labile asparagine residues and functional characterization of Asn→Asp mutant forms. *J. Biol. Chem.* **278** (17): 15142-15152.
- Solstad, T., Carvalho, R. N., Andersen, O. A., Waidelich, D., and Flatmark, T. 2003. Deamidation of labile asparagine residues in the autoregulatory sequence of human phenylalanine hydroxylase structural and functional implications. *Euro. J. Biochem.* **270**: 929-938.
- Strokopytov, B., Knegtel, R.M.A., Penninga, D., Rozeboom, H.J., Kalk, K.H., Dijkhuizen, L., Dijkstra, B.W. 1996. Structure of cyclodextrin glycosyltransferase complexed with a maltononaose inhibitor at 2.6 Å resolution. Implications for product specificity. *Biochemistry* **35**: 4241-4249.
- Suizdak, G. 1996. *Mass Spectrometry for Biotechnology*. London. Academic Press.
- Szejtli, J. 1988. *Cyclodextrins technology*. Netherland: Kluwer Academic Publisher.
- Szejtli, J. 1990. The cyclodextrins and their application in biotechnology. *Carbohydrate Polymers*. **12**, 375.
- Szejtli, J. 1998. Introduction and general overview of cyclodextrin chemistry. *Chem. Rev.* **98**: 1743-1753.
- Takaha, T., Smith, S. M., 1999. The functions of 4- $\alpha$ -glucanotransferases and their use for the production of cyclic glucans. *BiotechnolGen Eng Rev.* **16**:257-80.
- Takano, T., Fukuda, M., Kobayashi, S., Kainuma, K., and Yamane, K. 1986. Molecular cloning, nucleotide sequencing, and expression in *Bacillus subtilis* cells of *Bacillus macerans* cyclodextrin glucanotransferase gene. *J. Bacteriol.*: 1118-1122.
- Techaiyakul, W., Pongssawasdi, P., and Mongkolkl, P. 1990. in *Minutes of the 5th International Symposium on Cyclodextrins*, Duchêne, D., ed., Editions de Santé, Paris: 50–54.
- Tesana, S. 2001. Cyclodextrin glycosyltransferase from thermotolerant bacteria: screening, optimization, partial purification and characterization. Master's Thesis, Faculty of Science, Chulalongkorn University.

- Terada, Y., Sanbe, H., Takaha, T., Kitahata, S., Koizumi, K., and Okada, S. 2001. Comparative study of the cyclization reactions of three bacterial cyclomalto-dextrin glucanotransferases. *App Environ Microbiol.* **67** (4): 1453–1460.
- Tonkova, A. 1998. Bacterial cyclodextrin glucanotransferase. *Enzyme Microb. Technol.* **22**: 678-686.
- Tyler-Cross, R. and Schirch, V. 1991. Effects of amino acid sequence, buffers, and ionic strength on the rate and mechanism of deamidation of asparagine residues in small peptides. *J Biol Chem.* **266**(33): 22549-56.
- Uitdehaag, J.C.M., Mosi, R., Kalk, K.H., van der Veen, B.A., Dijkhuizen, L., Withers, S.G., and Dijkstra, B.W. 1999b. X-ray structures along the reaction pathway of cyclodextrin glycosyltransferase elucidate catalysis in the  $\alpha$ -amylase family. *Nature Struct. Biol.* **6**: 432–436.
- van der Veen, B. A., Joost, C.M., Uitdehaag, B. W. D., and Lubbert. D. 2000. Engineering reaction and production specificity of cyclodextrin glycosyltransferase from *Bacillus circulans* strain 251. *Biochemica et Biophysica Acta: Protein and proteomic.* **1543**(2): 336-360.
- van der Veen, B.A., Leemhuis, H., Kralj, S., Uitdehaag, J.C.M., Dijkstra, B.W., and Dijkhuizen, L. 2001. Hydrophobic amino acid residues in the acceptor binding site are main determinants for reaction mechanism and specificity of cyclodextrin-glycosyltransferase. *J. Biol. Chem.* **276**: 44557–44562.
- Volkova, D. A., Lopatin, S. A., and Varlamov, V. P. 2000. One-step affinity purification of cyclodextrin glucanotransferase from *Bacillus* sp.1070. *Biocatalysis.* **41**(6): 67-69.
- Volkova, D. A., Lopatin S. A., Gracheva I. M., Varlamov V. P. 2001. Preparation of high-purity cyclodextrin glucanotransferase from *Bacillus* sp. 1070. *App. Biochem. Microb.*, **37** (2): 138–141.
- Webb, E. C. 1964. Nonmenclature of multiple enzyme forms. *Nature.* **203**: 821.
- Wind, R. D., Liebl, W., Buitelaar, R. M., Penninga, D., Spreinat, A., Dijkhuizen, L., and Bahl, H. 1995. Cyclodextrin formation by the thermostable  $\alpha$ -amylase of

- Thermoanaerobacterium thermosulfurigenes* EM1 and reclassification of the enzyme as a cyclodextrin glycosyltransferase. *Appl. Environ. Microbiol.* **61**: 1257-1265.
- Wongsangwattana, W., 2000. Specificity of glycosyl acceptor in coupling and transglycosylation reactions of cyclodextrin glycosyltransferase from *Bacillus circulans* A11. Master's Thesis, Faculty of Science, Chulalongkorn University.
- Yenpetch, W. 2002. Purification and biochemical characterization of cyclodextrin glycosyltransferase from thermotolerant *Paenibacillus* sp. strain RB01. Master's Thesis, Faculty of Science, Chulalongkorn University.
- Zomber, G., Reuveny, S., Garti, N., Shafferman, A., and Elhanany, E. 2005. Effects of spontaneous deamidation on cytotoxic activity of the Bacillus anthracis protective antigen. *J. Biol. Chem.*, **280** (48): 39897-39906.



## APPENDICEA

## Appendix 1 Bacterial media culture

### Horikoshi medium (100 mL)

Soluble starch	1.0 g
Peptone	0.5 g
Yeast extract	0.5 g
$K_2HPO_4$	0.1 g
$MgSO_4 \cdot 7H_2O$	0.02 g
$Na_2CO_3$	0.75 g

The pH was adjust to 10.1-10.2 at 40 °C by NaOH

### LB medium (100 mL)

Tryptone	1.0 g
Yeast extract	0.5 g
NaCl	0.5 g

The pH should be around 7.0

## Appendix 2: Preparation for buffer solution

- 0.2 M Potassium Acetate pH 3.0, 4.0 and 5.0

$\text{CH}_3\text{COOK}$	1.96 g
--------------------------	--------

Adjusted to pH 3, 4 or 5 by 0.2 M acetic acid and adjusted volume to 100 ml with distilled water.

- 0.2 M Phosphate pH 6.0

$\text{KH}_2\text{PO}_4$	2.27 g
--------------------------	--------

$\text{K}_2\text{HPO}_4$	0.58 g
--------------------------	--------

distilled water	100 ml
-----------------	--------

- 0.2 M Phosphate pH 7.0

$\text{KH}_2\text{PO}_4$	0.91 g
--------------------------	--------

$\text{K}_2\text{HPO}_4$	2.32 g
--------------------------	--------

distilled water	100 ml
-----------------	--------

- 0.2 M Tris-HCl pH 8.0 and 9.0

Tris(hydroxymethyl)-aminometane	2.42 g
---------------------------------	--------

Adjusted to pH 8.0 or 9.0 by 1 M HCl and adjusted to 100 ml with distilled water.

- 0.2 M Tris-Glycine NaOH pH 10.0 and 11.0

Glycine	1.5 g
---------	-------

Adjusted to pH 10.0 or 11.0 by 1 M NaOH and adjusted volume to 1000 ml with distilled water.

- **Universal pH buffer**

Citric acid	6.008 g
-------------	---------

$\text{KH}_2\text{PO}_4$	3.893 g
--------------------------	---------

$\text{H}_3\text{BO}_3$	1.769 g
-------------------------	---------

Diethylbarbituric acid	5.266 g
------------------------	---------

Dissolve these mixtures to 100 ml with distilled water, then titrated with 0.2 M NaOH to give the appropriated pH (4.0-10.0).

**Appendix 3: Preparation for polyacrylamide gel electrophoresis****Stock reagents**

30% Acrylamide, 0.8% bis-acrylamide, 100 ml

Acrylamide	29.2	g
N,N'-methylene-bis-acrylamide	0.8	g

**Adjusted volume to 100 ml with distilled water**

1.5 M Tris-HCl pH 8.8 (100 ml)

Tris(hydroxymethyl)-aminomethane	18.17	g
----------------------------------	-------	---

**Adjusted pH to 8.8 with 1 M HCl and adjusted with distilled water****2 M Tris-HCl pH 8.8**

Tris(hydroxymethyl)-aminomethane	24.2	g
----------------------------------	------	---

Adjusted pH to 8.8 with 1 M HCl and adjusted volume to 100 ml with distilled water

0.5 M Tris-HCl pH 6.8

Tris(hydroxymethyl)-aminomethane	6.06	g
----------------------------------	------	---

Adjusted pH to 6.8 with 1 M HCl and adjusted volume to 100 ml with distilled water

**1 M Tris-HCl pH 6.8**

Tris(hydroxymethyl)-aminomethane	12.1	g
----------------------------------	------	---

Adjusted pH to 6.8 with 1 M HCl and adjusted volume to 100 ml with distilled water

**Solution B (SDS-PAGE)**

2 M Tris-HCl pH 8.8	75	ml
10% SDS	4	ml
distilled water	21	ml

**Solution C (SDS-PAGE)**

1 M Tris-HCl pH 6.8	50	ml
10% SDS	4	ml
distilled water	46	ml

## Appendix 3: Preparation for polyacrylamide gel electrophoresis (continue)

## Non-denaturing PAGE

## 7.5% Separating gel

30% acrylamide solution	2.5	ml
1.5 M Tris-HCl pH 8.8	2.5	ml
distilled water	5.0	ml
10% $(\text{NH}_4)_2\text{S}_2\text{O}_8$	50	$\mu\text{l}$
TEMED	10	$\mu\text{l}$

## 5.0% stacking gel

30% acrylamide solution	0.67	ml
0.5 M Tris-HCl pH 6.8	1.0	ml
distilled water	2.3	ml
10% $(\text{NH}_4)_2\text{S}_2\text{O}_8$	30	$\mu\text{l}$
TEMED	5	$\mu\text{l}$

#### Appendix 4: Preparation for isoelectric focusing and 2 dimension electrophoresis gel

##### Monomer-ampholyte solution

25% (w/v) Acrylamide solution	0.8	ml
Ampholyte pH 4-6	0.2	ml
Distilled water	2.2	ml
25% (w/v) glycerol	0.8	ml
0.1% (w/v) FMN	40	$\mu$ l
10% $(\text{NH}_4)_2\text{S}_2\text{O}_8$	12	$\mu$ l
TEMED	4	$\mu$ l

##### Fixative solution for IEF-PAGE, 100 ml

Sulfosalicylic acid	4	ml
Trichloroacetic acid	12.5	ml
Methanol	30	ml

Immerse gels in this solution for 30 minutes.

##### Staining solution for IEF-PAGE, 100 ml

Ethanol	27	ml
Acetic acid	10	ml
Coomassie brilliant blue R-250	0.04	ml
$\text{CuSO}_4$	0.5	ml
Distilled water	63	ml

Dissolve the  $\text{CuSO}_4$  in water before adding the alcohol. Either dissolve the dye in alcohol or add it to the solution at the end.

Immerse the gel in stain for approximately 1-2 hours.

Appendix 4: Preparation for isoelectric focusing and 2 dimension electrophoresis gel  
(continue)

1<sup>st</sup> Dimension reagent

- Rehydration buffer (8 M urea, 2% CHAPS, 0.5/2% Pharmalyte or IPG buffer, 0.002% bromophenolblue, 25 ml)\*

Reagent	Final concentration	Amount
Urea (FW 60.06)	8 M	12 g
CHAPS	2%	0.5 g
Phamalyte or IPG buffer	0.5% (v/v) or 2% (v/v)	125 µl or 500 µl
(same range as the IPG strip)		
1% bromophenolblue stock solution	0.002%	50 µl
Double-distilled water	-	To 25 ml (16 ml required)

\*DTT is added just prior to use: 7 mg DTT per 2.5 ml aliquot of rehydration stock solution. For rehydration loading, sample is also added to the aliquot of rehydration solution just prior to use.

Store in 0.5 ml aliquots at -20°C.

- SDS equilibration buffer solution

(6 M urea, 75 mM Tris-HCl ph 8.8, 29.3% glycerol, 2% SDS, 0.002% bromophenolblue, 200 ml)

Reagent	Final concentration	Amount
Urea (FW 60.06)	6 M	72.1 g
Tris-HCl, pH 8.8	75 mM	10.0 ml
Glycerol (87% w/w)	29.3% (v/v)	69 ml (84.2 g)
SDS (FW 288.38)	2% (w/v)	4.0 g
1% bromophenolblue stock solution	0.002% (w/v)	400 µl
Double-distilled water	-	To 25 ml (16 ml required)

\*This is a stock solution. Just prior to use, DTT 10 mg/ml or iodoacetamide 25 mg/ml (for first or second equilibration, respectively)

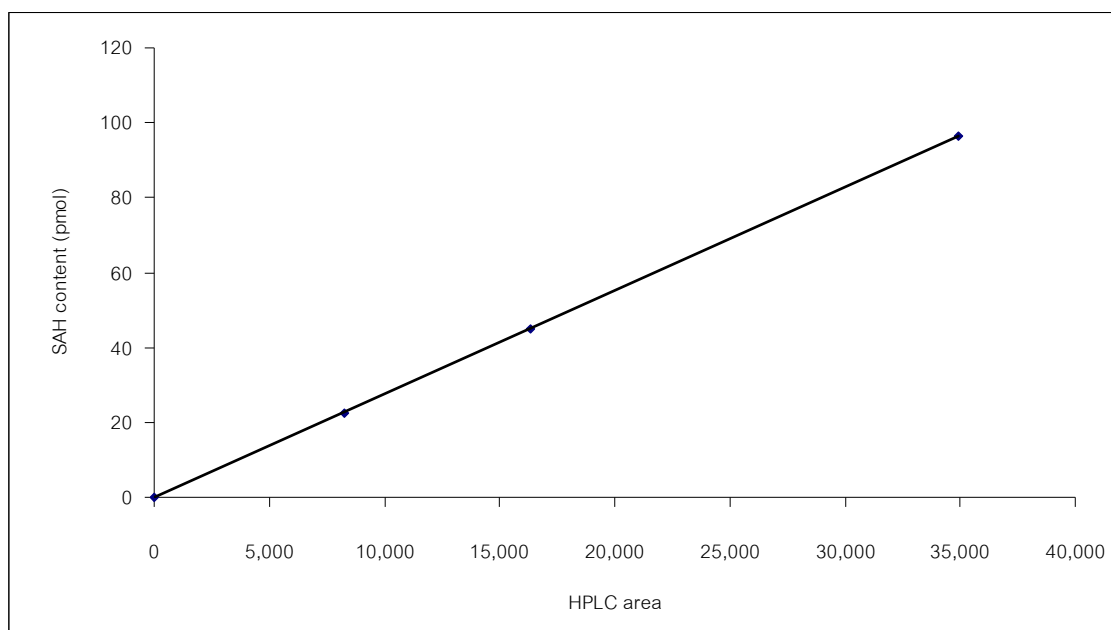
Store in 20- or 50 ml aliquote at -20°C.

## Appendix 5 Competent cell preparation (Sambrook, 2001)

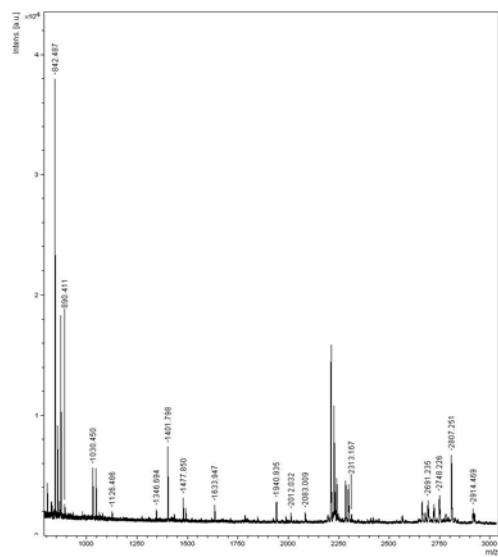
A single colony of *E. coli* BL21 (DE3) was cultured as the starter in 12 ml of LB broth and incubated at 37°C with 250 rpm shaking for overnight. One percent of starter was inoculated into 200 ml LB broth in 1,000 ml Erlenmeyer flask and cultivated at 37°C with 250 rpm shaking for about 3 hours until the absorbance at 650 nm of the cells reached 0.4-0.5. The cells were chilled on ice for 14-30 min and harvested by centrifugation at 8,000 x g for 15 min at 4°C. The supernatant was removed as much as possible. The cell pellet was washed with 800 ml of cold steriled water, resuspended by gentle mixing and centrifuged at 8,000 x g for 15 min at 4°C. The supernatant was discarded. The pellet was then wash and centrifuged with 400 ml of cold steriled water, followed by 20 ml of ice cold steriled 10% (v/v) glycerol, and finally resuspended in a final volume of 1.6-2.0 ml ice cold steriled 10% (v/v) glycerol. The cell suspension was divided into 40  $\mu$ l aliquots and stored at -80°C until used. Usually, these competent cells were good for at least 6 months under these conditions.



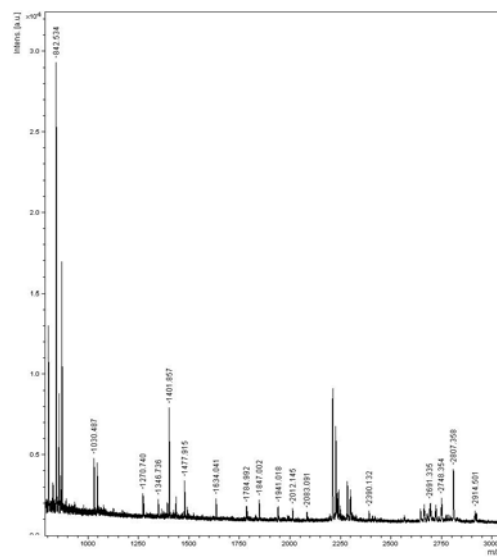
## Appendix 6 Standard curve for SAH content by reverse phase HPLC



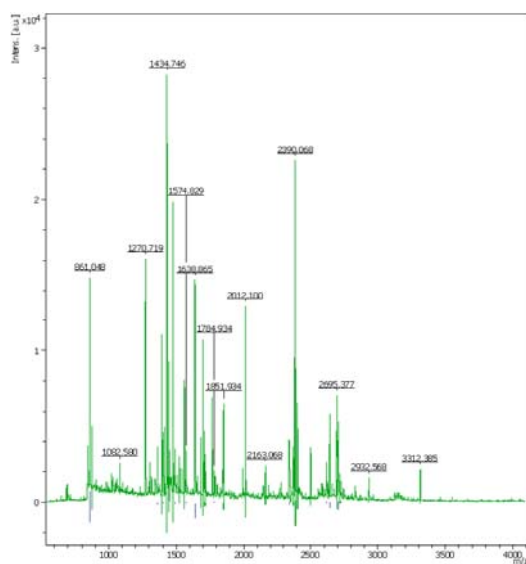
## Appendix 7 Chromatogram of monoisotopic mass of CGTase



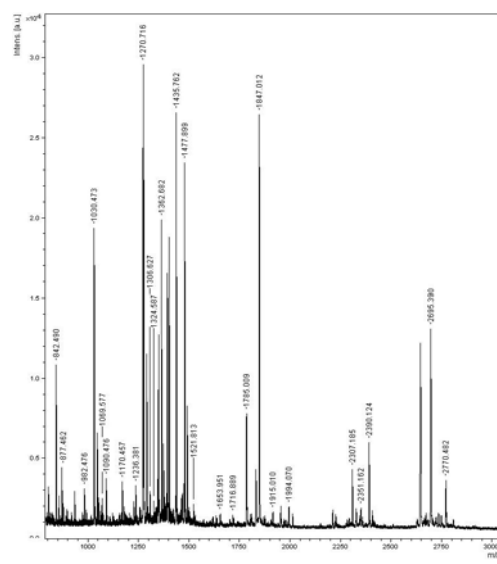
N336D



N415D



N427D



N336D/N415D

Appendix 8 Example calculation of  $T_{1/2}$  and CD value of labile Asn on human phenylalanine hydroxylase (PDB code 2PAH) (Carvalho, 2003)

Asn residue	Neighbor residues		$t_{1/2}$ mg (days)	Secondary structure	Three-dimensional localization		$C_D$
	( $n - 1$ )	( $n + 1$ )			H-bonding	Position	
133	Phe	Gln	60.0	Between C $\alpha$ 1-helix and C $\alpha$ 2a-helix	None	On the surface	4.1/73 <sup>a</sup>
167	Ala	Tyr	70.6	Just after C $\alpha$ 2b-helix	Asn <sup>167</sup> N $\delta$ 2-Asp <sup>163</sup> carbonyl oxygen (3.10 Å)	On the surface	740
207	Glu	His	10.2	In the middle of C $\alpha$ 4-helix	Asn <sup>207</sup> N $\delta$ 2-Ala <sup>202</sup> carbonyl oxygen (3.13 Å)	On the surface	85
223	Glu	Ile	298	In the loop between C $\alpha$ 4- and C $\alpha$ 5-helix	Asn <sup>223</sup> N $\delta$ 2-Gly <sup>218</sup> carbonyl oxygen (3.02 Å) Asn <sup>223</sup> O $\delta$ 1-H <sub>2</sub> O-Ile <sup>224</sup> carbonyl oxygen (2.89 and 2.72 Å)	On the surface (kept in position by H-bonding)	40
376	Ile	Tyr	94.5	Between C $\alpha$ 11- and C $\alpha$ 12-helix	None	On the surface, in the 380 loop that covers the active site crevice	5.5
393	Ser	Asp	27.4	Just in front of C $\alpha$ 12-helix	Asn <sup>393</sup> N $\delta$ 2 and O $\delta$ 1- Ser <sup>298</sup> O $\gamma$ (2.96 and 2.95 Å)	On the surface	230
401	Val	Phe	68.3	In the middle of C $\alpha$ 12-helix	None	On the surface	350
426	Leu	Thr	52.4	Just before C $\alpha$ 14-helix (the beginning of the tetramerization motif)	Asn <sup>426</sup> O $\delta$ 1-Phe <sup>410</sup> main chain N (2.71 Å)	Solvent-exposed	2100

## Biography

Mr. Wanchai Yenpetch born on September 25, 1975. He graduated with the Bachelor Degree of Science in Biochemistry from Khonkaen University in 1998. He has working at Department of Physiology, faculty of Veterinary Science, Chulalongkorn University. He graduated with Master Degree of Science in Biochemistry from Chulalongkorn University in 2002. He was back to work in the department of physiology, faculty of veterinary science until 2004. Then he further studied for the degree of PhD. in biochemistry at the department of biochemistry, faculty of science, Chulalongkorn university until 2009.